

UC Berkeley

UC Berkeley Electronic Theses and Dissertations

Title

Functional networks in aging and Alzheimer's disease: Contributions and consequences

Permalink

<https://escholarship.org/uc/item/6zj9m673>

Author

Ziontz, Jacob

Publication Date

2024

Peer reviewed|Thesis/dissertation

Functional networks in aging and Alzheimer's disease: Contributions and consequences

By

Jacob Ziontz

A dissertation submitted in partial satisfaction of the

requirements for the degree of

Doctor of Philosophy

in

Neuroscience

in the

Graduate Division

of the

University of California, Berkeley

Committee in charge:

Professor William Jagust, Chair

Professor Kevin Weiner

Professor Daniela Kaufer

Professor Kristopher Bouchard

Summer 2024

© Jacob Ziontz, 2024

Abstract

Functional networks in aging and Alzheimer's disease: Contributions and consequences

by

Jacob Ziontz

Doctor of Philosophy in Neuroscience

University of California, Berkeley

Professor William Jagust, Chair

Alzheimer's disease is characterized by two hallmark neuropathologies: A β plaques and hyperphosphorylated tau protein. A β tends to arise in a diffuse manner throughout cortex, whereas tau pathology accumulates in a stereotyped pattern first in medial temporal lobe and then in selectively vulnerable neocortical regions as the disease progresses. The processes facilitating the propagation of tau pathology are still unknown, but converging cellular and neuroimaging evidence suggests that tau spreads transneuronally along pathways of functional connectivity throughout the brain. In this work, we utilize multimodal human neuroimaging data in older adults without Alzheimer's disease to investigate the factors involved in the spread of tau at the earliest stages of pathology accumulation. First, we measure resting state functional connectivity between hippocampus and medial parietal cortex to show that greater connectivity strength along this pathway is associated with downstream tau pathology burden cross-sectionally, with consequences for memory function. Next, we identify networks of functional connectivity specific to either episodic memory or executive function, and show that these networks are altered by the presence of tau pathology before widespread neurodegeneration is evident. Finally, we show that baseline connectivity strength and AD pathology interact to predict longitudinal rate of tau pathology accumulation and rate of cognitive decline in a multicohort sample of cognitively unimpaired older adults. Together, this work reveals that functional connectivity can be used to better understand the extent and distribution of the earliest tau accumulation, and outlines what effects this accumulation has on changes in functional brain networks and the cognitive domains they support.

Table of Contents

Abstract.....	1
Table of Contents	i
Acknowledgements.....	ii
Introduction.....	iii
Chapter 1: Hippocampal connectivity with retrosplenial cortex is linked to neocortical tau accumulation and memory function.....	1
Abstract.....	2
Significance Statement.....	3
Introduction.....	4
Materials and Methods.....	5
Results.....	8
Discussion.....	15
Conclusion	17
Supplementary Materials	18
Foreword for Chapter 2.....	21
Chapter 2: Behaviorally meaningful functional networks mediate the effect of Alzheimer’s pathology on cognition.....	22
Abstract.....	23
Introduction.....	24
Materials and Methods.....	25
Results.....	29
Discussion.....	36
Supplementary Materials	39
Foreword for Chapter 3.....	43
Chapter 3: Pathology-connectivity interactions in unimpaired older adults predict longitudinal tau spatial progression	44
Abstract.....	45
Introduction.....	46
Methods.....	47
Results.....	51
Discussion.....	58
Conclusion	60
Supplementary Materials	61
Conclusion	65
References.....	66

Acknowledgements

I would like to extend my utmost thanks to my advisor William Jagust for inspiring me as a scientist and a mentor. I have learned so much about how to think like a scientist from Dr. Jagust, but even more than this he is a role model for how to be an exemplary academic: eternally curious and eternally kind. Throughout my career, I will strive to embody the respect that Dr. Jagust extends to colleagues, mentees, and students alike. I would also like to thank the many graduate students, postdocs, and scientists of the Jagust lab I have worked with and learned from over the years, including Jenna Adams, Tessa Harrison, Susan Landau, Suzanne Baker, Joe Winer, Joseph Giorgio, Xi Chen, Cecille Tissot, Samira Maboudian, Corrina Fonseca, and many others. They all have inspired and supported me more than I can express.

I would like to thank the graduate students, faculty, and administrators of the Helen Wills Neuroscience Institute at UC Berkeley, in particular my dissertation committee members Kevin Wiener, Daniela Kaufer, and Kristopher Bouchard for their guidance, mentorship, and invaluable scientific expertise. I also have so much gratitude for my cohort of neuroscience PhD students, the “Bananas in the Ocean”, and the neuroscience ultimate frisbee team “Hell on Wheels”, who each in their own way made each step of this process easier and more enjoyable, reminding me why I love scientists and the community that we create for each other.

Finally, I want to thank my family for their unending support, especially my parents Sue and Martin, my brother Aaron, and my late grandmother Charlotte, who I know would have been so proud of me for this accomplishment. And to my partner Emily, thank you for being a role model for me in so many ways, not the least of which is how to get a PhD while holding onto at least some of one’s sanity.

Introduction

Alzheimer's disease (AD) is a devastating neurodegenerative condition that accounts for or contributes to between 60-80% of all dementias worldwide¹, and exacts an immense emotional and financial toll on patients, caregivers, loved ones, and society more broadly. The disease can present clinically as a number of different subtypes and variants with different pathophysiological trajectories, but the most common type is sporadic late-onset AD, which can have a prodromal period of up to 20 years before cognitive deficits rise to the level of diagnosis². Though there is currently no cure or proven way to prevent the disease, a number of recent advances have raised the possibility of detecting and treating the disease early enough to have a meaningful impact on the lives of those affected by it. Reliable blood serum tests for AD pathological protein have been developed that are able to detect the presence of AD biomarkers prior to clinical diagnosis³, and several monoclonal antibody anti-amyloid therapies have recently been approved by the FDA that show promise in slowing the cognitive decline stemming from the disease⁴. Despite these advances, it is still relatively unknown what factors cause AD pathological protein to deposit throughout the brain in some individuals, and what the precise ties are between the accumulation of this pathology and resulting cognitive decline.

The hallmark neuropathologies of Alzheimer's disease (AD) are fibrillar beta-amyloid (A β) plaques and neurofibrillary tangles of hyperphosphorylated tau protein. A β plaques tend to accumulate in a diffuse manner across the cortex, whereas tau pathology tends to be localized originally within medial temporal lobe before accumulating in a stereotyped pattern in progressive neocortical areas, particularly in late-onset sporadic AD⁵. Most older adults display some degree of tau pathology confined to medial temporal lobe structures such as entorhinal cortex and hippocampus⁶, correlated with subtle changes in cognition⁷⁻⁹. However, the accumulation of tau pathology outside of medial temporal lobe in proximate structures of the neocortex marks a transition from healthy aging to AD, with consequences for cognitive function such as episodic memory and executive function that eventually lead to mild cognitive impairment and dementia¹⁰. Despite a variety of evidence from the staging of postmortem brain tissue characterizing the stereotyped accumulation of tau pathology, relatively little is known about the processes that facilitate the transition from the preclinical stage to the widespread neuropathology characteristic of AD. Investigation into these mechanisms provides greater insight into the risk factors that lead to the accumulation of tau pathology in AD, and may reveal potential targets for therapeutic intervention.

The advent of functional neuroimaging methods at the outset of the 21st century led to the characterization of so-called "intrinsic functional connectivity networks", networks of brain regions with correlated neural activity thought to underlie cognitive processes of the brain¹¹. This area of investigation was linked with neurodegenerative research by the striking observation that the spatial topography of these networks tends to overlap with patterns of AD syndrome-specific regional atrophy¹². In other words, individuals with different behavioral variants of AD tended to exhibit selective neurodegeneration in the same regions that tend to be functional coactive. Over time, this observation has led to the view that the stereotypical pattern of tau pathology accumulation may be due to transneuronal spread of this pathology throughout the brain along pathways of functional and/or structural connectivity, rather than arising spontaneously in areas of high metabolic activity as has also been suggested^{13,14}. The theory of transneuronal spread of tau has been corroborated by studies *in vitro* and in animal models showing activity-mediated spread of tau pathology from cell to cell¹⁵⁻¹⁸, and from variety of functional neuroimaging

evidence in living human participants showing that regions of high functional connectivity from medial temporal lobe tau epicenters also tend to covary in tau pathology burden^{13,19–25}. Despite accumulating evidence for tau pathology propagation along functional pathways in the brain, it is still not understood what factors facilitate the spread of this tau pathology at the earliest stages of disease, and why certain brain regions tend to be more vulnerable to tau pathology spread.

In this work, we outline both the ways in which functional brain networks in the aging brain contribute to Alzheimer’s disease pathology, as well as the reciprocal consequences of this pathology accumulation for functional networks and cognitive function. In Chapter 1, we show that a pathway of common connectivity between the medial temporal and medial parietal lobe exhibits greater downstream tau pathology burden for individuals with greater functional connectivity strength, with consequences for episodic memory function. In Chapter 2, we use a novel approach to identify behaviorally meaningful networks of brain regions that support cognitive domains such as memory and executive function and show that these networks may be impacted by the presence of tau pathology prior to the effects of widespread neurodegeneration. Finally in Chapter 3, we show that connectivity strength between hippocampus and key early areas of neocortical tau accumulation interacts with baseline AD pathology burden to predict the rate of tau accumulation and cognitive decline over time. Taken together, this work furthers our understanding of how features of functional brain networks at the individual level facilitate the spread of AD pathology to vulnerable regions of the brain, and how these networks play a critical role in the effects of AD pathology on cognition at the earliest stages of disease.

Chapter 1: Hippocampal connectivity with retrosplenial cortex is linked to neocortical tau accumulation and memory function

Jacob Ziontz¹, Jenna N. Adams¹, Theresa M. Harrison¹, Suzanne L. Baker², William J. Jagust^{1,2}.

¹ Helen Wills Neuroscience Institute, UC Berkeley, Berkeley, United States, 94720

² Molecular Biophysics and Integrated Bioimaging, Lawrence Berkeley National Laboratory, Berkeley, United States, 94720

Acknowledgments: R. La Joie assisted with selecting regions of interest and visualization of results. This work was supported by NIH grants T32-NS095939 (J.Z.), F31-AG062090 (J.N.A.), F32-AG057107 (to T.M.H.), R01-AG062542 (W.J.J.) and R01-AG034570 (W.J.J.), and by the Rainwater Charitable Foundation (W.J.J.). Avid Radiopharmaceuticals enabled the use and the ¹⁸F-Flortaucipir tracer but did not provide direct funding and were not involved in data analysis or interpretation.

Author Contributions: Study design - J.Z., J.N.A., W.J.J.; Data analysis - J.Z. Feedback and consultation - J.N.A., T.M.H.; Manuscript writing – J.Z., W.J.J.; PET imaging and methodology expertise – S.L.B.; Paper editing – all authors.

Published in Journal of Neuroscience (2021)

<https://doi.org/10.1523/JNEUROSCI.0990-21.2021>

Abstract

The mechanisms underlying accumulation of Alzheimer's disease (AD)-related tau pathology outside of the medial temporal lobe (MTL) in older adults are unknown but crucial to understanding cognitive decline. A growing body of evidence from human and animal studies strongly implicates neural connectivity in the propagation of tau in humans, but the pathways of neocortical tau spread and its consequences for cognitive function are not well understood. Using resting state fMRI and tau PET imaging from a sample of 97 male and female cognitively normal older adults, we examined MTL structures involved in medial parietal tau accumulation and associations with memory function. Functional connectivity between hippocampus and retrosplenial cortex, a key region of the medial parietal lobe, was associated with tau in medial parietal lobe. By contrast, connectivity between entorhinal and retrosplenial cortices did not correlate with medial parietal lobe tau. Further, greater hippocampal-retrosplenial connectivity was associated with a stronger correlation between MTL and medial parietal lobe tau. Finally, an interaction between connectivity strength and medial parietal tau was associated with episodic memory performance, particularly in the visuospatial domain. This pattern of tau accumulation thus appears to reflect pathways of neural connectivity, and propagation of tau from entorhinal cortex to medial parietal lobe via the hippocampus may represent a critical process in the evolution of cognitive dysfunction in aging and AD.

Significance Statement

The accumulation of tau pathology in the neocortex is a fundamental process underlying Alzheimer's disease. Here, we use functional connectivity in cognitively normal older adults to track the accumulation of tau in the medial parietal lobe, a key region for memory processing that is affected early in the progression of AD. We show that the strength of connectivity between the hippocampus and retrosplenial cortex is related to medial parietal tau burden, and that these tau and connectivity measures interact to associate with episodic memory performance. These findings establish the hippocampus as the origin of medial parietal tau and implicate tau pathology in this region as a crucial marker of the beginnings of Alzheimer's disease.

Introduction

Hyperphosphorylation of the microtubule-associated protein tau together with amyloid- β ($A\beta$) plaques represent the hallmark neuropathologies of Alzheimer's disease (AD). Early histopathology studies⁵ and more recent positron emission tomography (PET) imaging have characterized the distribution and extent of pathological tau burden in patients with AD as well as cognitively healthy older adults^{26,27}. Tau pathology has been observed to originate in the transentorhinal region, an area spanning the lateral entorhinal cortex and medial perirhinal cortex in humans^{28,29}, but its accumulation in cortical areas outside of the MTL, perhaps facilitated by $A\beta$ ³⁰, is often a feature of the earliest stages of AD.

A developing body of work investigating the mechanisms of tau accumulation supports the transsynaptic propagation of tau via coactive neurons. Studies *in vitro* and in animal models suggest that tau pathology can be transferred between synaptic connections, and that enhanced neuronal activity stimulates the release of pathological tau and increases downstream accumulation^{15,16,31}. In humans, transneuronal tau spread has been investigated by associating the topography of tau accumulation with measures of structural and functional connectivity^{19–21,25,32–34}. Connectivity measures between brain regions that exhibit early tau accumulation may therefore provide insights into the structures and processes involved in the spread of tau in aging and AD.

Tau appears to initially propagate to neocortex via connectivity with the anterolateral entorhinal cortex (alEC)¹⁹, but regions without strong structural connectivity to alEC such as the medial parietal lobe^{35,36} also develop tau pathology as AD progresses^{37,38}. Connectivity with other MTL structures that subsequently develop tau pathology, including the posteromedial entorhinal cortex (pmEC) and hippocampus, may thus underly tau spread into medial parietal lobe. This region also comprises a large part of the posterior medial (PM) memory network, which together with the anterior temporal (AT) memory network represent two distinct large-scale neocortical memory systems with separable anatomical and functional connectivity with the MTL that support different aspects of memory and cognitive function^{39,40}. Given the substantial increase in PM tau in mild cognitive impairment (MCI) and AD⁴¹, tau accumulation in regions of this memory system may be a key condition under which memory performance begins to worsen prior to the clinical presentation of disease.

In this study, we investigate how tau spreads from MTL to the medial parietal lobe using resting state functional magnetic resonance imaging (fMRI) in a sample of cognitively normal older adults. We measured functional connectivity between key MTL subregions (alEC, pmEC and hippocampus) and medial parietal lobe, and tested whether this connectivity was related to tau deposition in medial parietal lobe. Given strong structural connectivity between hippocampus and medial parietal lobe⁴², we hypothesized that the degree of functional connectivity with hippocampus would better predict tau burden in medial parietal lobe than functional connectivity with either entorhinal subregion. Because pmEC also demonstrates connectivity with some medial parietal areas³⁶ and alEC is the earliest cortical region of tau accumulation, we also tested whether these structures would also contribute to medial parietal tau. Further, we were interested in examining how connectivity between the MTL and medial parietal lobe was related to both the correspondence of tau between the two regions and to memory function. We hypothesized that MTL and medial parietal tau would be more correlated as functional connectivity between these regions increased, and that greater tau burden and functional connectivity together would be associated with worse memory performance.

Materials and Methods

Participants

To test these hypotheses, we included data from 97 male and female cognitively normal older adults from the Berkeley Aging Cohort Study. All participants underwent 3T structural MRI, and resting state 3T functional MRI, and a standard neuropsychological assessment. These participants also received tau PET imaging using ^{18}F -Flortaucipir (FTP) and $\text{A}\beta$ PET imaging using ^{11}C -Pittsburgh Compound B (PiB). Demographic information for all participants is shown in Table 1. There were 3 individuals who did not have PiB PET data available for analysis, and so were excluded from all analyses that adjusted for global $\text{A}\beta$ signal. We included only participants whose resting state fMRI data was collected within 146 days of their corresponding tau PET scan ($M = 42.5$, $SD = 37.9$). Additional inclusion criteria for this study were 60+ years of age, cognitively normal status (Mini Mental State Examination score ≥ 25 and normal neuropsychological examination, defined as within 1.5 SD s of age, education, and sex adjusted norms), no serious neurological, psychiatric, or medical illness, no major contraindications found on MRI or PET, and independent community living status. This study was approved by the Institutional Review Boards of the University of California, Berkeley, and the Lawrence Berkeley National Laboratory (LBNL). All participants provided written informed consent.

	Mean (SD) or n (%)	Range
Age (years)	76.4 (6.1)	60 – 93
Education (years)	16.8 (1.9)	12 – 20
MMSE	28.6 (1.3)	25 – 30
Global $\text{A}\beta$ PET	1.17 (0.25)	0.92 – 1.89
Sex (female)	58 (59.8%)	
$\text{A}\beta$ +	43 (45.7%)	
ApoE4+	28 (29.8%)	

Table 1. Participant characteristics. Demographic information for sample of 97 cognitively normal older adults including age, years of education, mini mental state examination (MMSE) score, global $\text{A}\beta$ PET signal, sex, $\text{A}\beta$ positivity status ($\text{A}\beta$ +), and apolipoprotein E positivity status (ApoE4+).

MRI acquisition

Structural and functional MRI data were acquired on a 3T TIM/Trio scanner (Siemens Medical System, software version B17A) using a 32-channel head coil. A T1-weighted whole brain magnetization prepared rapid gradient echo (MPRAGE) image was acquired for each subject (voxel size = 1mm isotropic, TR = 2300ms, TE = 2.98ms, matrix = 256 \times 240 \times 160, FOV = 256 \times 240 \times 160mm³, sagittal plane, 160 slices, 5 min acquisition time). Resting state functional MRI was then acquired using T2*-weighted echo planar imaging (EPI, voxel size = 2.6mm isotropic, TR = 1.067ms, TE = 31.2ms, FA = 45, matrix 80 \times 80, FOV = 210mm, sagittal plane, 300 volumes, anterior to posterior phase encoding, ascending acquisition, 5 min acquisition time). During resting state acquisition, participants were told to remain awake with eyes open and focused on a white asterisk displayed on a black background.

MRI preprocessing

Structural T1-weighted images were processed using Statistical Parametric Mapping (SPM12). Images were first segmented into gray matter, white matter, and cerebral spinal fluid (CSF) components in native space. DARTEL-imported tissue segments for all individuals in the sample were used to create a study-specific template, which was then used to warp native space T1 images and tissue segments to MNI space at 2mm isotropic resolution. Finally, native space T1 images were segmented with Freesurfer v.5.3.0 using the Desikan-Killiany atlas parcellation⁴³.

Resting state fMRI images were preprocessed using a standard SPM12 pipeline. Slice time correction was first applied to adjust for differences in acquisition time for each brain volume. Then, all echo planar images (EPIs) were realigned to the first acquired EPI, and translation and rotation realignment parameters were output. Each EPI was next coregistered to each individual's native space T1 image. Next all resting state EPIs and structural images were warped to the study-specific DARTEL template in 2mm isotropic MNI space from structural preprocessing. Unsmoothed fMRI data in MNI space was used to extract the time series correlation of all ROI seeds used in these analyses.

Regions of interest

We defined regions of interest (ROIs) for these analyses to examine the association of functional connectivity between these areas and tau burden. Most were obtained from the FreeSurfer segmentation of each participant's native space 3T structural image⁴³, including hippocampus (HC), retrosplenial cortex (RsC), posterior cingulate cortex (PCC), precuneus (PrC), whole entorhinal cortex (EC), and inferior temporal cortex (IT). In the case of RsC, we used the FreeSurfer region analog labeled as "isthmus cingulate." The composite medial parietal lobe ROI used throughout this study consisted of the RsC, PCC, and PrC regions. To test neocortical connectivity with HC outside of the medial parietal lobe, we also identified a region in the superior frontal gyrus (SFG) analogous to the medial portion of Brodman Area 10, labeled as A10m in the Brainnetome atlas parcellation⁴⁴.

Anterolateral entorhinal cortex and pmEC were defined in a previous study with high-resolution 7T MRI⁴⁵. In brief, anatomical borders of the entire entorhinal cortex were manually defined on a high-resolution T1-group template. Multivariate classification in a group of young adults was used to then identify clusters of voxels within this mask that showed preferential functional connectivity with perirhinal cortex, comprising the aIEC ROI, or with the parahippocampal gyrus, comprising the pmEC ROI. These aIEC and pmEC ROIs were then warped to a 2mm isotropic MNI template and made publicly available. In this study, we used these bilateral MNI space ROIs in our functional connectivity analyses. Because these regions are in close spatial proximity to one another, we extracted time series from the unsmoothed, denoised MNI space resting state data to avoid smoothing signal from each seed into each other.

To address signal dropout in the identified ROIs, we derived an explicit mask to remove regions of low signal across the whole brain. This mask was defined by calculating the mean functional MNI space image across all individuals, restricted to a group level grey matter mask. We then excluded voxels with less than 40% of the mean signal intensity of the image. Using this mean signal intensity threshold mask, a mean of 15.8% of voxels ($SD = 11.9\%$) were removed across all ROIs with the highest proportion of voxels being removed from the A10m region (34.8%).

Functional connectivity analyses

Seed-to-seed functional connectivity was assessed using the CONN functional connectivity toolbox (version 17e)⁴⁶ implemented in MATLAB version 2019b (The Mathworks Inc., Natick, MA). ART motion detection was first performed to identify volumes of high motion, using a movement threshold of $> 0.5\text{mm/TR}$ and a global intensity z-score of 3. Outlier volumes were flagged and included as spike regressors during denoising. No individuals were excluded from these analyses due to excess motion, as all participants had $< 20\%$ of outlier volumes ($M = 5.0\%$, $SD = 3.4\%$). Denoising was then performed with translation and rotation realignment parameters and their first-order derivatives, as well as anatomical CompCor (first five components of time series signal from white matter and CSF). A band pass filter of 0.008-0.1 Hz and linear detrending were then applied to the residual time-series.

We constructed a model of functional connectivity between each of three MTL regions (alEC, pmEC, and HC) and medial parietal lobe using bilateral ROIs. Within the medial parietal lobe, we identified the retrosplenial cortex as a region where tau is thought to spread to the neocortex via the MTL²⁹ and with known structural and functional connectivity with MTL^{36,39,42}. Semipartial correlations and unsmoothed data were used to minimize spillover of signal between adjacent MTL regions. Connectivity strength was defined as β -weights from region-to-region semipartial correlations adjusted for age and sex.

PET acquisition and processing

PET was acquired for all participants at LBNL. Tau accumulation was assessed with FTP synthesized at the Biomedical Isotope Facility at LBNL as previously described²⁷. Data were collected on a Biograph TruePoint 6 scanner (Siemens, Inc) 75-115 min post-injection in listmode. Data were then binned into 4 x 5 min frames from 80-100 min post-injection. CT scans were performed before the start of each emission acquisition. A β burden was assessed using ¹¹C-Pittsburgh Compound B (PiB), also synthesized at the Biomedical Isotope Facility at LBNL⁴⁷. Data were collected on the Biograph scanner across 35 dynamic frames for 90 min post-injection and subsequently binned into 35 frames (4 x 15, 8 x 30, 9 x 60, 2 x 180, 10 x 300, and 2 x 600s), and a computed tomography (CT) scan was performed. All PET images were reconstructed using an ordered subset expectation maximization algorithm, with attenuation correction, scatter correction, and smoothing with a 4mm Gaussian kernel.

Processing of FTP images was carried out in SPM12. Images were realigned, averaged, and coregistered to 3T structural MRIs. Standardized uptake value ratio (SUVR) images were calculated by averaging mean tracer uptake over the 80-100 min data and normalized with an inferior cerebellar gray reference region⁴⁸. The mean SUVR of each ROI (structural MRI FreeSurfer segmentation) was extracted from the native space images. This ROI data was partial volume corrected using a modified Geometric Transfer Matrix approach⁴⁹ as previously described⁴⁸. SUVR images were then warped to 2mm MNI space for voxelwise analyses using the study-specific DARTEL template produced from structural data (see above). No additional spatial smoothing was applied. PiB images were also realigned using SPM12. An average of frames within the first 20 min was used to calculate the transformation matrix to coregister the PiB images to the participants' 3T structural MRI; this transformation matrix was then applied to all PiB frames. Distribution volume ratio (DVR) images were calculated with Logan graphical analysis over 35-90 min data and normalized to a whole cerebellar gray reference region^{50,51}. Global A β was calculated across cortical FreeSurfer ROIs as previously described⁵², and a threshold of $DVR > 1.065$ was used to categorize participants as A β -positive or A β -negative. In

addition, mean DVR within each FreeSurfer ROI was extracted from coregistered, MNI space PiB images.

Tau PET quantification

To quantify tau deposition, we used the proportion of voxels above an *a priori* threshold of $SUVR > 1.4$ for FTP PET signal. This threshold has been shown to be a reliable marker of AD-related tau pathology, outperforming other thresholds in discriminating between A β - older adults and MCI/AD individuals³⁷. This suprathreshold measure has also been used in previous investigation of the relationship between functional connectivity and tau accumulation¹⁹. Another distinct advantage of using suprathreshold signal over mean SUVR is that it is not confounded by differing number of voxels within ROIs. To calculate this suprathreshold tau measure for each individual, we computed the number of suprathreshold FTP voxels within each ROI and divided by the total number of voxels in the region. In MTL and particularly hippocampus however, measuring tau is challenging given the confound of signal contamination from off-target FTP binding in choroid plexus. To address this, we quantified hippocampal tau using Rousset geometric transfer matrix partial volume corrected FTP SUVR, which minimizes choroid plexus spillover⁴⁸. As an additional precaution, we adjusted for choroid plexus FTP signal in regression analyses using this hippocampal tau signal.

Neuropsychological assessment

To assess episodic memory in our sample of cognitively normal older adults, we used neuropsychological assessment data collected closest in time to each individual's tau scan. There was a mean of 84.2 days ($SD = 56.9$) between each individual's cognitive assessment and tau PET scan. We computed an episodic memory composite measure by averaging the z-transformed individual test scores using mean and SD from the sample^{7,53} for four different tasks. These tasks were the California Verbal Learning Test (CVLT) immediate free recall, CVLT long-delay free recall, Visual Reproduction I (immediate recall), and Visual Reproduction II (delayed recall). We analyzed distinct verbal and visuospatial episodic memory components by considering performance in CVLT and Visual Reproduction tasks separately.

Experimental Design and Statistical Analyses

Functional connectivity analyses were carried out in the CONN functional connectivity toolbox (version 17e). Semipartial correlations were used for all first-level analyses to compute the time series correlation for all voxels of each ROI, controlling for the variance of all other ROIs entered into the same model. Statistically significant functional connectivity was determined by extracting β -weights from region-to-region semipartial correlations adjusted for age and sex. A one-sample t-test was then conducted on these β -values to test if connectivity between ROI pairs was significantly different from 0 (two-tailed, FDR corrected $p < 0.05$). Multivariate linear regression analyses were carried out in R (version 3.6.3) with a two-tailed significance level of $\alpha = 0.05$ throughout. All regression analyses were adjusted for age at time of tau scan, sex, and mean global A β burden. Analyses involving cognitive test performance were additionally adjusted for years of education and practice effects, quantified as the square root of the number of prior testing occasions⁵⁴. All models including interactions used mean-centered values for independent variables.

Results

Hippocampus exhibits strong resting state functional connectivity with retrosplenial cortex

We first investigated which structures of the MTL exhibit resting state functional connectivity with retrosplenial cortex, focusing on three regions of interest within MTL: alEC, pmEC, and hippocampus (Figure 1a). We observed significant functional connectivity between

hippocampus and retrosplenial cortex ($\beta = 0.45, p < 0.001$), as well as between pmEC and retrosplenial cortex ($\beta = 0.07, p = 0.007$). We directly compared the connectivity of these two pathways and found that hippocampal-retrosplenial (HC-RsC) connectivity was significantly greater than pmEC-RsC connectivity (two-tailed paired samples $t(96) = 15.74, p < 0.001$). By contrast, no significant connectivity was observed between alEC and retrosplenial cortex ($\beta = 0.00, p = 0.891$). Thus, hippocampus and to a lesser extent pmEC, but not alEC, exhibited resting state functional connectivity with retrosplenial cortex in our sample of cognitively normal older adults (Figure 1b).

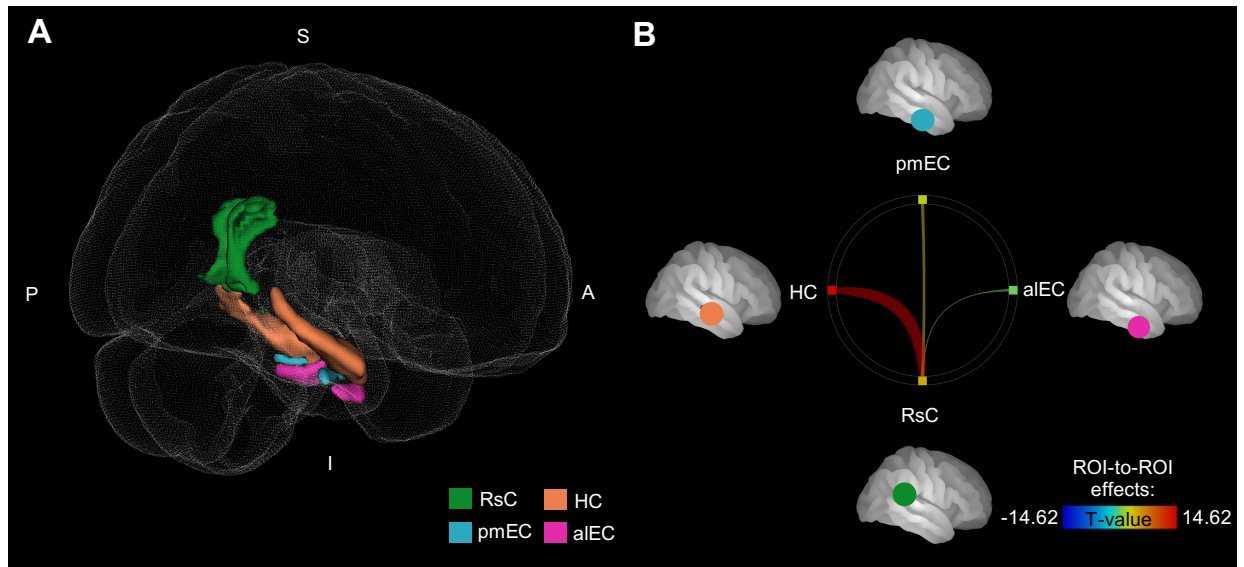


Figure 1. Hippocampus exhibits strong resting state functional connectivity with retrosplenial cortex. (A) Regions of interest for functional connectivity analysis. Anterolateral entorhinal cortex (alEC), posteromedial entorhinal cortex (pmEC), and hippocampus (HC) were included from MTL, as well as retrosplenial cortex (RsC). (B) RsC exhibits functional connectivity with HC and pmEC, but not alEC. Line color and thickness correspond to T-statistic of one-sample t-test of β values. See Figure S1 for resting state connectivity with superior frontal gyrus and association with medial parietal tau.

Hippocampal-retrosplenial connectivity strength is related to medial parietal tau pathology

Having observed strong functional connectivity between MTL and retrosplenial cortex, we next sought to investigate the extent to which this connectivity is associated with tau pathology in a medial parietal lobe composite region comprising the retrosplenial cortex, precuneus, and posterior cingulate cortex. To visualize this tau signal, we computed the proportion of participants above threshold in each voxel of the composite region (Figure 2a). Adjusting for age, sex, and global A β PET signal, we found that HC-RsC connectivity strength was associated with suprathreshold tau in the medial parietal lobe ($\beta = 0.145, p = 0.004$; Figure 2b). From this same model, global A β was also associated with suprathreshold medial parietal tau ($\beta = 0.113, p = 0.014$). In contrast with HC-RsC connectivity, neither alEC-RsC ($\beta = 0.120, p = 0.145$) nor pmEC-RsC connectivity strength ($\beta = 0.015, p = 0.842$) were associated with medial parietal lobe tau (Figure 2c-d) adjusting for age, sex, and global A β . In a separate model, we further examined whether individuals with more global A β exhibited a stronger relationship

between HC-RsC and medial parietal tau. Adjusting for age and sex, we did not observe a significant interaction between HC-RsC connectivity and global A β ($\beta = 0.442, p = 0.141$).

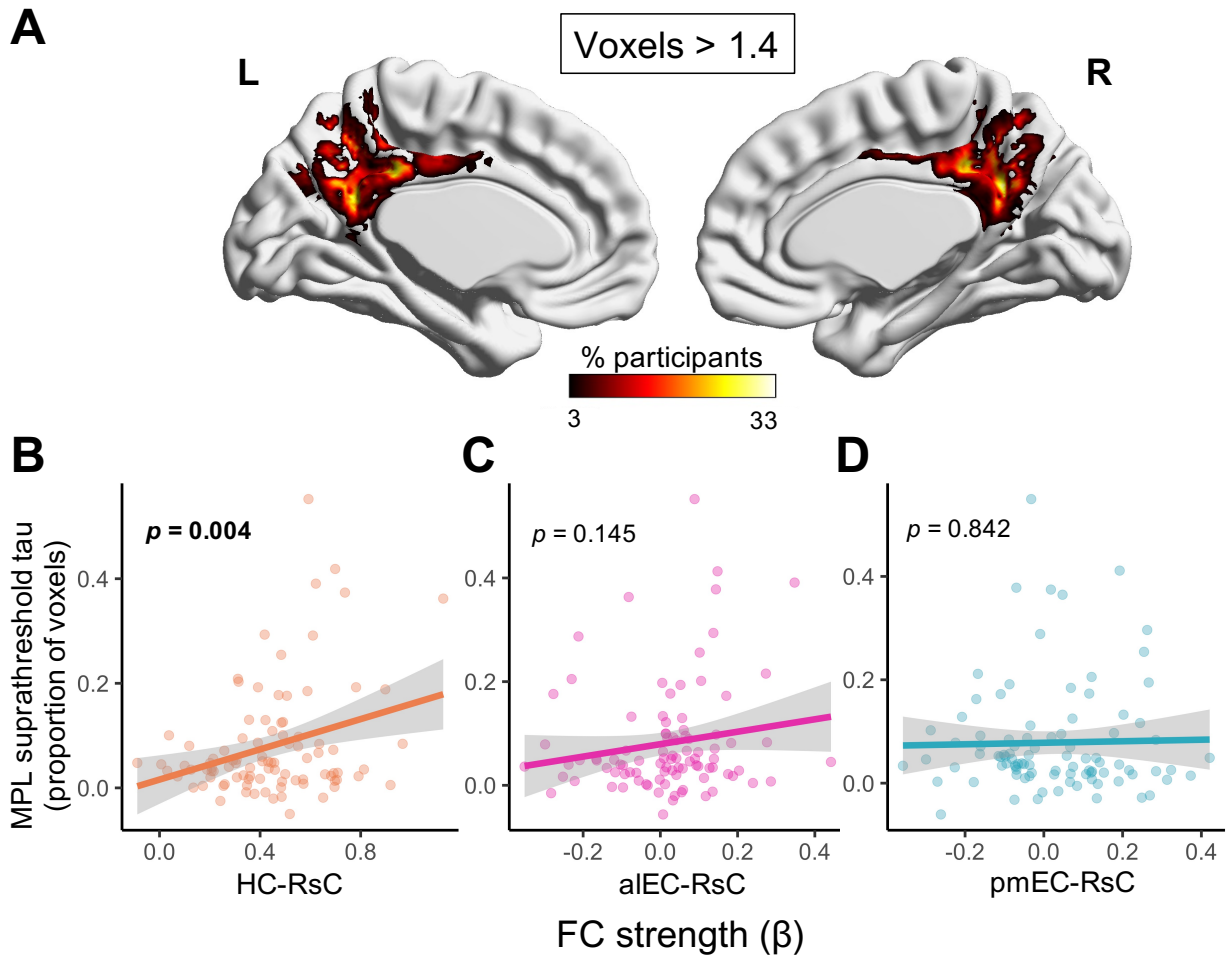


Figure 2. Hippocampal-retrosplenial connectivity strength is related to medial parietal tau pathology. (A) Percent of participants above tau threshold (FTP SUVR > 1.4) for each voxel in medial parietal lobe (MPL) region comprising retrosplenial cortex, precuneus, and posterior cingulate cortex. (B) Adjusting for age, sex, and global beta amyloid (A β), hippocampal-retrosplenial (HC-RsC) resting state functional connectivity strength is associated with mean suprathreshold tau within MPL. MPL suprathreshold tau defined as proportion of voxels above threshold within composite region. (C) aIEC-RsC and (D) pmEC-RsC connectivity strength are not associated with MPL tau. Significance value for each plot corresponds to effect of each term from linear regression model. Functional connectivity (FC) strength quantified as β -values from semipartial correlations between regions. See Figure S2 for association between HC-RsC connectivity and tau outside of medial parietal lobe, as well as medial parietal A β .

To confirm that the relationship between HC-RsC connectivity and medial parietal tau was specific to retrosplenial cortex and not a general effect of strong resting state functional connectivity, we identified a control region within the SFG analogous to the medial portion of Brodmann area 10 from the Brainnetome Atlas⁴⁴. Like retrosplenial cortex, this region is known to be part of the default mode network but does not have extensive structural connections with

hippocampus and exhibited low signal dropout in our sample. Similar to retrosplenial cortex, we observed significant resting state functional connectivity between hippocampus and SFG ($\beta = 0.40, p < 0.001$), though not between SFG and aIEC ($\beta = 0.02, p = 0.439$) or pmEC ($\beta = -0.02, p = 0.379$; Figure S2a). However, in contrast with retrosplenial cortex, we did not observe an association between the strength of hippocampus-SFG connectivity and medial parietal lobe tau ($\beta = 0.006, p = 0.907$; Figure S2b).

We further wanted to verify that connectivity between hippocampus and retrosplenial cortex was associated specifically with tau in medial parietal lobe and not also in other early tau-accumulating regions. To this end, we examined tau within entorhinal cortex and inferior temporal cortex, a region frequently used as a marker for early tau accumulation in aging^{55,56}. Again adjusting for age, sex, and global A β , we found that HC-RsC connectivity was not associated with suprathreshold tau in the entorhinal cortex ($\beta = -0.017, p = 0.843$; Figure 2-2a). Though suprathreshold tau in medial parietal lobe and inferior temporal cortex were highly correlated ($r = 0.796, p < 0.001$), HC-RsC was only associated at trend level with inferior temporal tau ($\beta = 0.150, p = 0.082$; Figure 2-2b). Finally, to confirm that the relationship between connectivity and pathology was specific to tau, we examined the association between HC-RsC and A β burden in the medial parietal lobe. Adjusting for age and sex, HC-RsC connectivity was not associated with medial parietal lobe A β PET signal ($\beta = 0.172, p = 0.193$; Figure 2-2c). Taken together, these results demonstrate the specificity of tau pathology accumulation in medial parietal lobe via direct connectivity with hippocampus in cognitively unimpaired older adults.

Hippocampal-retrosplenial connectivity strengthens tau correspondence

To further examine the role of functional connectivity in the accumulation of tau pathology from MTL, we tested whether HC-RsC connectivity strength modulated how closely MTL tau corresponded with medial parietal lobe tau. Adjusting for age, sex, global A β , and choroid plexus FTP signal, there was a significant main effect of hippocampal tau ($\beta = 0.263, p < 0.001$) as well as a main effect of HC-RsC ($\beta = 0.123, p = 0.005$) on medial parietal lobe suprathreshold tau (Table 2). Critically, we also observed an interaction between hippocampal tau and HC-RsC connectivity ($\beta = 0.607, p = 0.008$; Figure 3) such that there was a stronger association between MTL and medial parietal lobe tau with greater functional connectivity between these regions. To further verify that choroid plexus spillover into hippocampus was not driving these results, we replicated this analysis using partial volume corrected entorhinal tau PET, and found a trend-level interaction between entorhinal tau and HC-RsC in predicting medial parietal tau ($\beta = 0.357, p = 0.073$; Figure S3). Because tau in entorhinal cortex and hippocampus were highly correlated with one another ($r = 0.719, p < 0.001$), it is not surprising that using entorhinal tau yielded a similar result, and suggests that contamination of hippocampal signal from non-specific choroid plexus FTP binding is likely not driving this finding.

Independent variables	Dependent variable: MPL suprathreshold tau
age	$\beta = -0.002, p = 0.321$
sex	$\beta = 0.007, p = 0.708$
global A β	$\beta = 0.050, p = 0.241$
choroid plexus signal	$\beta = -0.012, p = 0.208$
hippocampus mean tau	$\beta = 0.263^{***}, p < 0.001$
HC-RsC FC strength	$\beta = 0.123^{**}, p = 0.005$
hippocampus mean tau x HC-RsC FC strength	$\beta = 0.607^{**}, p = 0.008$
Constant	$\beta = 0.066, p = 0.281$

Table 2. Summary of model results with medial parietal tau as outcome. Effects from linear regression model examining the relationship between medial parietal lobe (MPL) suprathreshold tau and age, sex, global A β , choroid plexus signal (partial volume corrected FTP SUVR), hippocampus mean tau (partial volume corrected FTP SUVR), hippocampal-retrosplenial (HC-RsC) functional connectivity (FC) strength, and hippocampus mean tau x HC-RsC FC strength interaction. Bolded term indicates interaction effect visualized in Figure 3. See Table S1 for model results using FTP SUVR from entorhinal cortex instead of hippocampus.

* $p < 0.05$; ** $p < 0.01$; *** $p < 0.001$.

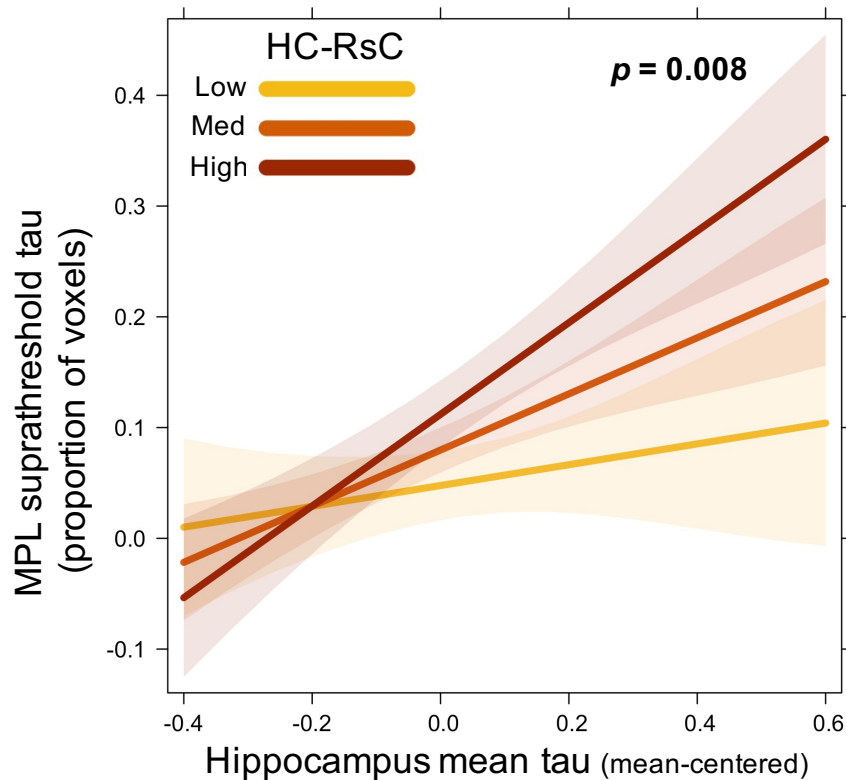


Figure 3. Hippocampal-retrosplenial connectivity modulates the relationship between medial temporal and medial parietal tau. Visualization of interaction between hippocampus mean tau (partial volume corrected FTP SUVR) and hippocampal-retrosplenial functional connectivity strength (HC-RsC) from linear regression model (see Table 2). Medial parietal lobe (MPL) suprathreshold tau is associated with a hippocampal tau x HC-RsC interaction. Plot displays the relationship predicted by linear regression at low (10th percentile), median, and high (90th percentile) HC-RsC. See Figure S3 for visualization of the same interaction effect using FTP SUVR from entorhinal cortex in place of hippocampus.

Episodic memory is related to an interaction between tau and connectivity

We next sought to test if connectivity and tau might also interact to associate with episodic memory performance. Adjusting for age, years of education, practice effects, and global A β , we did not observe a significant main effect of either medial parietal lobe tau ($\beta = 1.111, p = 0.318$) or HC-RsC connectivity ($\beta = 0.073, p = 0.861$) on episodic memory. Critically, there was a significant interaction between medial parietal tau and hippocampal-retrosplenial connectivity ($\beta = -9.482, p = 0.018$), such that episodic memory performance was poorest when both medial parietal tau and hippocampal-retrosplenial connectivity were greatest (Table 3). Examining episodic memory subdomains separately, the interaction between medial parietal tau and hippocampal-retrosplenial connectivity was significantly associated with visuospatial memory performance ($\beta = -12.016, p = 0.006$; Figure 4a), but not verbal memory performance ($\beta = -6.933, p = 0.145$; Figure 4b).

Independent variables	Dependent variable: Episodic memory composite
age	$\beta = -0.048^{**}, p = 0.005$
sex	$\beta = -0.105, p = 0.540$
years education	$\beta = 0.037, p = 0.420$
practice effects	$\beta = 0.253^*, p = 0.019$
global A β	$\beta = -0.308, p = 0.395$
MPL suprathreshold tau	$\beta = 1.130, p = 0.284$
HC-RsC FC strength	$\beta = 0.079, p = 0.843$
MPL suprathreshold tau x HC-RsC FC strength	$\beta = -9.531^*, p = 0.018$
Constant	$\beta = 0.139, p = 0.772$

Table 3. Summary of model results with episodic memory performance as outcome. Effects from linear regression model examining the relationship between episodic memory performance (California Verbal Learning Test immediate and long-delay free recall, Visual Reproduction immediate and delay recall) and age, years of education, practice effects (see Materials & Methods), global A β , MPL suprathreshold tau, HC-RsC FC strength, and MPL suprathreshold tau x HC-RsC FC strength interaction. Bolded term indicates interaction effect visualized in Figure 4. * $p < 0.05$; ** $p < 0.01$; *** $p < 0.001$.

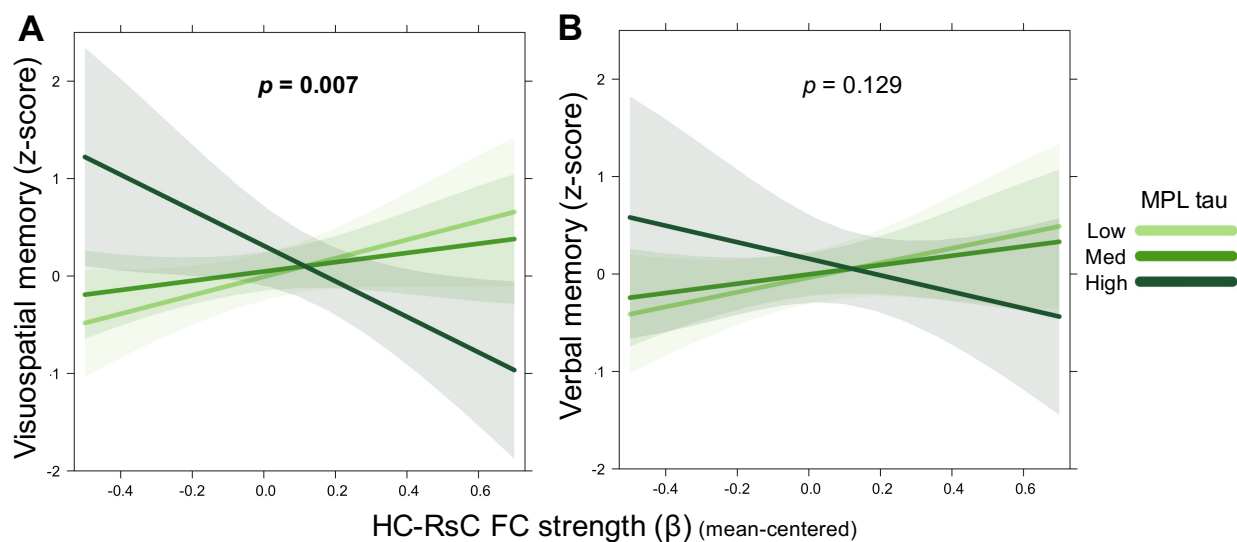


Figure 4. Episodic memory performance is associated with the interaction of hippocampal-retrosplenial connectivity and medial parietal tau. Visualization of interaction between hippocampal-retrosplenial (HC-RsC) functional connectivity (FC) strength (beta value) and medial parietal lobe (MPL) suprathreshold tau in relation to visuospatial and verbal memory, adjusting for age, sex, years of education, practice effects, and global $A\beta$. (A) Visuospatial memory (Visual Reproduction immediate and delay recall) is associated with the interaction of MPL tau and HC-RsC FC strength. (B) Verbal memory (CVLT immediate and long delay free recall) does not exhibit a significant interaction. Plots display the relationship predicted by linear regression at low (10th percentile), median, and high (90th percentile) MPL suprathreshold tau.

Discussion

In this study of cognitively unimpaired older adults, we measured functional connectivity between the MTL and medial parietal lobe using resting state fMRI and examined tau and $A\beta$ pathology with PET imaging. Overall, our findings suggest that AD-related tau accumulates in medial parietal lobe via connectivity with hippocampus, and that this may reflect early disruption of memory processing via tau spread. A growing literature has linked patterns of resting state functional connectivity to greater tau accumulation and correspondence of tau between these regions^{19,20}. Though recent data suggest heterogeneity in patterns of tau deposition in patients with AD, these distinct profiles all include medial parietal lobe as a vulnerable region⁵⁷. Further, computational modeling of tau spread using functional connectivity closely resembles the observed pattern of tau deposition in the brain^{25,32}. Our finding that connectivity between retrosplenial cortex and hippocampus, but not aIEC or pmEC, was associated with medial parietal tau suggests that tau originating in MTL accumulates in hippocampus before later spreading directly to medial parietal lobe via connectivity with retrosplenial cortex. Because pmEC-RsC connectivity was weaker than HC-RsC connectivity and did not correlate with medial parietal tau, it is not likely to be the primary structure involved in the propagation of tau to this region despite connectivity with several posterior medial areas^{19,58}.

Instead, tau may spread to aIEC-connected neocortex and hippocampus at a comparable rate, later accumulating in medial parietal areas with connections to the hippocampus. This is consistent with histopathological data indicating that although the earliest cortical region to exhibit tau pathology is the aIEC/transentorhinal area^{28,59}, tau is typically observed in

hippocampus prior to limbic areas such as the retrosplenial region²⁹. Our findings also corroborate recent work that found that structural connectivity between hippocampus and posterior cingulate cortex (PCC) was associated with tau pathology in PCC³³. Importantly, our finding of greater correspondence between hippocampal and medial parietal tau with greater HC-RsC connectivity strength further suggests that neural connectivity may reflect patterns of tau to spread from early-accumulating regions to connected downstream areas.

The specificity of this key finding in our study is striking. The lack of association between HC-RsC connectivity and tau in entorhinal cortex suggests this connectivity is specifically related to tau in the downstream medial parietal region of this pathway. Though the inferior temporal cortex is one of the first areas of neocortical tau pathology and is often used as a marker of AD disease progression^{55,56}, we found the strength of HC-RsC connectivity was only associated at trend level with tau in this region. In addition, functional connectivity between hippocampus and the superior frontal gyrus was significant but not associated with medial parietal tau, suggesting that functional connections with other brain areas are not related to tau in medial parietal lobe. We also did not find an association between HC-RsC and A β burden within medial parietal lobe, which is not surprising given that A β does not originate in the MTL and is not thought to spread in the same transneuronal manner as tau. Taken together, these results support the view that tau pathology in hippocampus spreads to medial parietal lobe in cognitively unimpaired older adults, reflected by resting state functional connectivity between these regions.

Some studies have in fact found a negative association between tau pathology and functional connectivity across the cortex^{55,60,61}, though these tended to use global measures of tau or focused on A β -positive individuals. However, our findings together with previous work help illustrate how the relationship between tau and connectivity may vary between different brain areas and time scales. Initially, greater connectivity within an individual pathway may facilitate the spread of tau from regions of early accumulation to downstream cortical areas, perhaps enhanced by the presence of A β . Over time, however, the influence of tau throughout this circuit leads to neurodegeneration and disruption of neuronal signaling, and tau pathology may in fact show an inverse correlation with functional connectivity. These distinct short- and long-term effects may help explain regional differences in the tau-connectivity relationship such that pathways of early tau propagation are first to show local degeneration, whereas later pathways, such as the MTL-medial parietal lobe, may concurrently demonstrate increased connectivity leading to further tau spread.

We also found that episodic memory performance, particularly visuospatial memory, was related to the combination of greater medial parietal lobe tau accumulation and greater HC-RsC strength. Because we did not observe a main effect of connectivity on memory, it does not appear likely that greater connectivity alone is related to worse cognition. However, the interaction between connectivity strength and medial parietal tau suggests that the presence of tau in conjunction with greater connectivity along this pathway may indeed be detrimental for memory performance. Existing work has yet to establish a clear relationship between memory performance and connectivity changes in aging. Greater functional connectivity between MTL and medial parietal areas is related to poorer memory performance both cross-sectionally and over time⁶¹. By contrast, a positive association has been reported between MTL-medial parietal connectivity and memory performance^{62,63}, though these studies did not include tau PET measures. Abnormal diffusivity of the hippocampal cingulum bundle has also been shown to be related to greater decline in memory performance in older individuals with high PCC tau and high A β ³³.

It may be that the propagation of tau, reflected by greater connectivity and correspondence of pathology between regions, is associated with the earliest deficits in cognitive function. Converging theoretical frameworks including the ‘molecular nexopathies’ paradigm have proposed that the conjunction of pathology and intrinsic circuit characteristics can lead to a state of mild peptide-dependent network disruption, marking the onset of neurodegenerative disease^{64,65} prior to widespread neurodegeneration and cascading network failure⁶⁶. Tau spread to the medial parietal lobe may be an indicator of consequences for the PM memory system, which while not affected by tau as early as the AT system may begin to be disrupted in MCI and AD⁴¹. It is also striking that we found a particularly strong association with visuospatial memory, given medial parietal areas have long been implicated in processing of spatial information^{67–69}. The representation of visuospatial context is also thought to be a key function of the PM memory system³⁹, and spatial information processing is one of the earliest-affected domains in cognitive aging and Alzheimer’s disease⁷⁰. Connectivity-mediated accumulation of tau may thus underlie the beginnings of cognitive decline in healthy older adults.

There are a number of limitations to the conclusions drawn from this study. The cross-sectional and correlational nature of these results means that caution is required in inferring a causal relationship between connectivity and tau spread. Still, in view of longitudinal studies showing that tau propagates to different regions over time via connectivity^{21,34}, our findings are consistent with a relationship that could be causal. In addition, though we adjusted for A β PET signal throughout this study, we did not find that the relationships described here were stronger in individuals with greater global A β burden. This was a somewhat surprising finding given a number of studies that have found a stronger association between tau and connectivity for those with greater A β pathology^{19,21,33}. It is possible that our sample did not provide us with enough statistical power to observe this interaction, though it was enriched to include nearly half A β -positive individuals. Further study is needed to assess the role of A β in the association between medial parietal lobe tau and functional connectivity in cognitively normal older adults.

Conclusion

The findings described here support the view that tau pathology accumulates in medial parietal lobe via direct connectivity with hippocampus in cognitively normal older individuals. Though the accumulation of tau pathology in MTL and even some areas of the AT network has been observed in older adults without cognitive impairment, tau spread into the PM network and subsequent domain-specific memory decline may reflect a significant transition between normal aging and the processes involved in Alzheimer’s disease. Future work with longitudinal data can help establish tau propagation into the medial parietal lobe as a crucial marker of the beginnings of Alzheimer’s disease.

Supplementary Materials

Independent variables	Dependent variable: MPL suprathreshold tau
age	$\beta = -0.002, p = 0.359$
sex	$\beta = 0.006, p = 0.791$
global A β	$\beta = 0.033, p = 0.527$
choroid plexus signal	$\beta = 0.006, p = 0.566$
entorhinal mean tau	$\beta = 0.139^{**}, p = 0.008$
HC-RsC FC strength	$\beta = 0.133^{**}, p = 0.006$
entorhinal mean tau x HC-RsC FC strength	$\beta = 0.357, p = 0.073$
Constant	$\beta = 0.017, p = 0.790$

Table S1. Summary of model results with medial parietal tau as outcome. Effects from linear regression model examining the relationship between medial parietal lobe (MPL) suprathreshold tau and age, sex, global beta amyloid (A β), choroid plexus signal (partial volume corrected FTP SUVR), entorhinal mean tau (partial volume corrected FTP SUVR), hippocampal-retrosplenial (HC-RsC) functional connectivity (FC) strength, and entorhinal mean tau x HC-RsC FC strength interaction. Bolded term indicates interaction effect visualized in Figure S3. * $p < 0.05$; ** $p < 0.01$; *** $p < 0.001$.

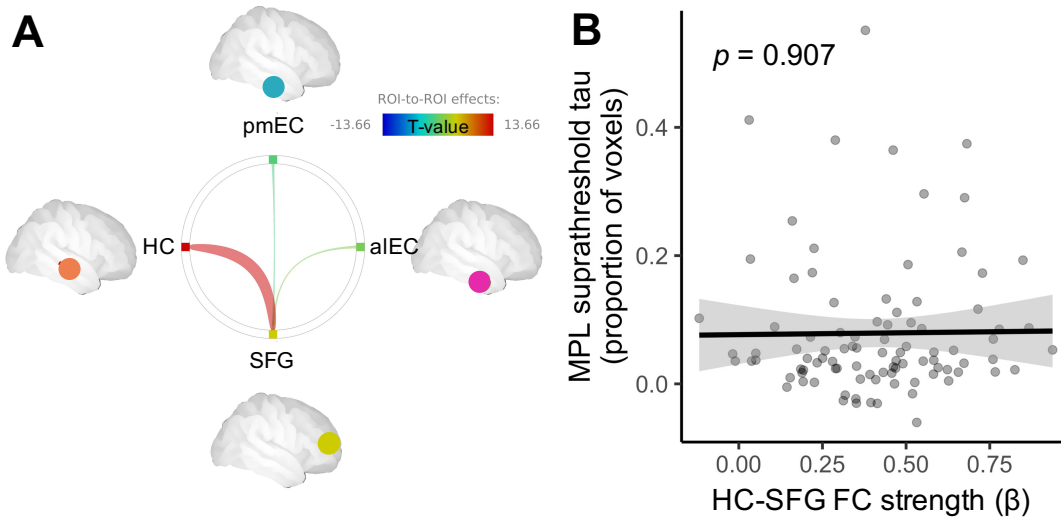


Figure S1. Hippocampal-superior frontal resting state functional connectivity is not associated with medial parietal lobe tau accumulation. (A) Superior frontal gyrus (SFG; medial portion of Brodmann Area 10) exhibits resting state functional connectivity with hippocampus ($\beta = 0.40$, $p < 0.001$), but not with pmEC ($\beta = -0.02$, $p = 0.379$) or alEC ($\beta = 0.02$, $p = 0.439$). Line color and thickness correspond to T-statistic of one-sample t-test of β values. (B) Adjusting for age, sex, and global A β , HC-SFG functional connectivity strength is not associated with proportion of voxels above threshold (SUVR > 1.4) within medial parietal lobe. Connectivity strength measured by extracting β -values of semipartial correlations between hippocampus and SFG.

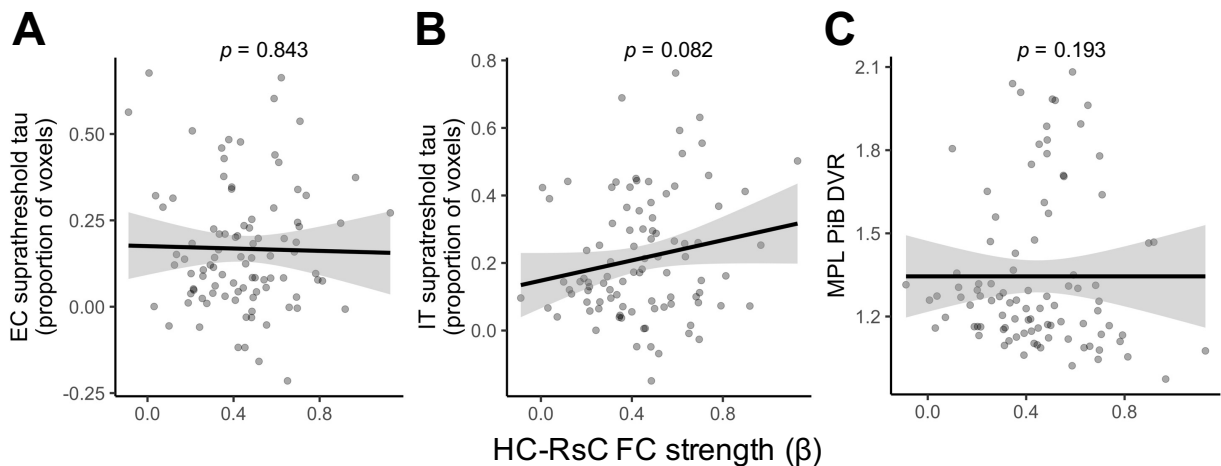


Figure S2. Hippocampal-retrosplenial resting state functional connectivity is specifically associated with medial parietal lobe tau accumulation. (A) HC-RsC is not associated with entorhinal cortex (EC) suprathreshold tau. (B) HC-RsC shows a trend-level association with inferior temporal (IT) suprathreshold tau. (C) HC-RsC is not associated with MPL A β measured by PiB PET DVR. Plots show residualized values from linear regression models adjusting for age, sex, and global A β . Connectivity strength measured by extracting β -values of semipartial correlations between HC and RsC. Suprathreshold tau defined as proportion of voxels above threshold (SUVR > 1.4) within each region of interest.

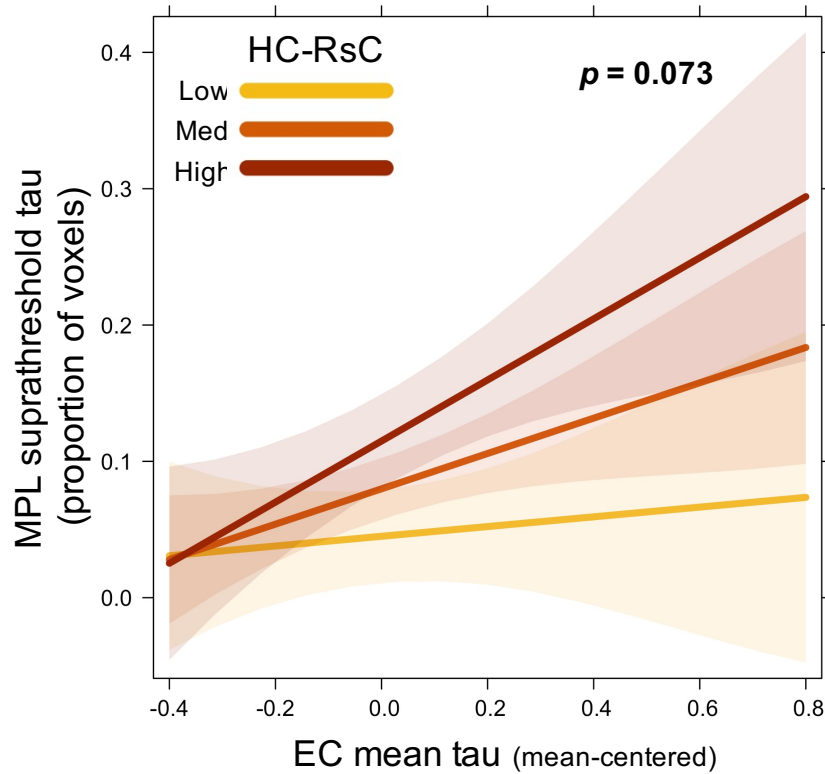


Figure S3. Entorhinal tau pathology exhibits greatest association with medial parietal lobe tau when hippocampal-retrosplenial connectivity is greatest. Visualization of interaction between entorhinal cortex (EC) mean tau (partial volume corrected FTP SUVR) and hippocampal-retrosplenial (Table S1). Medial parietal lobe (MPL) suprathreshold tau is associated with an entorhinal tau x HC-RsC interaction at trend level. Plot displays the relationship predicted by linear regression at low (10th percentile), median, and high (90th percentile) HC-RsC.

Foreword for Chapter 2

In the previous chapter, we demonstrated that resting state functional connectivity strength along the pathway from hippocampus to medial parietal cortex is associated with downstream tau pathology burden cross-sectionally. Further, this association is strengthened in individuals with higher upstream hippocampal tau pathology, and the combination of tau accumulation and high connectivity strength has consequences for memory function. This first analysis investigated the possible correlation between an individual's connectivity between regions vulnerable to tau pathology and the degree of tau accumulation in the downstream region, implicating neural activity in the spread of tau pathology. In the next chapter, we utilize whole-brain neural connectivity and investigate the opposite direction of this effect: Does tau pathology accumulation influence the integrity of networks of functional connectivity? In Chapter 2, we investigate whether measures of connectivity across the entire brain—connectivity networks defined using cognitive performance—are affected by tau pathology, even before the onset of widespread neurodegeneration. This line of inquiry provides insight into the connections in the brain most likely to be altered by the presence of tau pathology, and highlights the intercorrelated relationship between pathology accumulation and network connectivity in aging and Alzheimer's disease.

Chapter 2: Behaviorally meaningful functional networks mediate the effect of Alzheimer's pathology on cognition

Jacob Ziontz¹, Theresa M. Harrison¹, Xi Chen¹, Joseph Giorgio^{1,2}, Jenna N. Adams³, Zehao Wang¹, William Jagust^{1,4} for the Alzheimer's Disease Neuroimaging Initiative*

¹ Helen Wills Neuroscience Institute, UC Berkeley, Berkeley, United States

² School of Psychological Sciences, College of Engineering, Science and the Environment, University of Newcastle, Newcastle, New South Wales, Australia

³ Department of Neurobiology and Behavior and Center for the Neurobiology of Learning and Memory, University of California, Irvine, California, United States

⁴ Lawrence Berkeley National Laboratory, Berkeley, United States

**Part of the data used in preparation of this article were obtained from the Alzheimer's Disease Neuroimaging Initiative (ADNI) database (adni.loni.usc.edu). As such, the investigators within the ADNI contributed to the design and implementation of ADNI and/or provided data but did not participate in the analysis or the writing of this report. A complete listing of ADNI investigators can be found at:*

http://adni.loni.usc.edu/wpcontent/uploads/how_to_apply/ADNI_Acknowledgement_List.pdf

Author Contributions: Study design - J.Z., T.M.H., W.J.J.; Data organization and processing – J.Z., T.M.H., J.N.A., Data analysis and visualization - J.Z., W.W., Feedback and consultation – T.M.H., J.N.A., X.C., J. G. Manuscript writing – J.Z., W.J.J.; Paper editing – all authors.

Published in Cerebral Cortex (2024)

<https://doi.org/10.1093/cercor/bhae134>

Abstract

Tau pathology is associated with cognitive impairment in both aging and Alzheimer's disease (AD), but the functional and structural basis of this relationship remain unclear. We hypothesized that the integrity of behaviorally-meaningful functional networks would help explain the relationship between tau and cognitive performance. Using resting state fMRI, we identified unique networks related to episodic memory and executive function. The episodic memory network was particularly related to tau pathology measured with positron emission tomography (PET) in entorhinal and temporal cortices. Further, episodic memory network strength mediated the relationship between tau pathology and cognitive performance above and beyond neurodegeneration. We replicated the association between these networks and tau pathology in a separate cohort of older adults, including both cognitively unimpaired and mild cognitive impairment individuals. Together, these results suggest that behaviorally-meaningful functional brain networks represent a functional mechanism linking tau pathology and cognition.

Introduction

The microtubule-associated protein tau is primarily involved in stabilizing the neural cytoskeleton⁷¹, but when hyperphosphorylated it becomes pathological and dissociates to form neurofibrillary tangles both intra- and extracellularly⁷². Along with diffuse fibrillar amyloid-beta (A β), the stereotyped spread of tau from medial temporal lobe to areas across the cortex is one of the hallmark neuropathologies of Alzheimer's disease (AD)⁵. Tau pathology is also known to be present in aging, with accumulation in the medial temporal lobe observed in almost all older adults even without cognitive impairment⁶. In contrast to the weak relationship found between A β and cognitive performance, tau pathology burden is closely associated with cognitive performance both cross-sectionally and over time^{7-9,73,74} in older adults. Episodic memory is one of the cognitive domains that declines earliest in the presence of AD pathology even in cognitively unimpaired (CU) older adults^{7,8,73}, but executive function may also be impaired shortly after, particularly for individuals with mild cognitive impairment (MCI) and AD⁷⁵⁻⁷⁹. Still, despite the preponderance of evidence linking tau to cognitive performance in aging and AD, the mechanisms by which tau deposition results in cognitive decline are not well understood.

Most explanations of the link between tau pathology and cognition have focused on the role of neurodegeneration. Tau pathology is associated with lower regional brain volume and cortical thickness⁸⁰⁻⁸² and the baseline spatial pattern of tau accumulation predicts future atrophy rate beyond the effects of baseline A β or cortical thickness⁸³. Indeed, tau may lead to neural death and regional atrophy via disruption of cytoskeletal integrity in brain regions where it accumulates^{80,84}, and the presence of tangles in affected regions may further disrupt cell signaling and maintenance⁶⁵. Still, studies examining neurodegeneration as a potential mechanism have shown that much of the association between tau and cognition is unexplained by structural measures, particularly for individuals in the earliest stages of decline. A mediating effect of grey matter volume⁷⁶ and cortical thickness⁸⁵ has been observed in individuals diagnosed with AD, though CU individuals often do not show a definitive mediating role for brain structure in the relationship between tau pathology and cognition^{82,85}. In each of these studies, a great degree of variance in the relationship between tau pathology and cognition remains after accounting for brain structure. It may be that factors related to brain function, rather than structure, explain greater degree of variance in the relationship between tau pathology and cognition in the earliest stages of disease.

Inter-correlation of the spontaneous blood oxygen level-dependent (BOLD) signal, reflecting neural activity and measured with functional magnetic resonance imaging (fMRI), has been used for decades to define functionally correlated regions of the brain. This phenomenon is described as intrinsic connectivity as regional patterns of coherence arise in the absence of external stimulus, with topography at rest robust across individuals and closely matching functional connections observed during task performance^{11,86}. Networks reflecting these patterns of functional connectivity (FC) can be observed during many different cognitive tasks or in the absence of a specific paradigm⁸⁷, and functional architecture at rest may in fact shape networks observed during task performance⁸⁸. Interestingly, atrophy patterns of different neurodegenerative syndromes topographically resemble distinct intrinsic connectivity networks in healthy individuals¹². Furthermore, patterns of tau accumulation in different clinical variants of AD mirror⁸⁹ and can be predicted by patterns of connectivity of distinct brain networks²³. Some of these networks, such as the default mode and salience networks, show alterations in the strength of connectivity that is related to A β and tau pathologies⁹⁰ and decline in cognitive

function over time ⁹¹. Given the close relationship between intrinsic FC and patterns of tau accumulation, network connectivity may be a critical factor in the relationship between tau pathology and cognitive performance.

Functional networks can be identified using a wide array of approaches, with one of the most well-known parcellations organizing the brain into 7 distinct, stable networks that span the entire cerebral cortex ⁹². Alternatively, networks of functional connections can be identified in terms of their relationship to specific cognitive performance. One influential study ⁹³ defined a whole-brain network of functional connections most closely related to performance on a sustained attention task, and found that overall strength of this network during task predicted attentional performance in an independent cohort, both during a different attention task and at rest. Similar methods have been used to identify brain networks reflecting varied outcomes such as pain ⁹⁴ and creative ability ⁹⁵, as well as cognitive performance in domains including executive function ⁹⁶, short-term memory ⁹⁷, fluid intelligence ^{98,99}, attention ¹⁰⁰, and processing speed ¹⁰¹. Still, though considerable evidence indicates that intrinsic brain networks are robust and generalizable, few studies to date have leveraged these kinds of functional networks to understand the impact of pathology on cognitive function. Further, this type of approach relies on selecting *a priori* thresholds for identifying connections, and often results in networks of hundreds or thousands of components that make it difficult to explore biologically meaningful pathways and regional interactions. Approaches that result in much sparser networks have a particular advantage in the study of aging and AD, as evidenced by a recent study identifying highly sparse functional networks predicting cognitive reserve in older adults ¹⁰². Sparse networks can be viewed as more biologically and cognitively relevant in that it is easier to examine those connections that are involved in cognitive performance, and simplifies the analysis of which connections may be impacted by pathology and/or atrophy in regions known to be affected in neurodegenerative disease. In this way, network sparsity allows for the examination of the relevance of specific connections and regions involved in both cognitive function and neurodegenerative disease.

In this study, we investigated the role of behaviorally-meaningful functional brain networks in mediating the relationship between tau pathology accumulation and cognitive performance. We utilized a data-driven network definition procedure to identify networks of resting state functional connections in older adults that are closely related to performance on neuropsychological tests in two distinct cognitive domains: episodic memory and executive function. We hypothesized that this approach, allowing for network identification without introducing *a priori* thresholds for selecting connections, would nonetheless yield networks with a much sparser and interpretable subset of connections than conventional approaches ^{93,103}. We further hypothesized that the overall strength of these networks would be related to tau pathology accumulation and would play a mediating role in the relationship between tau and cognitive function, particularly in the episodic memory domain. Finally, to assess the robustness of this approach, we replicated our findings in an independent dataset, demonstrating that behaviorally-defined networks represent a functional mechanism for the relationship between pathology and cognitive performance.

Materials and Methods

Participants

Berkeley Cohort. We included data from 120 cognitively unimpaired (CU) older adults from the Berkeley Aging Cohort Study (BACS). Demographic information for all BACS participants is shown in Table 1. All participants underwent 3T structural MRI, resting state 3T

functional MRI, and a standard neuropsychological assessment. We excluded 2 participants on the basis of excessive head motion during the rsfMRI scan, defined as >20% of all volumes being flagged as outliers during artifact detection. Of the remaining sample, 103 individuals underwent tau PET imaging using ^{18}F -Flortaucipir (FTP), and we excluded an additional 9 participants whose resting state fMRI data was collected more than 1 year from the closest corresponding tau PET scan ($M = 125.6$, $SD = 138.4$ days). Additional inclusion criteria for this study were 60+ years of age, cognitively normal status (Mini Mental State Examination score ≥ 25 and normal neuropsychological examination, defined as within 1.5 SD s of age, education, and sex adjusted norms), no serious neurological, psychiatric, or medical illness, no major contraindications found on MRI or PET, and independent community living status. This study was approved by the Institutional Review Boards of the University of California, Berkeley, and the Lawrence Berkeley National Laboratory (LBNL). All participants provided written informed consent.

ADNI cohort. We included data from 140 older adults aged 60-100 years old from the Alzheimer’s Disease Neuroimaging Initiative 3 (ADNI3) who had all undergone 3T structural MRI and resting state 3T functional MRI, and tau PET imaging using ^{18}F -Flortaucipir (FTP). Demographic information for all ADNI participants is shown in Table 1. We excluded 8 participants due to errors in warping rsfMRI data to MNI space. We excluded an additional 13 participants due to excessive head motion, again defined as >20% of all volumes being flagged as outliers. Individuals aged 60+ years from ADNI3 were included based on the availability of high temporal resolution rsfMRI (TR=0.607) within 1 year of a corresponding FTP PET scan ($M = 29.4$, $SD = 94.5$ days).

	BACS rsfMRI	ADNI3 rsfMRI		BACS vs. ADNI
	Mean (SD) or n (%)			
Sample	CU ($n = 118$)	CU ($n = 75$)	MCI ($n = 44$)	
Age	78.2 (6.5)	70.9 (8.1)	72.6 (7.1)	$p < 0.001$
MMSE	28.7 (1.2)	28.9 (1.6)	27.5 (2.6)	$p = 0.15$
Education (yrs)	16.9 (2.0)	16.5 (2.4)	16.3 (2.6)	$p = 0.07$
Sex (female)	68 (58%)	52 (69%)	14 (32%)	$p = 0.84$

Table 1. Demographics for participants with resting state functional magnetic resonance imaging data (rsfMRI) from the Berkeley Aging Cohort Study (BACS) and Alzheimer’s Disease Neuroimaging Initiative (ADNI) samples. CU = Cognitively unimpaired, MCI = mild cognitive impairment, MMSE = Mini mental state examination.

MRI acquisition and processing

In BACS, structural and functional MRI data were acquired on a 3T TIM/Trio scanner (Siemens Medical System, software version B17A) using a 32-channel head coil. A T1-weighted whole brain magnetization prepared rapid gradient echo (MPRAGE) image was acquired for each subject (voxel size = 1mm isotropic, TR = 2300ms, TE = 2.98ms, matrix = 256×240×160, FOV = 256×240×160mm³, sagittal plane, 160 slices, 5 min acquisition time). Resting state functional MRI was then acquired using T2*-weighted echo planar imaging (EPI, voxel size = 2.6mm isotropic, TR = 1.067s, TE = 31.2ms, FA = 45, matrix 80×80, FOV = 210mm, sagittal

plane, 300 volumes, anterior to posterior phase encoding, ascending acquisition, 5 min acquisition time). During resting state acquisition, participants were told to remain awake with eyes open and focused on a white asterisk displayed on a black background.

In ADNI3, structural and functional MRI data were acquired on 3T scanners with a standardized protocol across all sites. A T1-weighted whole brain magnetization prepared rapid gradient echo (MPRAGE) image was acquired for each subject (voxel size = 1mm isotropic, TR = 2300ms, TE = min full echo, matrix = 208×240×256, FOV = 208×240×256mm³, sagittal plane, 256 slices, 6 min acquisition time). Resting state functional MRI was then acquired using EPI-BOLD (voxel size = 2.5mm isotropic, TR = 0.607s, TE = 30ms, FA = 53, matrix 220x220, FOV = 160mm, sagittal plane, 976 volumes, anterior to posterior phase encoding, ascending acquisition, 10 min acquisition time, further details at <https://adni.loni.usc.edu/wp-content/uploads/2017/07/ADNI3-MRI-protocols.pdf>).

Structural T1-weighted images were processed using Statistical Parametric Mapping (SPM12). Images were first segmented into gray matter, white matter, and CSF components in native space. DARTEL-imported tissue segments for all individuals in the sample were used to create a study-specific template, which was then used to warp native space T1 images and tissue segments to MNI space at 2mm isotropic resolution. Finally, native space T1 images were segmented with Freesurfer v.5.3.0 using the Desikan-Killiany atlas parcellation⁴³. Separate DARTEL study-specific templates were created for BACS and ADNI, such that functional and structural images were warped to MNI space using a template defined separately in each cohort.

Resting state fMRI images from BACS and ADNI3 were preprocessed using a nearly identical SPM12 pipeline, with slight differences to account for different acquisition parameters. Slice time correction was applied in BACS to adjust for differences in acquisition time for each brain volume, but this was not done in ADNI because of the low TR resting state data. In both cohorts, all EPIs were realigned to the first acquired EPI, and translation and rotation realignment parameters were output. Each EPI was next coregistered to each individual's native space T1 image. Next all resting state EPIs and structural images were warped to a cohort-specific DARTEL template in 2mm isotropic MNI space from structural preprocessing. These smoothed rsfMRI images in MNI space were used to extract the time series of each ROI in seed-to-seed functional connectivity analyses. To further adjust for confounds of head motion, mean framewise displacement was computed for each rsfMRI scan and included as a covariate in all subsequent analyses. Across all subjects after excluding participants with excessive head motion, mean framewise displacement was 0.18mm (*SD*: 0.06) in BACS and 0.19mm (*SD*: 0.07) in ADNI.

Functional connectivity analyses

ROI-to-ROI functional connectivity was assessed using the CONN functional connectivity toolbox (version 17e)⁴⁶ implemented in MATLAB version 2019b (The Mathworks Inc., Natick, MA). ART motion detection was first performed to identify volumes of high motion, using a movement threshold of > 0.5mm/TR and a global intensity *z*-score of 3. Outlier volumes were flagged and included as spike regressors during denoising. Denoising was performed with translation and rotation realignment parameters and their first-order derivatives, as well as anatomical CompCor (first five components of time series signal from white matter and CSF). A band pass filter of 0.008-0.1 Hz and linear detrending were applied to the residual time-series. For each individual denoised time series were extracted for 246 ROIs from the Brainnetome atlas⁴⁴. Each of these time series were then correlated (Pearson's *r*) and transformed (*r* to Fisher *z*), resulting in a 246x246 connectivity matrix.

Network definition procedure

Behaviorally-meaningful functional networks were defined in a similar fashion to previous network-building approaches¹⁰³, taking a functional connectivity matrix and behavioral outcome measure for each individual as inputs and generating a network across the sample consisting of a subset of all possible connections in the brain. Each connection (30,135 unique ROI-ROI pairs in a 246 x 246 matrix) was treated as a regressor in a regularized linear model with behavioral performance as the outcome. A least absolute shrinkage and selection operator (LASSO)¹⁰⁴ penalty (λ) was applied to the beta weights of each regressor, such that only a sparse subset of regressors survived the penalty to remain nonzero. An appropriate λ penalty was selected by computing the Bayesian Information Criterion (BIC)¹⁰⁵ using the equation:

$$LL = -\frac{n}{2} \left(1 + \ln \left(\frac{1}{n} \sum_{i=1}^n (y_i - \hat{y}_i)^2 \right) \right)$$

where LL is the log likelihood of the model, n is the sample size, y is the observed data and \hat{y} is the outcome predicted by each model with a given λ , and the using the equation:

$$BIC = -2LL + a \ln n$$

where a is the number of nonzero features included in the model. BIC was computed for models iterating through 1000 λ hyperparameter values, and the model with the lowest BIC (i.e., best explanatory power adjusting for the number of regressors) was selected. This data-driven LASSO+BIC procedure does not require selection of an arbitrary significance threshold and only keeps regressors with very high beta values, meaning those that are the most relevant to the behavioral outcome measure. The resulting networks tend to exclude spurious or collinear relationships between behavior and connectivity, making them highly sparse and more interpretable. Overall network strength was then computed for each individual by summing the connectivity values (Fisher z -transformed correlations) for every ROI-ROI connection in the network¹⁰³.

PET acquisition and processing

In BACS, PET was acquired for all participants at the Lawrence Berkeley National Laboratory (LBNL). Tau burden was assessed with ¹⁸F-Flortaucipir (FTP) synthesized at the Biomedical Isotope Facility at LBNL as previously described²⁷. Data were collected on a Biograph TruePoint 6 scanner (Siemens, Inc) 75-115 min post-injection in listmode. Data were then binned into 4 x 5 min frames from 80-100 min post-injection. CT scans were performed before the start of each emission acquisition. In ADNI, PET data were collected using a standardized protocol of six 5-min time windows 75 to 105 min after injection. All PET images were reconstructed using an ordered subset expectation maximization algorithm, with attenuation correction, scatter correction, and smoothing with an 8mm Gaussian kernel.

Processing of FTP images was carried out in SPM12 and Freesurfer. Images were realigned, averaged, and coregistered to 3T structural MRIs. Standardized uptake value ratio (SUVR) images were calculated by averaging mean tracer uptake over the 80-100 min data and normalized with an inferior cerebellar gray reference region. The mean SUVR of each ROI (structural MRI FreeSurfer segmentation) was extracted from the native space images. SUVR images were then warped to 2mm MNI space for voxelwise analyses using the cohort specific

DARTEL template produced from structural data (see above). No additional spatial smoothing was applied.

Neuropsychological measures

Episodic memory and executive function cognitive domain performance was measured using neuropsychological assessment data collected closest in time to each individual's rsfMRI scan ($M = 129.5$, $SD = 73.2$ days). Composite measures were computed by averaging the z -transformed individual test scores using mean and SD from the sample⁷. The episodic memory domain composite included scores from the California Verbal Learning Test (CVLT) immediate free recall, CVLT long-delay free recall, Visual Reproduction I (immediate recall), and Visual Reproduction II (delayed recall) tasks. The executive function domain composite included scores from the Trails A, Trails B, Stroop Correct in 60s, and Digit Symbol Substitution tasks. In the ADNI sample, episodic memory (adni_mem) and executive function (adni_ef2) cognitive domain scores were downloaded from the publicly available computed online repository using methods described previously (https://ida.loni.usc.edu/download/files/study/ce0a4966-84bf-4a17-bacc-99e98277e325/file/adni/ADNI_Methods_UWNPSYCHSUM_March_2020.pdf).

Statistical analyses

Following functional connectivity analyses, network definition was carried out in python using a combination of internal code and the *pycasso* package (<https://pypi.org/project/pycasso/>). All subsequent statistical analyses were carried out in R version 4.2.0. Linear regression models in the `{stats}` package were used to assess the relationship between network strength and tau pathology adjusting for age, sex, mean framewise displacement, the interval between rsfMRI and tau PET acquisition, and the interval between rsfMRI and cognitive testing. All analyses involving neuropsychological measures additionally adjusted for years of education. The `{lavaan}` package was used to carry out multiple mediation analyses, with 1000 bootstrapped iterations used to determine statistical significance. Percent mediated by each factor was computed by dividing the indirect effect of each factor by the total effect of the relationship.

Data visualization

Networks were rendered and visualized using the BioImage Suite Connectivity Viewer, part of the BioImage Suite Web 1.2.0 browser tool (<https://bioimagesuiteweb.github.io/webapp/index.html>). Voxelwise analysis results were visualized using the *nilearn* glassbrain plotting function in python (https://nilearn.github.io/dev/modules/generated/nilearn.plotting.plot_glass_brain.html). Scatter plots were created using the `{ggplot2}` package in R to visualize effects from linear regression models.

Results

Network identification captures cognition-specific connections across the brain

Resting state fMRI data from 118 CU older adults aged 60-94 ($M = 78.2$, $SD = 6.5$ years) from the Berkeley Aging Cohort Study (BACS; Table 1) were used to identify distinct episodic memory and executive function networks. We computed resting state functional connectivity (rsFC) as the Pearson's correlation coefficient (z -transformed) between all regions of interest (ROIs) in a 246-ROI parcellation (Brainnetome atlas)⁴⁴. Using the data-driven network definition procedure (Materials and Methods), we selected pairwise connections specific to each behavioral domain by regressing each unique connection against either an episodic memory or executive function composite score measured close to the fMRI scan ($M = 129.5$, $SD = 73.2$ days). A LASSO penalty (λ) was applied to identify connections with the greatest positive association to the behavioral domain score, iterating over many possible λ values to select the

model with the lowest Bayesian Information Criterion (BIC). The resulting sample network masks were then applied to each individual's connectivity matrix, and rsFC values for each connection in the network were summed to determine subject-specific overall network strength (Figure 1a).

This approach identified an episodic memory network comprising 63 functional connections, including between brain areas often implicated in memory processing such as hippocampus, medial parietal, anterior temporal, and prefrontal regions (Figure 1b). An executive function network comprising 60 connections between prefrontal, superior parietal, and lateral temporal regions was also identified (Figure 1c). Networks defined by these two cognitive domains were markedly distinct, with only 2 identical ROI-ROI connections and limited spatial overlap of connected regions (Dice similarity coefficient = 0.07). After adjusting for age, sex, years of education, mean framewise displacement, and time between rsfMRI and cognitive testing, subject-specific network strength was unsurprisingly highly correlated with performance in the cognitive domain by which it was defined; episodic memory network strength with episodic memory performance ($r = 0.58$), and executive function network strength with executive function performance ($r = 0.55$). Episodic memory network strength exhibited a weaker correlation with executive function performance ($r = 0.18$), as did executive function network strength with episodic memory performance ($r = 0.18$; Figure S1).

Tau pathology burden is associated with lower memory network strength

We next aimed to characterize how the strength of these networks was related to age and tau pathology burden. Age was negatively correlated with the overall strength of both episodic memory ($r = -0.24$, $p = 0.010$) and executive function networks ($r = -0.19$, $p = 0.038$; Figure S2). We then examined tau PET standard uptake value ratio (SUVR) in the entorhinal cortex (EC) as well as a previously-validated AD-signature temporal meta-ROI comprising EC, amygdala, parahippocampal, fusiform, inferior temporal, and middle temporal gyri¹⁰⁶. We used linear regression models adjusting for age, sex, mean framewise displacement, the interval between rsfMRI and tau PET, and the interval between rsfMRI and cognitive testing to test the association between network strength and tau pathology burden. Greater tau PET signal in EC was associated with lower episodic memory network strength ($\beta = -4.11$, $p = 0.019$; Figure 2a), as was greater temporal meta-ROI tau signal ($\beta = -4.94$, $p = 0.017$; Figure 2b). By contrast, neither tau PET burden in EC ($\beta = -0.97$, $p = 0.51$; Figure 2d) nor the temporal meta-ROI ($\beta = -1.00$, $p = 0.57$; Figure 2e) was associated with executive function network strength.

To verify EC and the temporal meta-ROI were appropriate regions to test the association between network strength and tau pathology burden and to explore other potential regional relationships, we examined the voxelwise association between tau PET signal and strength of each network separately, adjusting for age and sex. Using an exploratory threshold ($k > 100$, $p < 0.05$ unc.), we found an association between tau PET and episodic memory network strength in medial temporal and lateral temporal regions that captures the typical pattern of tau deposition in AD¹⁰⁷ and which largely overlaps with the temporal meta-ROI (Figure 2c). A notably sparser pattern of associations was observed between tau PET and executive function network strength (Figure 2f).

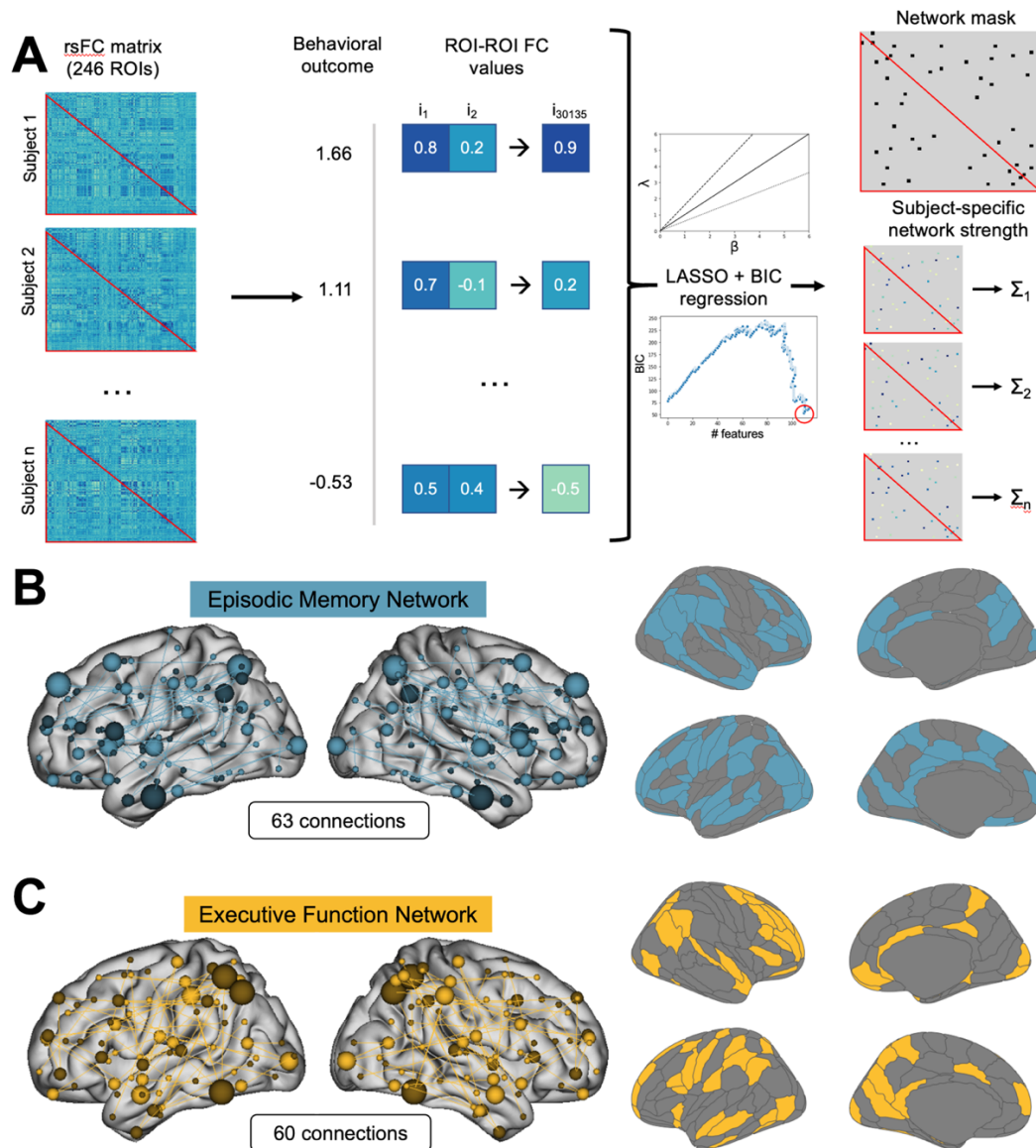


Figure 1. Behavioral functional networks in cognitively unimpaired older adults. (A) In network definition, all unique pairwise rsFC values for each individual were regressed against a behavioral outcome measure. A LASSO penalty (λ) was applied to the β of each positive pairwise connection to select a sparse subset of connections, iterating over 1000 λ values to identify the model with the lowest Bayesian Information Criterion (BIC). A network mask can then be projected onto cortical ROIs, and subject-specific network strength is computed by summing rsFC values for each network connection (see Methods). (B) Episodic memory and (C) executive function networks, with spheres centered within connected regions and size corresponding to the number of connections to each region. Darker-colored spheres correspond to nodes in the left hemisphere, and lighter-colored spheres correspond to nodes in the right hemisphere. Cortical surface renderings (right) depict regions connected by each network.

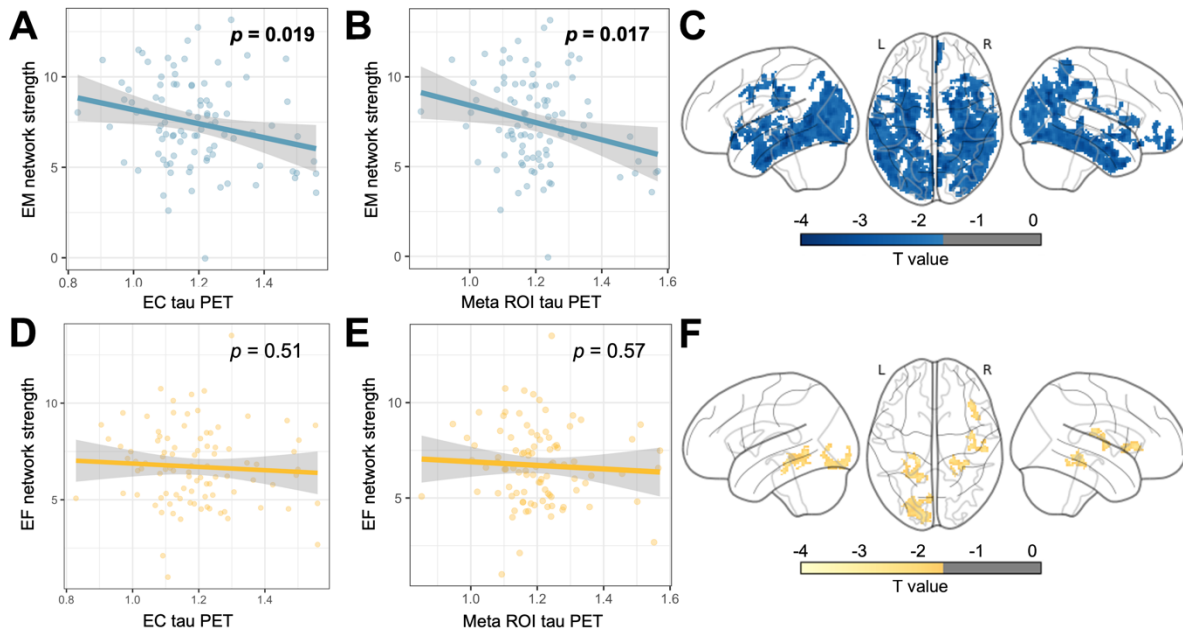


Figure 2. Tau pathology burden is associated with lower memory network strength. (A) Association between episodic memory (EM) network strength and tau PET signal in entorhinal cortex (EC) and (B) temporal meta-ROI adjusting for age and sex. (C) Voxelwise association between episodic memory network strength and tau PET signal adjusted for age and sex. (D) Association between executive function (EF) network strength and tau PET signal in EC and (E) temporal meta-ROI adjusting for age and sex. (F) Voxelwise association between executive function (EF) network strength and tau PET signal. Voxelwise analyses used an exploratory threshold ($k > 100$, $p < 0.05$ unc.) to validate the use of EC and temporal meta-ROI for as relevant regions for associations with network strength.

Memory network strength mediates the association between pathology and cognition

Next, we tested whether episodic memory or executive function networks would mediate the relationship between tau pathology and cognitive function, particularly compared to structural measures of neurodegeneration. We used multiple mediation models to measure the extent to which the association between temporal meta-ROI tau accumulation and cognitive domain score is mediated by both network strength and cortical thickness in this same meta-ROI, including both functional and structural effects in the same model. We found that episodic memory network strength significantly mediated 50.1% of the total effect of entorhinal cortex (EC) tau on memory performance ($p = 0.026$), while EC cortical thickness only mediated a nonsignificant ($p = 0.18$, 15.8%) proportion of this relationship (Figure 3a). Similarly, episodic memory network strength mediated 48.5% of the total effect of meta-ROI tau on episodic memory performance ($p = 0.009$), while meta-ROI cortical thickness only mediated a nonsignificant (20.8%, $p = 0.13$) proportion of this relationship (Figure 3b). Using bilateral hippocampal volume as an alternative structural measure did not change this result, as episodic memory network strength mediated 51.5% of the total effect ($p = 0.003$), while hippocampal volume mediated a nonsignificant ($p = 0.25$, 10.9%) proportion of the effect. In contrast, neither executive function network strength ($p = 0.42$) nor EC cortical thickness ($p = 0.24$) mediated the relationship between EC tau and executive function performance (Figure 3c), nor did the executive function network ($p = 0.41$) or meta-ROI cortical thickness ($p = 0.09$) mediate the

relationship between meta-ROI tau and cognition (Figure 3d). As an additional control, we found that episodic memory network strength did not mediate the relationship between meta-ROI tau and executive function performance ($p = 0.14$), nor did executive function network strength mediate the relationship between meta-ROI tau and episodic memory performance ($p = 0.48$; Figure S3).

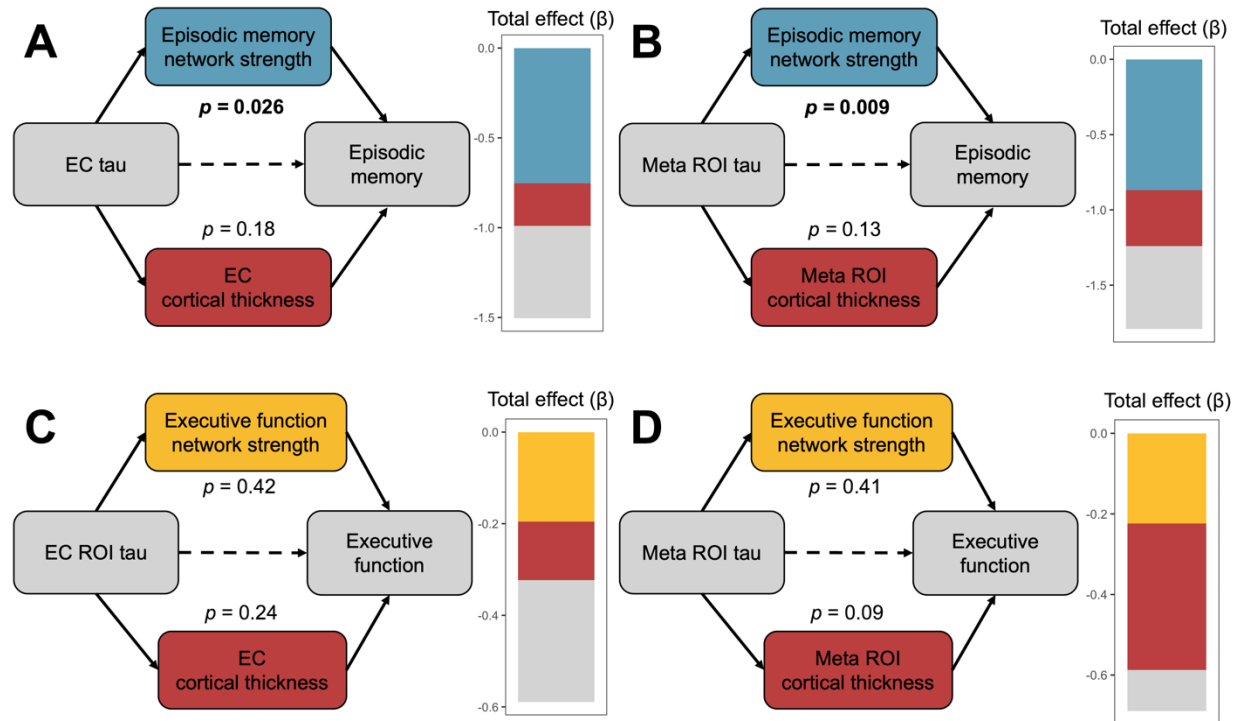


Figure 3. Episodic memory network strength mediates the association between tau pathology and cognitive performance. Multiple mediation models demonstrate that episodic memory network strength mediates the relationship between tau pathology and cognition to a greater degree than cortical thickness, both (A) in entorhinal cortex (EC) and (B) in the meta-ROI. Neither executive function network strength nor cortical thickness mediates the relationship between tau pathology and cognition (C) in entorhinal cortex or (D) in the meta-ROI. Stacked bar charts visualize proportion of total effect mediated by each factor.

Network strength association with tau generalizes to an independent cohort

Finally, we assessed the extent to which these networks were associated with tau pathology in an independent cohort of older adults. We utilized rsfMRI and tau PET data from an ADNI3 sample of CU older individuals as well as patients with MCI (Table 1) to test the generalizability of the BACS-defined networks in their association with tau pathology burden. We computed rsFC between all 246 regions of the same whole-brain atlas⁴⁴ in ADNI participants, and network strength was derived by summing rsFC values of the BACS-defined episodic memory (Figure 4a) and executive function (Figure 4d) network connections in the independently collected and processed sample. We then used linear regression models adjusting for age, sex, mean framewise displacement, and the interval between rsfMRI and cognitive testing to examine the association between BACS-defined network strength and age as well as tau pathology in the ADNI sample. As in BACS, we observed a negative correlation between network strength and age for both episodic memory ($r = -0.30$, $p = 0.001$) and executive function

($r = -0.29, p = 0.001$; Figure S2). Similar to the BACS sample, episodic memory network strength showed a moderate correlation with both EC tau ($\beta = -2.11, p = 0.083$; Figure 4b) and a somewhat stronger association with meta-ROI tau ($\beta = -2.65, p = 0.031$; Figure 4c) adjusting for age, sex, mean framewise displacement, rsfMRI-PET interval, and rsfMRI-cognitive testing interval.

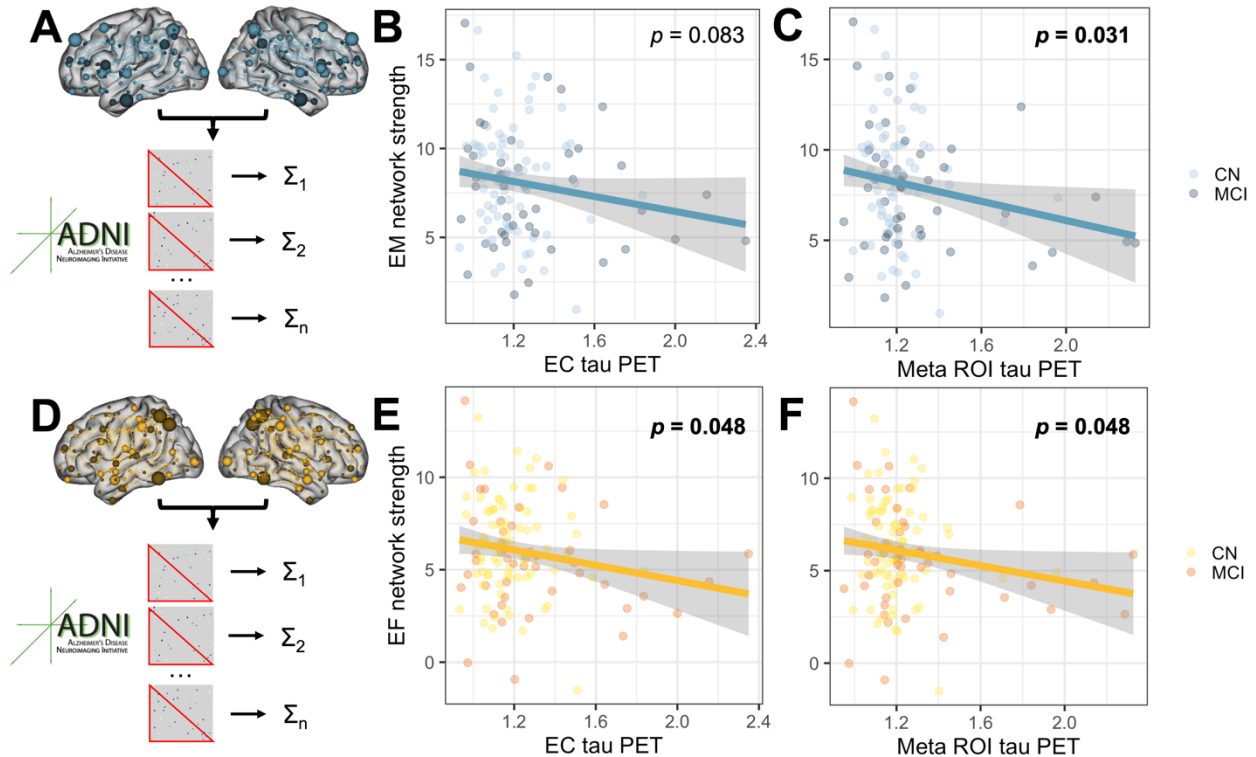


Figure 4. Strength of BACS-defined networks is associated with tau pathology burden in ADNI participants. BACS-defined episodic memory (A) and executive function networks (D) were applied to ADNI participants and network strength was computed for each individual. (B) Association between overall episodic memory network strength and entorhinal cortex (EC) tau PET. (C) Association between episodic memory network strength and meta-ROI tau PET. (E) Association between executive function network strength and EC tau PET. (F) Association between executive function network strength and meta-ROI tau PET. Scatter plots are visualized effects of interest from linear regression models adjusted for age, sex, mean framewise displacement, rsfMRI-PET interval, and rsfMRI-cognitive testing interval.

In contrast with the BACS sample of only CU individuals, however, executive function network strength was also correlated with tau pathology in EC ($\beta = -2.06, p = 0.048$; Figure 4e) and in the meta-ROI ($\beta = -2.08, p = 0.048$; Figure 4f).

To examine associations between BACS-defined network strength and cognition in the ADNI sample, we utilized previously computed memory and executive function cognitive domain scores¹⁰⁸ collected closest in time to each participant's fMRI scan ($M = 22.0, SD = 52.2$ days). Episodic memory network strength exhibited a bivariate correlation with memory performance ($r = 0.22, p = 0.012$), as did executive function network strength with executive

function performance in ADNI ($r = 0.34, p < 0.001$). Adjusting for age, sex, mean framewise displacement, rsfMRI-cognitive testing interval, and years of education, the relationship between episodic memory network strength and memory performance in ADNI was no longer significant ($\beta = 0.03, p = 0.31$), but executive function network strength remained significantly associated with executive function performance ($\beta = 0.08, p = 0.003$). Adjusting for these same factors, episodic memory network strength was weakly correlated with executive function performance ($\beta = 0.04, p = 0.07$), as was executive function network strength with memory performance ($\beta = 0.05, p = 0.07$; Figure S4). Finally, we again examined the roles of network strength and cortical thickness in the tau-cognition relationship using multiple mediation analyses in the ADNI sample. We found that episodic memory network strength did not significantly mediate the association between entorhinal cortex (7.2%, $p = 0.23$) or meta-ROI (7.6%, $p = 0.22$) tau burden and episodic memory performance, while entorhinal cortical thickness (29.8%, $p = 0.01$) and meta-ROI cortical thickness (28.0%, $p = 0.02$), did mediate this relationship (Figure 5a-b). Executive function network strength exhibited a weak mediating role in the association between entorhinal cortex (14.0%, $p = 0.06$) and meta-ROI (13.5%, $p = 0.07$) tau burden and executive function performance, as did entorhinal cortical thickness (18.0%, $p = 0.07$) and meta-ROI cortical thickness (17.2%, $p = 0.13$; Figure 5c-d). Taken together, our findings suggest that the strength of these functional networks in a separately collected and processed cohort of older adults exhibit similar relationships with age and tau pathology burden, but did not demonstrate robust associations with cognitive performance per se.

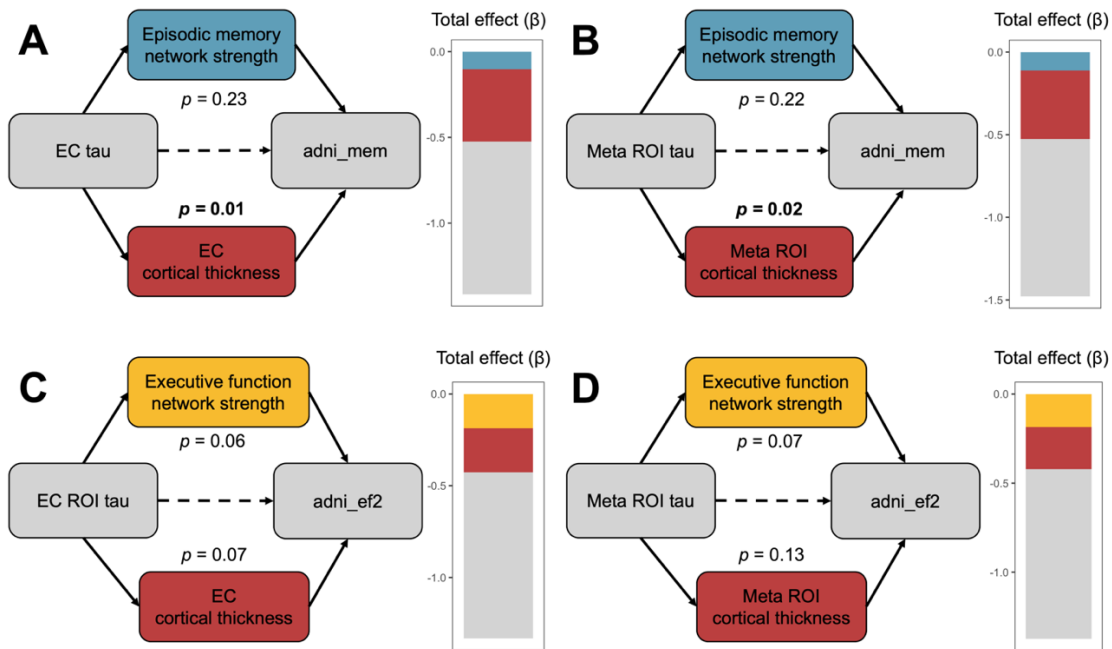


Figure 5. Network strength does not robustly mediate the association between tau pathology and cognitive performance in an independent cohort. Multiple mediation models demonstrate that cortical thickness, but not episodic memory network strength, mediates the relationship between tau pathology and cognition, both (A) in entorhinal cortex (EC) and (B) in the meta-ROI. Executive function network strength and cortical thickness show a weak mediating effect in the relationship between tau pathology and cognition (C) in entorhinal cortex and (D) in the meta-ROI. Stacked bar charts visualize proportion of total effect mediated by each factor.

Discussion

In this study, we used resting state fMRI in a cohort of CU older adults to identify functional networks related to both episodic memory and executive function performance. The episodic-memory defined network was characterized by connections between medial and lateral temporal cortex, medial parietal and inferior parietal cortex, and frontal regions including medial parietal prefrontal cortex. Parahippocampal gyrus, precuneus, and supramarginal gyrus tended to have the most connections with other brain areas in this network. Notably, the episodic memory network included connections between hippocampus and anterior temporal as well as posterior medial regions. This pattern of connectivity is thought to be critical for memory processing and susceptible to age- and pathology-related alterations³⁹. The executive function-defined network was characterized by connections between lateral temporal, superior parietal, and many superior frontal regions. Regions in the inferior parietal lobule and inferior temporal gyrus were particularly well-connected with the rest of the brain by this network. One striking anatomical feature of the executive function-defined network was connections with a cluster of regions in dorsolateral prefrontal cortex (dlPFC). The dlPFC has long been implicated in the ability to manipulate information in the environment such as rearranging of digits, and making plans for the future¹⁰⁹. Further comparing the anatomy of the two networks, the episodic memory network contained more regions such as parahippocampal gyrus, fusiform gyrus, and posterior cingulate cortex that are part of the limbic system affected early in the accumulation of tau pathology in aging and AD. Overall, the topography of these networks suggests that using cognitive performance to identify a sparse network of functional connections in the brain may provide insight into which connections throughout the brain are likely to be altered by the presence of tau pathology in aging and Alzheimer's disease.

In the BACS sample of CU older adults, we found that greater tau pathology in both entorhinal cortex and the temporal meta-ROI was related to lower overall strength of the episodic memory-defined network, but not the executive function-defined network. Episodic memory is often observed to be one of the first cognitive domains to decline in preclinical AD, and pathology-related disruption of connections specifically related to episodic memory plausibly underlies this deficit. Aberrant resting state FC between hippocampus and other memory-related brain regions has previously been shown to differentiate CU older adults and those with impaired memory performance¹¹⁰. Further, brain aging predicted from rsfMRI is accelerated in individuals with a history of familial AD and significant pathology burden¹¹¹, and discrepancy between chronological and brain age determined using rsfMRI has been shown to capture cognitive impairment¹¹². The networks identified in our study replicate these negative associations with age, but the relationship between episodic memory network strength and tau burden even after adjusting for participant age indicates that AD pathology may be driving functional impairment beyond the effects of normal aging. Indeed, the observed spatial distribution of tau pathology associated with reduced episodic memory network strength in our study resembles the typical pattern of AD-related tau deposition¹⁰⁷, revealing a phenotype typical of AD in CU older individuals.

Examination of the BACS-defined networks in the ADNI cohort provide replication and extension of our findings in BACS. We found associations between tau and reduced network strength for both episodic memory and executive function networks in ADNI participants, which may reflect more progressed disease given the inclusion of patients with MCI in the ADNI sample. Associations with the strength of both networks supports the notion that both episodic memory and executive function domains tend to become impaired as individuals transition to

MCI^{75,78}. This was particularly the case for tau pathology in the temporal meta-ROI, a group of regions where tau accumulation is thought to occur outside of the effects of normal aging¹⁰⁶. Though tau was correlated with lower strength of both networks, the executive function network showed a stronger association with cognitive performance than did the episodic memory network after adjusting for factors such as age and sex. Though neither of these networks were observed to robustly mediate the effects of tau on cognition in the ADNI sample, measures of brain structure mediated this relationship more so than episodic memory network strength. Thus, the executive function network showed a somewhat more convincing association with cognition in the cohort of CU and MCI individuals, which may be related to the more progressed disease stage of the ADNI sample affecting cognitive domains other than episodic memory.

Another potential explanation for the limited replication of the functional network mediation is differences in data acquisition between BACS and ADNI. Although fMRI data was processed as similarly as possible between the two samples, differences in scanners between sites and acquisition parameters make an exact comparison challenging. Further, although composite measures of episodic memory and executive function were used in both samples, the precise neuropsychological tests that were used to construct these measures differed between samples and may introduce additional variability. These differences are also informative, however, as they suggest that relationships between network strength and AD pathology can be replicated despite nonidentical data acquisition across samples. It should also be noted that replication of associations between cognitive and resting-state fMRI networks is challenging given the relatively high degree of variability inherent to this modality. Furthermore, the approach used here tends to identify networks of relatively few functional connections compared to previous approaches (Rosenberg et al. 2015; Shen et al. 2017), favoring interpretability of these networks in the context of aging and AD. However, it is possible that this sparsity may make it less likely to capture all of the many connections in the brain that are important for cognitive function, emphasizing the need for ongoing work to balance both interpretability and generalizability of these behaviorally-meaningful functional networks.

The mediating roles of brain structure and function also hint at the differing biological consequences that this pathology can have in the aging brain. Though tau accumulation has been convincingly linked to neurodegeneration⁸³, the role of structural measures in mediating its relationship with cognition has been inconsistently demonstrated^{76,82}, particularly for CU individuals⁸⁵. Indeed, tau pathology has been shown to be more sensitive for detecting early cognitive change than either A β PET or structural measures¹¹⁴, and it has been proposed that functional changes such as network disruption may be a crucial mechanism for the effect of tau pathology on cognition^{85,115}. Consistent with our results, tau pathology may eventually cause cognitive dysfunction through synaptic loss and neurodegeneration, but also more immediately via alterations in synaptic function⁶⁵. These distinct effects may help explain the limited role of neurodegeneration in cognitive impairment early in disease progression, and suggest that the functional consequences of tau are more relevant for study and intervention at the earliest stages of decline⁸⁵.

This study has several limitations. First, the BACS sample includes individuals with rsfMRI, tau PET, and cognitive testing collected within 1 year of each other. Although alterations in brain tau and cognition are likely to occur very slowly in cognitively normal people and we adjust for the time difference between the acquisition of these data in our analyses, our results may be impacted by these relatively liberal inclusion criteria. We also did not analyze the role of A β and chose to focus on tau pathology due to its closer relationship with cognition, but it is

possible that there be interactions between tau and A β that we lack the statistical power to test. In addition, we took the approach of including only connections with a positive relationship to behavior in order to increase network sparsity and interpretability, but it is possible that functional connections that are negatively associated with behavior may also be important for cognition and influenced by the presence of pathology. We also did not precisely replicate associations between the BACS networks and cognition in ADNI, so further work is needed to identify generalizable networks with a more robust influence on cognition, perhaps defined using task fMRI. Finally, in order to make inferences about the role of these networks in cognitive decline, future work should utilize longitudinal cognitive data rather than focusing exclusively on cross-sectional cognitive performance.

Taken together, our results suggest that behaviorally meaningful functional networks in fact play an important role in cognition in the early stages of AD. Despite skepticism over the relevance of resting state fMRI for predicting cognition¹¹⁶, the ubiquity and ease of collecting resting state data makes it a modality of great interest for potential clinical relevance^{19,34,57}. Overall, this study presents evidence that these networks are a compelling functional mechanism for the effect of tau pathology on cognitive performance in older adults. While neurodegeneration may account for more broad effects on cognition in the later stages of Alzheimer's disease when tau pathology has been present for many years, reduced network integrity helps explain the impact of tau accumulation on cognitive function in older individuals without obvious structural atrophy.

Supplementary Materials

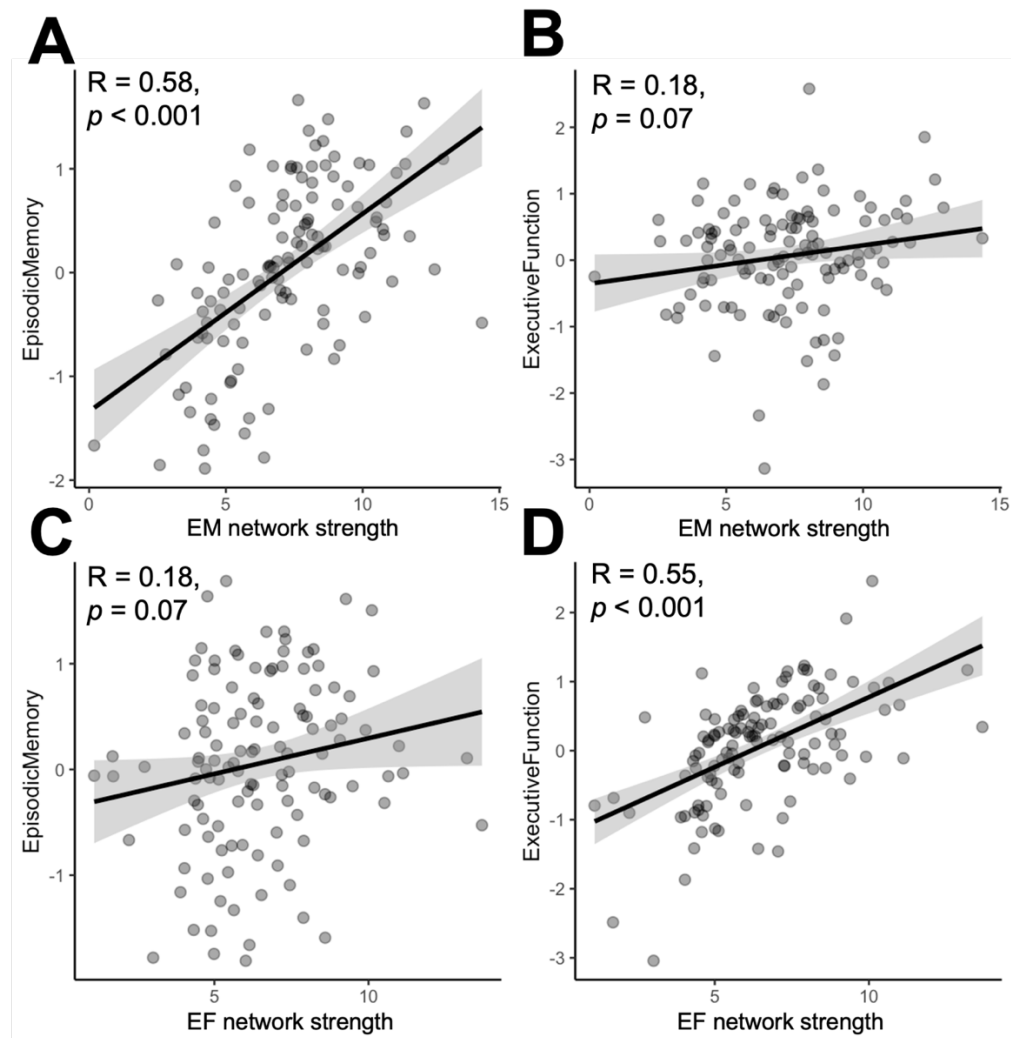


Figure S1. Network strength is highly correlated with performance in the domain by which it is defined. (A) In BACS, correlation between episodic memory (EM) network strength and EM performance. (B) Correlation between EM network strength and executive function (EF) performance. (C) Correlation between EF network strength and EM performance. (D) Correlation between EF network strength and EF performance.

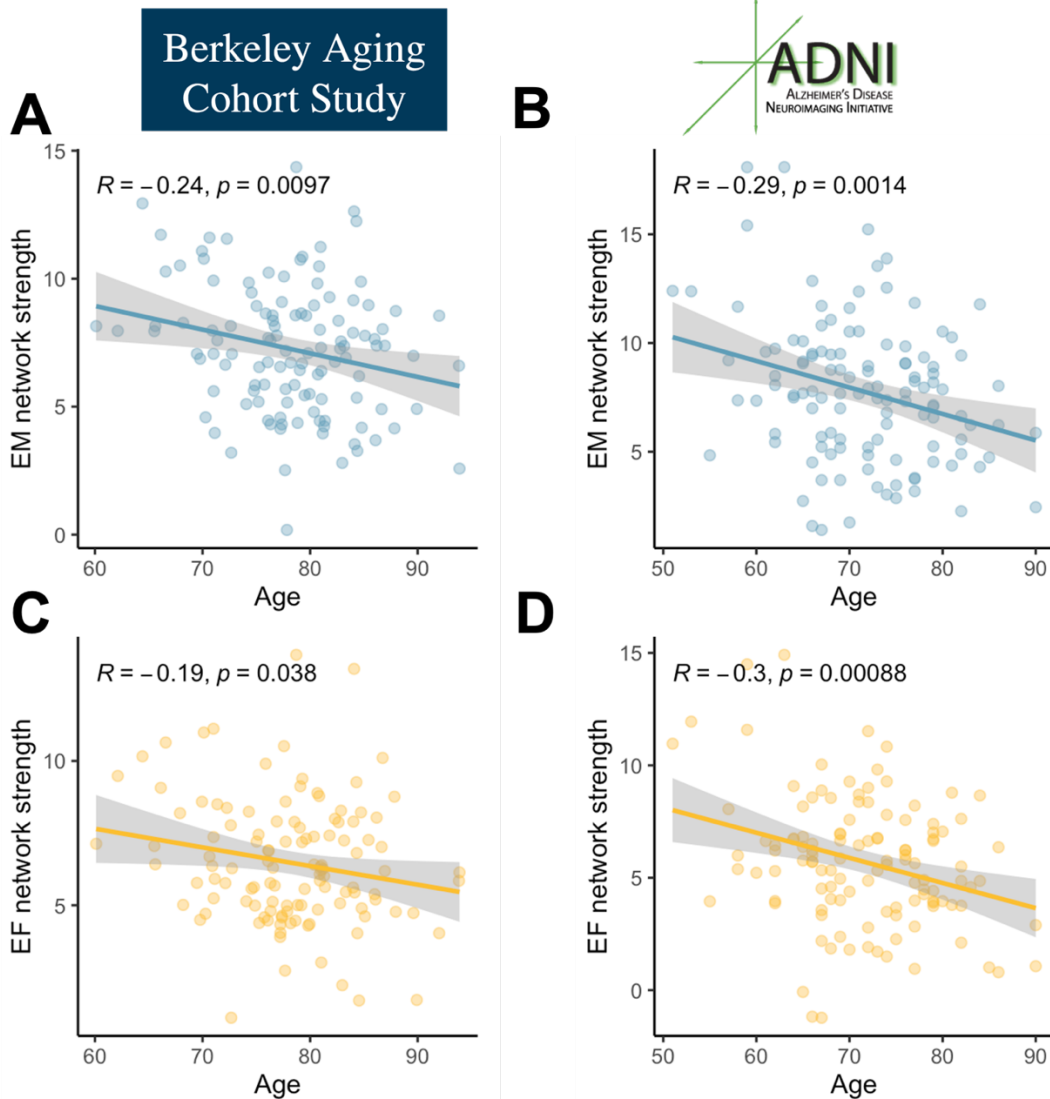


Figure S2. Age is associated with lower network strength across cohorts. (A) In BACS, greater age is correlated with lower overall episodic memory (EM) network strength. (B) In ADNI, greater age is correlated with lower overall EM network strength. (C) In BACS, greater age is correlated with lower overall executive function (EF) network strength. (D) In ADNI, greater age is associated with lower overall EF network strength.

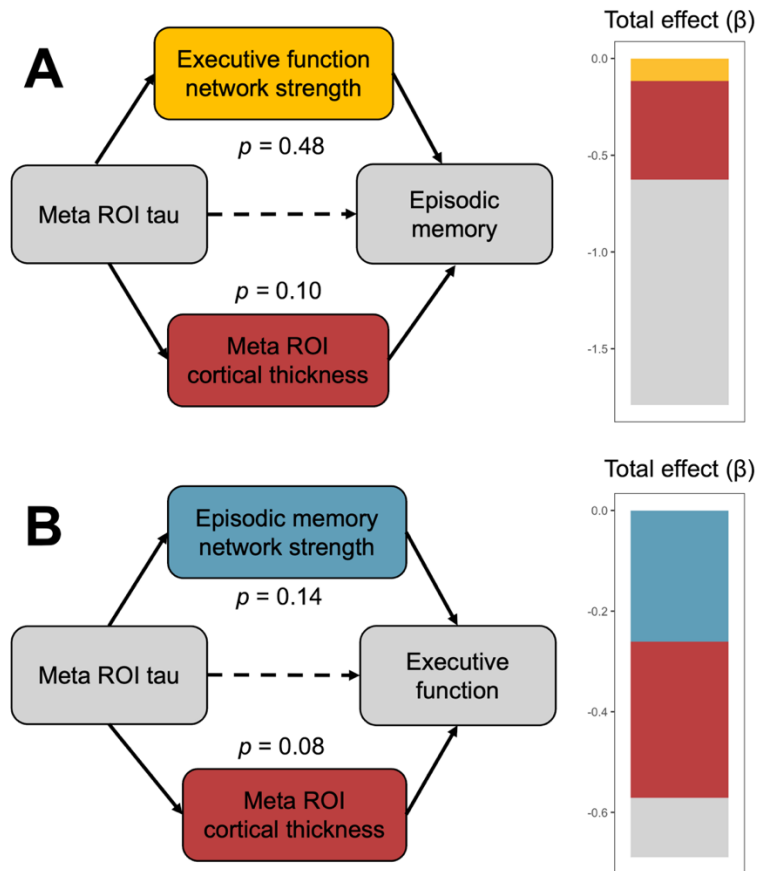


Figure S3. Network strength does not mediate performance in a distinct cognitive domain.

(A) Neither executive function network strength nor meta-ROI cortical thickness significantly mediate the relationship between meta-ROI tau burden and episodic memory performance. (B) Neither episodic memory network strength nor meta-ROI cortical thickness mediate the relationship between meta-ROI tau burden and executive function performance.

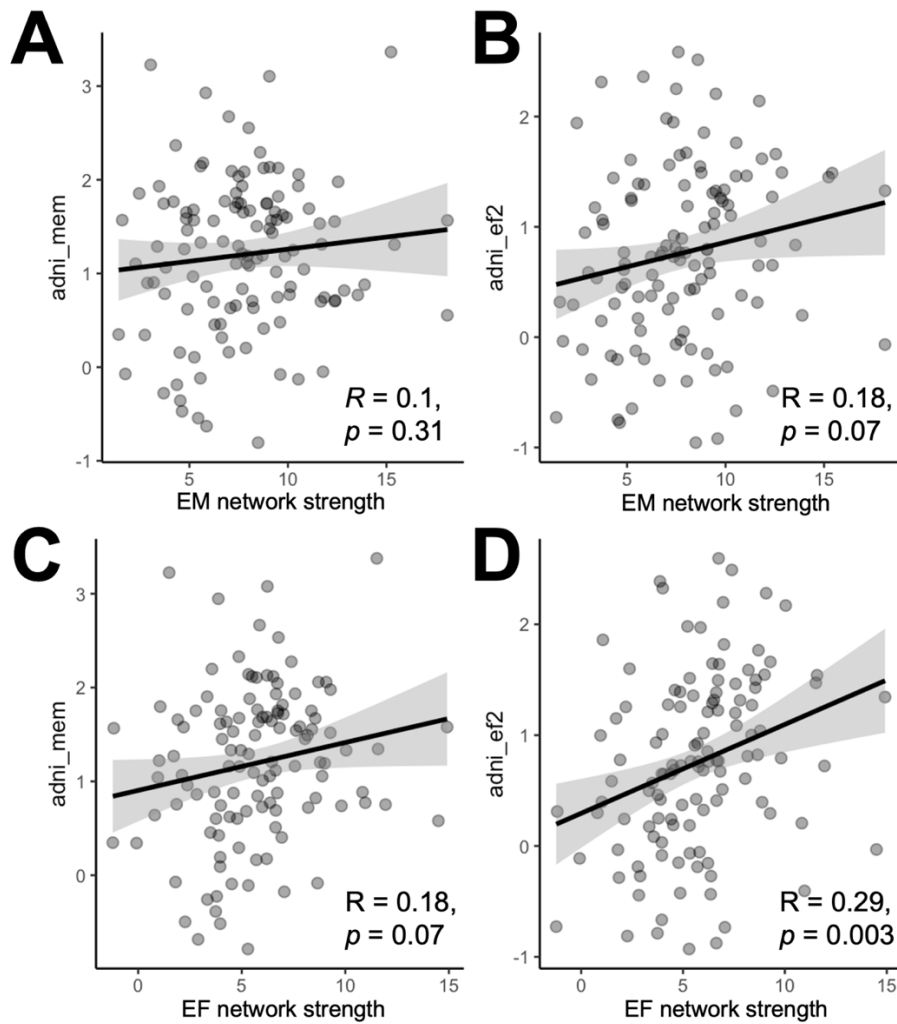


Figure S4. Replication of cognitive analyses in ADNI. Adjusting for age, sex, mean framewise displacement, rsfMRI-cognitive testing interval, and years of education, strength of the BACS-defined episodic memory (EM) network is not associated with the adni_mem measure of memory performance (A), and weakly associated with the adni_ef2 measure of executive function performance (B) in the ADNI cohort. Adjusting for these same factors, strength of the BACS-defined executive function (EF) network is weakly associated with the adni_mem measure of memory performance (C), and significantly correlated with the adni_ef2 measure of EF performance (D).

Foreword for Chapter 3

In Chapter 2, we identified functional connectivity networks specific to episodic memory or executive function performance and demonstrated that these networks are altered by the presence of tau pathology even before the onset of obvious widespread neurodegeneration. These results are an important step toward understanding whether tau pathology impacts the connectivity of networks supporting cognitive function in the aging brain. However, it is unknown whether connectivity is itself a predictor of tau spread over time, influencing both the rate and spatial progress of tau accumulation over time. Further, following the idea that connectivity may reflect pathways along which tau pathology propagates, it is unknown whether the degree of tau pathology at baseline interacts with the intrinsic connectivity of the brain to predict rate of tau accumulation. Finally, it remains to be seen if factors that have been shown to influence neural excitability, such as A β deposition and ApoE4 genotype, further modulate the interaction between baseline tau pathology and connectivity. In Chapter 3, using a multicohort sample of cognitively unimpaired older adults, we test whether the baseline connectivity strength and AD pathology in the medial temporal lobe interact with one another to predict the longitudinal rate of both tau pathology accumulation and cognitive decline. This interaction provides a possible explanation for the individual differences in both the rate and distribution of tau accumulation seen in the early stages of cognitive impairment.

Chapter 3: Pathology-connectivity interactions in unimpaired older adults predict longitudinal tau spatial progression

Jacob Zions¹, Theresa M. Harrison¹, Corrina Fonseca¹, Joe Giorgio^{1,2}, Feng Han¹, JiaQie Lee¹, William J. Jagust^{1,3} for the Alzheimer's Disease Neuroimaging Initiative

¹ Helen Wills Neuroscience Institute, UC Berkeley, Berkeley, United States

² School of Psychological Sciences, College of Engineering, Science and the Environment, University of Newcastle, Newcastle, New South Wales, Australia

³ Lawrence Berkeley National Laboratory, Berkeley, United States

**Part of the data used in preparation of this article were obtained from the Alzheimer's Disease Neuroimaging Initiative (ADNI) database (adni.loni.usc.edu). As such, the investigators within the ADNI contributed to the design and implementation of ADNI and/or provided data but did not participate in the analysis or the writing of this report. A complete listing of ADNI investigators can be found at:*

http://adni.loni.usc.edu/wpcontent/uploads/how_to_apply/ADNI_Acknowledgement_List.pdf

Author Contributions: Study design - J.Z., W.J.J.; Data organization and processing – J.Z., T.M.H., C.F., J.L., Data analysis and visualization - J.Z., C.F., W.W., Feedback and consultation – T.M.H., J. G., F.H., W.J.J., Manuscript writing – J.Z., W.J.J.; Paper editing – all authors.

Manuscript under review

Abstract

The propagation of pathological tau protein outside of medial temporal lobe and its accumulation in neocortex indicates a transition from healthy aging to Alzheimer's disease (AD). Still, the mechanisms underlying this transition are not well understood and likely rely on a confluence of detrimental factors. We investigated these processes using resting state functional MRI and longitudinal PET imaging from a multi-cohort sample of cognitively unimpaired older adults from the Berkeley Aging Cohort Study (BACS) and Alzheimer's Disease Neuroimaging Initiative (ADNI). We first measured resting state functional connectivity between hippocampus as a medial temporal lobe epicenter of tau pathology and two key regions of neocortical tau accumulation: precuneus and inferior temporal cortex. We then examined how baseline tau PET, A β PET, and ApoE4 status interacted with functional connectivity strength to predict rate of tau accumulation in downstream neocortical regions. We found that the 3-way interaction between connectivity, baseline tau, and baseline A β or ApoE4 status was associated with tau accumulation both in precuneus and inferior temporal cortex. We further showed that pathology-connectivity interactions were associated with longitudinal memory decline. Together, these findings indicate that tau propagation is influenced by the interaction of baseline functional connectivity and AD pathology, and suggest these factors may be used to predict the extent and distribution of future tau accumulation.

Introduction

Hyperphosphorylated tau protein and fibrillar beta-amyloid (A β) are the hallmark neuropathologies of Alzheimer's disease, with neurofibrillary tangles of tau accumulating both intra- and extra-cellularly and A β plaques largely found in the extracellular space¹¹⁷. A β accumulates in a diffuse manner across neocortex, but tau pathology has a stereotyped pattern of deposition, originating in medial temporal lobe before accumulating in proximal areas of the temporal and medial parietal cortices⁵. Tau pathology is found in the medial temporal lobe (MTL) of most older adults, even those without cognitive impairment¹¹⁸, but its accumulation in other areas of cortex is thought to represent a transition to Alzheimer's disease and is associated with neurodegeneration and cognitive decline^{9,119}. A variety of evidence suggests that substantial tau deposition outside of MTL occurs only with the presence of A β pathology, which is likely a key component of this process^{120,121}. However, the mechanisms of tau accumulation and its transition out of the MTL are poorly understood.

Though the spread of tau pathology in Alzheimer's disease does not always follow a single homogeneous trajectory⁵⁷, in sporadic AD tau spread outside of medial temporal lobe predominantly occurs in inferior and lateral regions of the temporal cortex, as well as frequently in medial parietal regions such as the retrosplenial cortex and precuneus^{26,38,122,123}. In particular, the inferior temporal cortex (IT) has been proposed as a key region of tau spread, with pathology in this region representing a transition to mild cognitive impairment (MCI) and AD¹²⁴. Indeed, several studies have identified inferior temporal tau accumulation as indicative of future atrophy, cognitive impairment, and functional decline^{73,125,126}. Medial parietal tau has also been observed to be an area of relatively early tau accumulation^{37,38,127}, and substantial increase in accumulation in this region is observed in MCI and AD⁴¹. This region is also notable as a site of early A β deposition and subsequent network disruption¹²⁸, and thus the pathway between medial temporal lobe structures such as hippocampus and medial parietal regions may be of particular importance for the interaction of tau and A β pathologies. Furthermore, following the proposed role of anterior temporal brain regions in object/item memory and posterior medial region in scene/context memory^{39,40,129}, there may be distinct cognitive consequences for tau accumulation in IT and medial parietal cortices. As tau spreads from its origin in medial temporal lobe to these regions, likely along distinct neuronal pathways, disruptions in neuronal signaling and neurodegeneration may lead to differentiable declines in cognitive function over time^{65,77,79}.

Considerable evidence from *in vitro* studies¹⁶, animal models^{15,31}, and human neuroimaging investigation^{13,25} suggests that tau pathology spreads throughout the cortex in a transsynaptic manner. Tau has been observed to propagate via the extracellular space from one neuron to another, and the release of tau is enhanced by neuronal activity and increases tau pathology accumulation *in vivo*^{15,16,31}. The spread of tau pathology throughout the brain has been corroborated by analysis of functional neuroimaging measures in older adults and individuals with Alzheimer's disease. In particular, resting state functional magnetic resonance imaging (rsfMRI) has been used as a way to model the spread of tau throughout the cortex^{19,20}. This work is based in the principle that functionally connected brain regions, i.e., areas of the brain that show correlated blood oxygen level-dependent (BOLD) signal over time, may represent pathways between coactive regions that facilitate the transsynaptic spread of tau pathology. Early graph theoretical analysis of rsfMRI functional connectivity in Alzheimer's disease indicated that more positively correlated (i.e., strongly connected) nodes exhibit greater tau pathology burden, favoring the notion of transneuronal tau spread rather than tau arising in areas of high metabolic demand¹³. More recently, converging evidence has shown that functional connectivity strength

between tau epicenters and other areas of cortex correlates with the degree and covariance of tau pathology in these downstream areas^{19,20,130}. Resting state functional connectivity has also been used to model future tau accumulation²⁵ and baseline functional connectivity has been shown to associate with rate of tau accumulation in individuals across the AD continuum^{21,23,34}, emphasizing the critical role of functional connectivity in AD-phenotype patterns of tau accumulation across the neocortex. However, little attention has been given to the factors that drive tau pathology spread along the pathways of earliest accumulation in cognitively unimpaired individuals.

Functional pathways in the brain have been proposed as the conduits along which neurodegenerative pathologies tend to spread²², but additional factors are needed to explain the variability in extent and distribution of pathology across individuals, particularly at the earliest stages of accumulation. If tau spreads to downstream neocortical areas along pathways of functional connectivity, the degree of tau pathology in upstream medial temporal lobe regions should influence the rate of this spread. Indeed, increased rate of tau spread into neocortex is associated with greater baseline medial temporal tau pathology and global A β burden¹²³. Further, the presence of cortical A β has been associated with hyperexcitability¹³¹ and changes in network connectivity¹¹⁴, and may in fact be a critical factor in driving medial temporal lobe excitability and tau accumulation¹³². In addition, carriers of the apolipoprotein E (ApoE) ϵ 4 allele have exhibited hyperexcitability medial temporal lobe structures such as hippocampus^{133,134}, as well as differences in connectivity of functional brain networks including default mode and temporal networks^{135,136}. ApoE4 status has also been linked to greater rates of tau accumulation^{137–139}, and recent evidence has suggested that A β may be a critical mediating factor in the relationship between ApoE genotype and connectivity-mediated tau spreading¹⁴⁰. Taken as a whole, high functional connectivity between areas of early pathology accumulation, modulated by greater baseline tau, A β , and/or ApoE genotype, may be the conditions under which tau accumulates most quickly, and therefore represent a useful framework for predicting future regional tau accumulation at the earliest stages of disease.

In the present study, we used rsfMRI and longitudinal PET imaging to investigate the spread of tau pathology from medial temporal lobe to neocortex in a multi-cohort sample of cognitively unimpaired older adults. For each individual, we measured resting state functional connectivity between hippocampus and both inferior temporal cortex and precuneus, two key potential pathways of neocortical tau accumulation^{33,123,124,130}. We then assessed the relationship between rate of longitudinal tau accumulation in these regions and interactions between baseline pathology and functional connectivity, i.e., the 3-way interaction between baseline connectivity strength, tau pathology, and cortical A β . We further tested whether ApoE genotype in these same individuals modulated this tau-connectivity relationship. Finally, we examined the relationship between pathology-connectivity interaction and decline in memory performance over time. We hypothesized that the relationship between higher functional connectivity and downstream tau accumulation would be modulated by baseline tau and A β pathology, as well as ApoE genotype, to show to strongest relationships with downstream tau accumulation. In addition, we hypothesized that the interaction of these factors would be associated with a decline in memory performance.

Methods

Participants

We included data from 110 cognitively unimpaired (CU) older adults from the Berkeley Aging Cohort Study (BACS) and Alzheimer's Disease Neuroimaging Initiative (ADNI).

Demographic information for all participants is shown in Table 1, and demographics for each sample separately is shown in Table S1. All participants had data from 3T structural MRI, resting state 3T functional MRI, flortaucipir (FTP) PET scan within 1 year of MRI ($M = 45$ days, $SD = 52$ days), A β PET imaging, and at least 2 separate FTP PET scans. We excluded 6 participants on the basis of excessive head motion during the rsfMRI scan, defined as >20% of all volumes being flagged as outliers during artifact detection. Additional inclusion criteria in BACS were 60+ years of age, cognitively normal status (Mini Mental State Examination score ≥ 25 and normal neuropsychological examination, defined as within 1.5 SD s of age, education, and sex adjusted norms; no serious neurological, psychiatric, or medical illness, no major contraindications found on MRI or PET, and independent community living status. ADNI participants were all cognitively normal or had subjective memory complaints at time of their rsfMRI scan. This study was approved by the Institutional Review Boards of the University of California, Berkeley, and the Lawrence Berkeley National Laboratory (LBNL). All participants provided written informed consent. The final sample of 110 cognitively unimpaired individuals included 67 cognitively normal BACS participants and 43 cognitively unimpaired ADNI participants.

	All ($n = 110$)	A β - ($n = 58$)	A β + ($n = 52$)
	Mean (SD) or n (%)		
Age (years)	76.4 (6.4)	74.4 (7.0)	78.7 (4.8)
Centiloids	28.0 (38.5)	3.1 (6.5)	55.7 (40.5)
Meta-ROI tau slope (SUVR/year)	0.02 (0.01)	0.01 (0.01)	0.03 (0.01)
rsfMRI-tau interval (days)	45.0 (52.0)	52.1 (53.6)	37.1 (49.4)
# FTP PET scans	2.81 (0.88)	2.79 (0.83)	2.81 (0.94)
Sex (female)	67 (60.9%)	33 (56.9)	34 (65.4%)
ApoE4+	35 (33.0%)	9 (16.0%)	26 (52%)

Table 1. Demographics of combined BACS and ADNI sample. SUVR = standard uptake value ratio, rsfMRI = resting state functional magnetic resonance imaging, FTP = flortaucipir, PET = positron emission tomography.

MRI acquisition and processing

In BACS, structural and functional MRI data were acquired on a 3T TIM/Trio scanner (Siemens Medical System, software version B17A; Siemens, Erlangen, Germany) using a 32-channel head coil. A T1-weighted whole brain magnetization prepared rapid gradient echo (MPRAGE) image was acquired for each subject (voxel size = 1mm isotropic, TR = 2300ms, TE = 2.98ms, matrix = 256 \times 240 \times 160, FOV = 256 \times 240 \times 160mm³, sagittal plane, 160 slices, 5 min acquisition time). Resting state functional MRI was then acquired using T2*-weighted echo planar imaging (EPI, voxel size = 2.6mm isotropic, TR = 1.067s, TE = 31.2ms, FA = 45, matrix 80 \times 80, FOV = 210mm, sagittal plane, 300 volumes, anterior to posterior phase encoding, ascending acquisition, 5.3 min acquisition time). During resting state acquisition, participants were told to remain awake with eyes open and focused on a white asterisk displayed on a black background.

In ADNI, structural and functional MRI data were acquired on 3T scanners with a standardized protocol across all sites (Siemens Medical Solutions, Siemens, Erlangen, Germany).

A T1-weighted whole brain magnetization prepared rapid gradient echo (MPRAGE) image was acquired for each subject (voxel size = 1mm isotropic, TR = 2300ms, TE = min full echo, matrix = 208×240×256, FOV = 208×240×256mm³, sagittal plane, 256 slices, 6 min acquisition time). Resting state functional MRI was then acquired using EPI-BOLD (voxel size = 2.5mm isotropic, TR = 0.607s, TE = 30ms, FA = 53, matrix 220x220, FOV = 160mm, sagittal plane, 976 volumes, anterior to posterior phase encoding, ascending acquisition, 10 min acquisition time, further details at <https://adni.loni.usc.edu/wp-content/uploads/2017/07/ADNI3-MRI-protocols.pdf>). Structural T1-weighted images were processed using Statistical Parametric Mapping (SPM12; <https://www.fil.ion.ucl.ac.uk/spm/software/spm12/>). Images were first segmented into gray matter, white matter, and CSF components in native space. Native space T1 images were segmented with Freesurfer v.5.3.0 (<https://surfer.nmr.mgh.harvard.edu/>) using the Desikan-Killiany atlas parcellation⁴³.

Resting state fMRI images from BACS and ADNI were preprocessed using a nearly identical SPM12 pipeline, with minimal differences to account for different acquisition parameters. Slice time correction was applied in BACS to adjust for differences in acquisition time for each brain volume, but this was not done in ADNI because of the low TR resting state data. In both cohorts, all EPIs were realigned to the first acquired EPI, and translation and rotation realignment parameters were output. Each EPI was next coregistered to each individual's native space T1 image, and these native space rsfMRI scans were used to extract the time series of each ROI in seed-to-seed functional connectivity analyses.

Functional connectivity analyses

ROI-to-ROI functional connectivity was assessed using the CONN functional connectivity toolbox (version 17e)⁴⁶ implemented in MATLAB version 2021a (The Mathworks Inc., Natick, MA). ART motion detection (https://www.nitrc.org/projects/artifact_detect/) was first performed to identify volumes of high motion, using a movement threshold of > 0.5mm/TR and a global intensity z-score of 3. Outlier volumes were flagged and included as spike regressors during denoising; no volumes were discarded. Denoising was performed with translation and rotation realignment parameters and their first-order derivatives, as well as anatomical CompCor (first five components of time series signal from white matter and CSF). A band pass filter of 0.008-0.1 Hz and linear detrending were applied to the residual time-series. For each individual, denoised time series were extracted for 87 ROIs from the Desikan-Killiany atlas⁴³. Each of these time series were then correlated (Pearson's r) and transformed (r to Fisher z). As a final step to compare functional connectivity between the BACS and ADNI samples, these values were z -scored within each sample using the mean and standard deviation of A β -individuals for each ROI-ROI connection.

We examined pathology-connectivity interactions as the 3-way interaction between functional connectivity, tau pathology, and A β pathology burden. We conducted seed-target connectivity analyses with linear regression models to assess the relationship between rate of tau pathology accumulation in the downstream target region (either precuneus or inferior temporal cortex) and the resting state functional connectivity strength between the seed region (hippocampus) and this target region, modulated by baseline tau and either baseline A β or ApoE4 status. The seed-target analysis was carried out with linear regression models and included all 2-way interactions and main effects related to the 3-way interaction of interest.

PET acquisition and processing

In BACS, PET was acquired for all participants at the Lawrence Berkeley National Laboratory (LBNL). Tau burden was assessed with ¹⁸F-Flortaucipir (FTP) synthesized at the

Biomedical Isotope Facility at LBNL as previously described²⁷. Data were collected on a Biograph TruePoint 6 scanner (Siemens, Inc) 75-115 min post-injection in listmode. Data were then binned into 4 x 5 min frames from 80-100 min post-injection. CT scans were performed before the start of each emission acquisition. In ADNI, PET data were collected using a standardized protocol of six 5-min time windows 75 to 105 min after injection. All PET images were reconstructed using an ordered subset expectation maximization algorithm, with attenuation correction, scatter correction, and smoothing with an 8mm Gaussian kernel.

Processing of FTP images was carried out in SPM12 and Freesurfer. Images were realigned, averaged, and coregistered to 3T structural MRIs. Standardized uptake value ratio (SUVR) images were calculated by averaging mean tracer uptake over the 80-100 min data and normalized with an inferior cerebellar gray reference region. The mean SUVR of each ROI (structural MRI FreeSurfer segmentation) was extracted from the native space images. Because hippocampal FTP signal is often thought to have low validity due to contamination from off-target choroid plexus signal¹⁴⁸, regional SUVRs were partial volume corrected (PVC) using a modified Geometric Transfer Matrix approach⁴⁹ as previously described⁴⁸ to minimize spillover signal between adjacent regions. Additionally, all analyses with hippocampal FTP included choroid plexus PVC SUVR as a covariate. Regional rate of tau pathology accumulation was computed using a longitudinal PET processing pipeline that defines a midpoint average MRI from all baseline and follow-up scans to coregister PET images³⁸. Tau slopes were extracted from linear mixed effects models with time from baseline as the only predictor and random effects of slope and intercept. All available FTP PET scans were included in each individual's slope calculation, and SUVR values were normalized to a hemispheric eroded white matter reference region prior to modeling to reduce variability over time. Slopes were computed for the 110 individuals in our final sample from a total of 309 FTP PET scans ($M = 2.81$, $SD = 0.88$). Defining rsfMRI scan as baseline, 72.7% of FTP scans were prospective and 27.2% of FTP scans were retrospective across all individuals. Voxelwise tau slope images were computed using all available FTP PET scans for each individual, with slope values from standard linear regression extracted for each voxel in the brain.

IN BACS, A β burden was assessed using ¹¹C-Pittsburgh Compound B (PiB), also synthesized at the Biomedical Isotope Facility at LBNL⁴⁷. Data were collected on the Biograph scanner across 35 dynamic frames for 90 min post-injection and subsequently binned into 35 frames (4 x 15, 8 x 30, 9 x 60, 2 x 180, 10 x 300, and 2 x 600s), and a CT scan was performed. All PET images were reconstructed using an ordered subset expectation maximization algorithm, with attenuation correction, scatter correction, and smoothing with a 4mm Gaussian kernel. An average of frames within the first 20 min was used to calculate the transformation matrix to coregister the PiB images to the participants' 3T structural MRI; this transformation matrix was then applied to all PiB frames. Distribution volume ratio (DVR) images were calculated with Logan graphical analysis over 35-90 min data and normalized to a whole cerebellar gray reference region^{50,51}. Global A β was calculated across cortical FreeSurfer ROIs as previously described⁵², and a threshold of DVR > 1.065 was used to categorize participants as A β -positive or A β -negative in BACS. In ADNI, A β burden was assessed using either florbetapir (FBP) or florbetaben (FBB), with an SUVR cutoff of 1.08 and 1.11 respectively used to categorize A β -positive and A β -negative participants. Finally, A β PET measures were converted to Centiloids using standard conversion formulae¹⁴⁹.

Neuropsychological measures

The visuospatial and verbal memory composites in BACS were constructed from longitudinal cognitive data taken from a standard neuropsychological battery. Longitudinal cognitive data included a total of 541 observations for the 67 individuals in BACS ($M = 8.1$, $SD = 3.3$ observations per individual). Participants had an average of 4.4 cognitive time points prior to baseline MRI ($SD = 2.3$), and an average of 3.7 cognitive time points after baseline MRI ($SD = 1.8$). Visuospatial memory was defined as a composite of Visual Reproduction I and II total recall scores. Verbal memory was defined as a composite of California Verbal Learning Test short- and long-delay free recall components. All scores were z -scored using the mean and standard deviation of each test from baseline, defined as the cognitive time point closest to each participant's rsfMRI scan. We computed rate of cognitive decline for each individual by extracting slopes from linear mixed effects models with time from baseline as the only predictor and random effects of slope and intercept.

Statistical Analyses

All terms used in linear models with interactions were mean-centered. All linear mixed effects modeling of regional tau slopes, pathology-connectivity interactions, and cognitive decline in BACS were conducted using `{nlme}` in R. Standard linear regression was carried out with `{lm}` in R. Leave-one-out cross validation modeling of tau accumulation was conducted with `{sklearn}` in python.

Data Visualization

Surface renderings of voxelwise tau slope images were visualized using the BrainNet Viewer toolbox (<http://www.nitrc.org/projects/bnv/>) in MATLAB Version 23.a. Ball-and-stick plots to visualize connectivity were created using the *nilearn* glassbrain plotting function in python (https://nilearn.github.io/dev/modules/generated/nilearn.plotting.plot_glass_brain.html). Scatter plots were created using the `{ggplot2}` package in R version 4.2.0 to visualize effects from linear regression models. The `{effects}` package in R was used to visualize interaction effects from linear regression models. The *seaborn.regplot* was used for scatter plots to visualize the correlation between predicted and observed outcomes from leave-one-out cross validation.

Results

Baseline tau, $A\beta$, and functional connectivity interaction is associated with longitudinal tau

To investigate the association between functional connectivity, baseline pathology, and longitudinal rate of tau accumulation, we utilized a sample of 110 cognitively unimpaired older adults (Table 1), $n = 67$ individuals from the Berkeley Aging Cohort Study (BACS) and $n = 43$ individuals from the Alzheimer's Disease Neuroimaging Initiative (ADNI). Participants were between 61 – 93 years of age ($M = 76.4$ years, $SD = 6.4$ years) cognitively unimpaired at baseline with an interval between 3T rsfMRI and flortaucipir (FTP) PET scans of no greater than 1 year ($M = 45$ days, $SD = 52$ days). Participants also had a concurrent $A\beta$ PET scan, and at least 2 FTP PET time points. A subset of 106 individuals had genotype data available to determine ApoE4 status. There were no significant differences in demographics between participants from the BACS and ADNI cohorts (Table S1), though ADNI individuals had a shorter interval between baseline rsfMRI scan and FTP PET scan ($p = 0.02$). For all participants, resting state functional connectivity between native space Desikan-Killiany atlas regions was computed, and functional connectivity values were normalized within cohorts to be able to account for acquisition differences when comparing these values between BACS and ADNI (see Methods). In addition, we computed FTP slope using linear regression for each subject in each voxel of the brain. Visualizing this average voxelwise longitudinal rate of change, tau accumulation over time

was observed primarily in lateral and inferior temporal cortices as well as medial parietal areas bilaterally, and was visibly higher in A β ⁺ compared to A β ⁻ individuals (Figure 1).

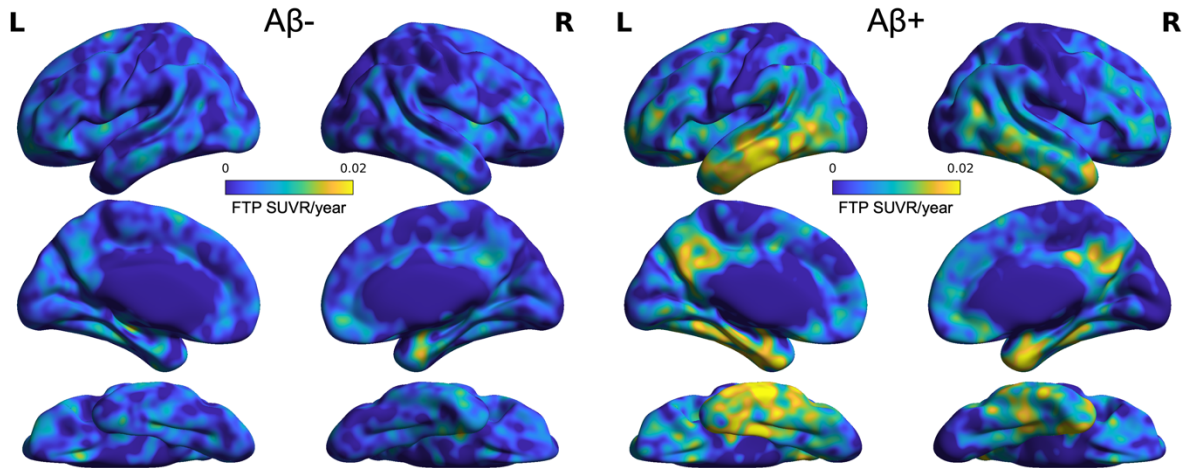


Figure 1. Voxelwise tau accumulation in combined sample of cognitively unimpaired older adults. Longitudinal rate of tau accumulation was computed using a simple linear regression model for all flortaucipir (FTP) PET scans for each cognitively unimpaired (CU) individual in the combined sample of BACS and ADNI participants. Group average voxelwise FTP slopes (SUVR/year) are plotted for A β ⁻ (*left*) and A β ⁺ (*right*) subjects.

We next investigated the association between rate of tau pathology accumulation and functional connectivity in 2 regions of interest: precuneus (PrC) and inferior temporal cortex (IT). Partial-volume corrected (PVC) rate of tau accumulation in each region was first calculated using linear mixed effects models with time from baseline as the only predictor and random effects of slope and intercept. These tau accumulation rates were then used as the dependent variable in linear mixed effects models testing the 3-way interaction (and all related 2-way interactions and main effects) between hippocampus-precuneus resting state functional connectivity (HC-PrC), baseline hippocampal tau, and baseline cortical A β burden (Centiloids), with additional fixed effects for age, sex, and choroid plexus FTP SUVR and a random effect of cohort. We found a main effect of greater baseline HC tau on rate of tau accumulation in downstream precuneus ($\beta = 0.014$, $p = 0.025$), and further observed a 2-way interaction between HC-PrC and baseline HC tau, such that there was a closer association between HC tau and precuneus tau accumulation for stronger HC-PrC connectivity ($\beta = 0.016$, $p = 0.016$). Critically, we also observed a 3-way interaction between HC-PrC, baseline HC tau, and baseline Centiloids ($\beta = 0.006$, $p = 0.038$), indicating that the strongest association between HC tau and precuneus tau accumulation was present in individuals with greater HC-PrC connectivity and greater baseline A β burden (Figure 2). This 3-way interaction was also significant in the BACS and ADNI cohorts separately (Figure S1). To test the specificity of these pathology-connectivity interactions along this hypothesized hippocampus-precuneus pathway, we repeated these analyses using parahippocampal gyrus as a control upstream medial temporal lobe region and did not find that precuneus tau accumulation was related to the 3-way interaction between baseline parahippocampal-precuneus connectivity, parahippocampal tau, and Centiloids ($\beta = 0.00002$, $p = 0.90$). Examining superior parietal cortex as a control downstream neocortical region, we did not

find that tau accumulation in this region was related to the 3-way interaction between hippocampus-superior parietal connectivity, hippocampal tau, and Centiloids ($\beta = 0.0001$, $p = 0.41$).

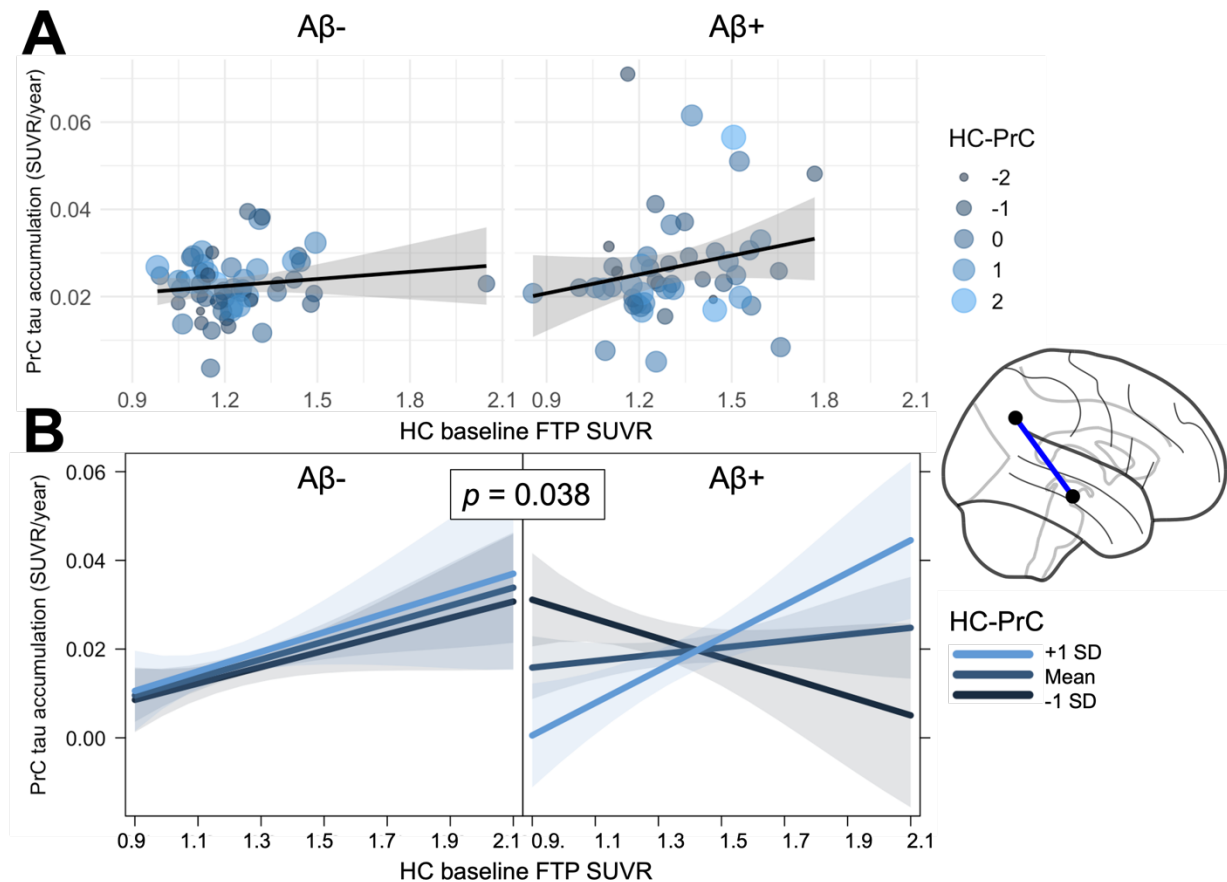


Figure 2. Hippocampus-precuneus pathology-connectivity interaction is associated with precuneus tau accumulation. (A) Rate of tau accumulation in precuneus (PrC) as a function of baseline hippocampal (HC) tau signal. Points represent a single $A\beta^-$ (left) or $A\beta^+$ (right) subject, with size and color corresponding to strength of functional connectivity between hippocampus and precuneus (HC-PrC). (B) From a linear model adjusting for age, sex, and choroid plexus FTP signal, visualization of association between precuneus rate of tau accumulation and the 3-way interaction of baseline HC tau, Centiloids, and HC-PrC functional connectivity. Lines represent predicted association for 3 different levels of HC-PrC connectivity. Panels visualize predicted associations at mean Centiloid value of $A\beta^-$ (left) and $A\beta^+$ (right) participants.

Similarly, we examined the association between rate of tau accumulation in IT and the 3-way interaction between hippocampus-inferior temporal resting state functional connectivity (HC-IT), baseline hippocampal tau, and baseline cortical $A\beta$. We found a main effect of greater baseline HC tau on rate of tau accumulation in IT ($\beta = 0.028$, $p = 0.049$), though the 2-way interaction between HC-IT and baseline HC tau did not reach significance ($\beta = 0.016$, $p = 0.23$). The 3-way interaction between HC-IT, baseline HC tau, and baseline Centiloids was associated with IT tau accumulation ($\beta = 0.007$, $p = 0.067$), suggesting a trend towards the relationship between HC-IT connectivity being modulated by baseline tau and $A\beta$ pathology (Figure 3).

Modeling these relationships in each cohort separately, this 3-way interaction was significantly associated with IT tau accumulation in ADNI, but not in BACS (Figure S2). Again, we repeated these analyses using parahippocampal gyrus as a control upstream medial temporal lobe region and did not find that inferior temporal tau accumulation was related to the 3-way interaction between baseline parahippocampal-inferior temporal connectivity, parahippocampal tau, and Centiloids ($\beta = -0.0001, p = 0.64$). Examining superior temporal cortex as a control downstream neocortical region, we did not find that tau accumulation in this region was related to the 3-way interaction between hippocampus-superior temporal connectivity, hippocampal tau, and Centiloids ($\beta = -0.00006, p = 0.83$).

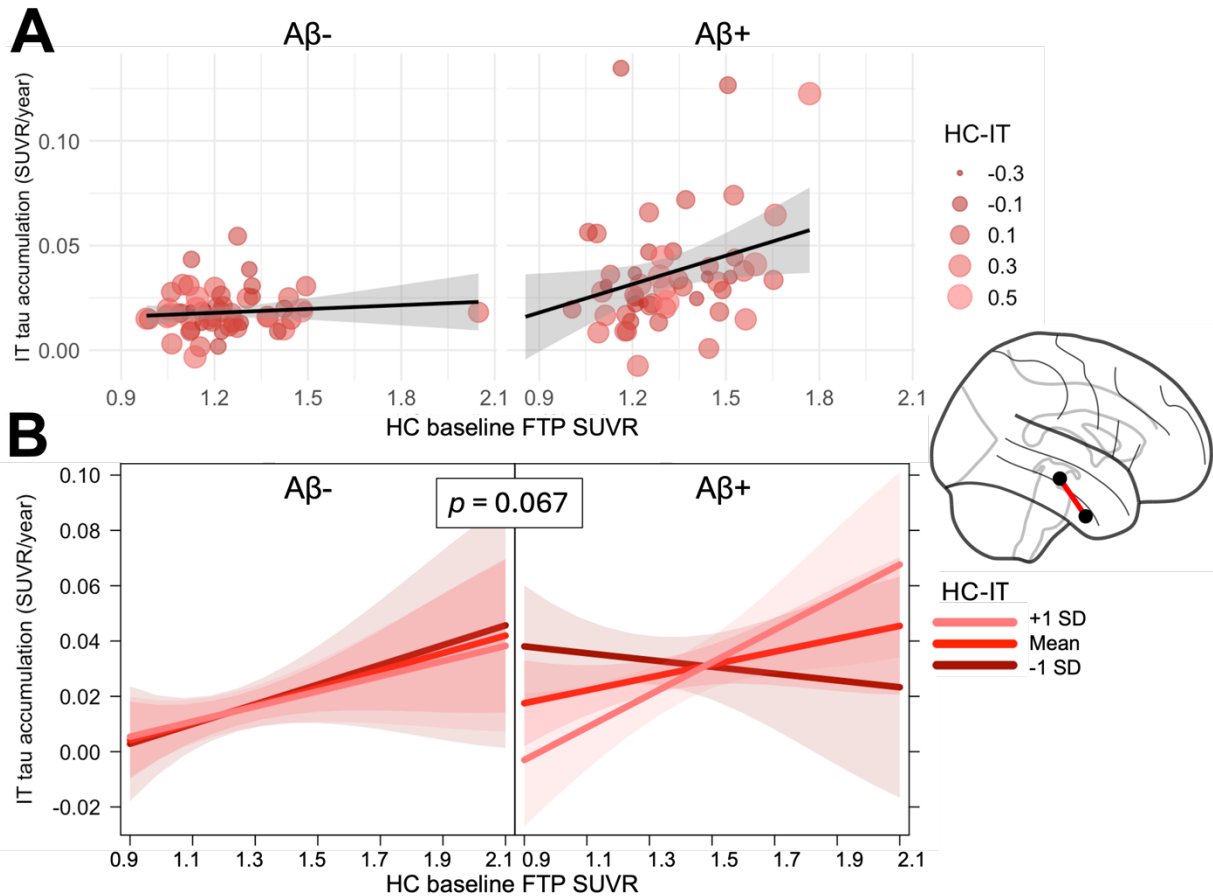


Figure 3. Hippocampus-precuneus pathology-connectivity interaction is associated with inferior temporal tau accumulation. (A) Rate of tau accumulation in inferior temporal (IT) cortex as a function of baseline hippocampal (HC) tau signal. Points represent a single $A\beta^-$ (left) or $A\beta^+$ (right) subject, with size and color corresponding to strength of functional connectivity between hippocampus and inferior temporal cortex (HC-IT). (B) From a linear model adjusting for age, sex, and choroid plexus FTP signal, visualization of association between precuneus rate of tau accumulation and the 3-way interaction of baseline HC tau, Centiloids, and HC-IT functional connectivity. Lines represent predicted association for 3 different levels of HC-PrC connectivity. Panels visualize predicted associations at mean Centiloid value of $A\beta^-$ (left) and $A\beta^+$ (right) participants.

ApoE4 genotype modulates connectivity association with tau accumulation

We next tested if there were dissociable effects of ApoE4 status and A β on the relationship between baseline tau, connectivity, and longitudinal tau accumulation. We again used linear mixed effects modeling with a random effect of cohort to assess the relationship between precuneus tau accumulation and the 3-way interaction between ApoE4 carrier status, baseline HC tau, and HC-PrC connectivity. We did not observe any significant main effects or 2-way interactions, but the 3-way interaction was associated with precuneus tau accumulation ($\beta = 0.032$, $p = 0.04$), such that the strongest association between baseline HC tau and precuneus tau accumulation tended to be present in ApoE4+ individuals with greatest HC-PrC connectivity (Figure 4a). This 3-way interaction remained significantly associated with precuneus tau accumulation in a separate model adjusting for the main effect of baseline Centiloids ($\beta = 0.034$, $p = 0.028$). In analyses separated by cohort, the interaction was significantly associated with PrC tau accumulation in BACS, but not in ADNI (Figure S3). Next, in a model predicting IT accumulation, we found a significant 3-way interaction between ApoE4 carrier status, baseline tau, and HC-IT connectivity ($\beta = -0.087$, $p = 0.001$), indicating that HC-IT connectivity tended to modulate the association between HC baseline tau and precuneus tau accumulation specifically in ApoE4- individuals (Figure 4b). This interaction remained significantly associated with IT tau accumulation in a separate model with baseline Centiloids as a main effect ($\beta = -0.083$, $p = 0.001$), but not when analyzed in each cohort independently (Figure S4).

Pathology-connectivity interactions are linked to memory decline

Finally, we investigated whether pathology-connectivity interactions were also related to decline in episodic memory, a critical downstream consequence of tau pathology accumulation. For this analysis, we focused on the subsample of 67 BACS participants with 546 longitudinal neuropsychological testing time points spanning up to 18 years ($M = 8.9$, $SD = 4.0$) and up to 15 cognitive time points per individual ($M = 8.1$, $SD = 3.3$). Similar to rate of tau accumulation, rate of memory decline was calculated using linear mixed effects models with time from baseline as the only fixed predictor and random effects of slope and intercept. Given the proposed role of the medial parietal cortex in spatial processing and memory¹²⁹, we examined the relationship between pathology-connectivity interactions and a visuospatial memory composite of Visual Reproduction I and II performance, as well as a verbal memory composite of the California Verbal Learning Test (CVLT) short- and long-delay free recall components.

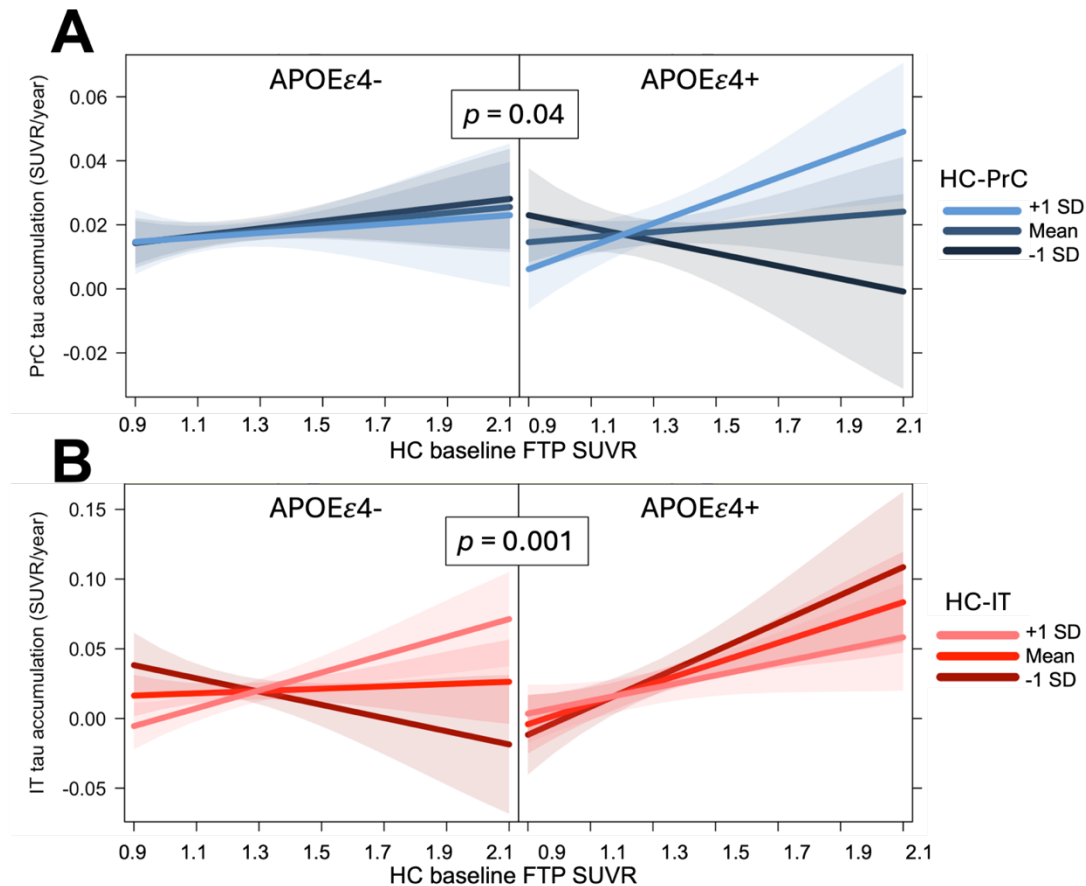


Figure 4. Connectivity modulated by ApoE4 genotype is associated with rate of tau accumulation. (A) Visualization of 3-way interaction between hippocampus-precuneus functional connectivity (HC-PrC), baseline HC tau, and ApoE4+ status. From a linear model adjusting for age, sex, and choroid plexus FTP signal, association between HC baseline tau is modulated by HC-PrC and ApoE4 positivity. (B) Visualization of 3-way interaction between hippocampus-inferior temporal functional connectivity (HC-IT), baseline HC tau, and ApoE4+ status. From a linear model adjusting for age, sex, and choroid plexus FTP signal, association between HC baseline tau is modulated by HC-IT and ApoE4 negativity. Lines represent predicted association for 3 different levels of functional connectivity. Panels visualize predicted associations for ApoE4- (left) and ApoE4+ (right) participants.

We first assessed the association between rate of visuospatial memory decline and pathology- connectivity interactions at baseline using linear regression models adjusting for age, sex, and choroid plexus FTP SUVR. We observed a main effect of baseline HC tau on rate of visuospatial memory decline ($\beta = -0.08$, $p = 0.01$), as well as a 2-way interaction of HC-PrC and Centiloids ($\beta = -0.34$, $p = 0.03$) indicating that greater HC-PrC connectivity was associated with less steep memory decline at lower baseline Centiloids. Critically, we also observed a significant 3-way interaction between baseline HC-PrC connectivity, HC tau, and Centiloids ($\beta = -3.97$, $p = 0.008$), such that the greatest decline in visuospatial memory performance occurred in individuals with highest baseline A β , HC-PrC connectivity, and HC tau (Figure 5a). We repeated this analysis examining the interaction between baseline connectivity, pathology, and ApoE

genotype and including a main effect of Centiloids in the linear regression model, and again found a significant 3-way interaction between baseline HC-PrC connectivity, HC tau, and ApoE genotype ($\beta = -0.68, p = 0.017$), such that the greatest decline in visuospatial memory performance was observed in ApoE4+ individuals with greater HC-PrC connectivity and greater HC tau (Figure 5b). We replicated this analysis using HC-IT connectivity in place of HC-PrC but did not observe any significant pathology-connectivity interactions associated with decline in visuospatial memory performance.

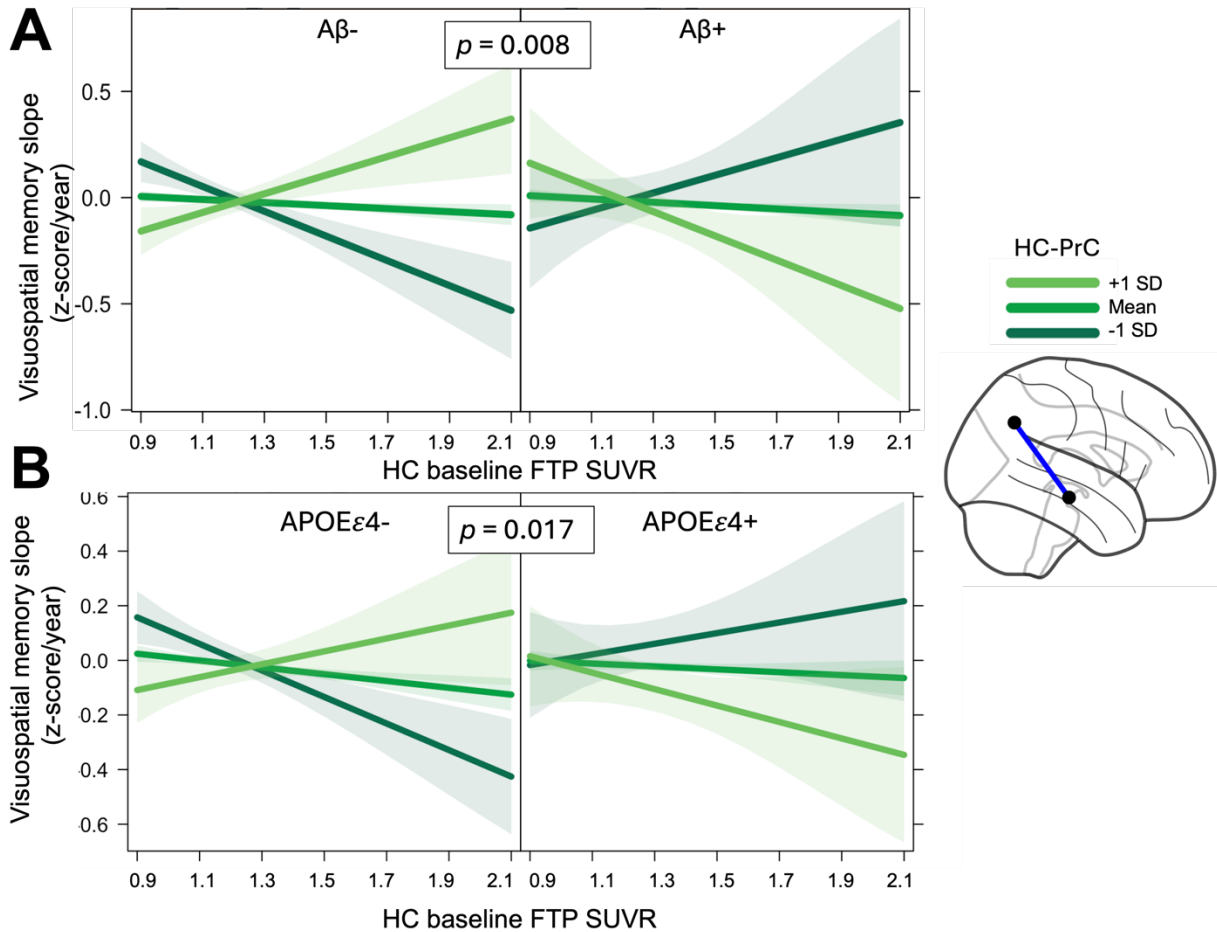


Figure 5. HC-PrC pathology-connectivity interaction is associated with visuospatial memory decline. (A) Visualization of 3-way interaction between hippocampus-precuneus functional connectivity (HC-PrC), baseline HC tau, and Centiloids. Adjusting for age, sex, and choroid plexus FTP signal, association between HC baseline tau and rate of decline in visuospatial memory performance is modulated by HC-PrC and Centiloids. Panels visualize predicted associations at mean Centiloid value of $A\beta^-$ (left) and $A\beta^+$ (right) participants. (B) Visualization of 3-way interaction between hippocampus-precuneus functional connectivity (HC-PrC), baseline HC tau, and ApoE4 status. Adjusting for age, sex, and choroid plexus FTP signal, association between HC baseline tau and rate of decline in visuospatial memory performance is modulated by HC-PrC and ApoE4 positivity. Lines represent predicted association for 3 different levels of functional connectivity. Panels visualize predicted associations for ApoE4- (left) and ApoE4+ (right) participants.

In assessing rate of change in verbal memory performance, we observed a main effect of baseline HC tau on verbal memory decline ($\beta = -0.05, p = 0.04$), and again observed a 2-way interaction of HC-PrC and Centiloids ($\beta = -0.29, p = 0.01$). The 3-way interaction between baseline HC-PrC connectivity, HC tau, and Centiloids was not significant ($\beta = -1.99, p = 0.07$), but suggested a trend toward individuals with highest baseline A β , HC-PrC connectivity, and HC tau exhibiting the steepest verbal memory decline (Figure S5). Again, we repeated this analysis examining the interaction between baseline connectivity, pathology, and ApoE genotype and including a main effect of Centiloids in the linear regression model, but did not find a significant 3-way interaction ($\beta = -0.10, p = 0.66$). Finally, we again carried out these analyses using HC-IT connectivity in place of HC-PrC, but did not observe any significant pathology-connectivity interactions associated with decline in verbal memory performance.

Discussion

This study utilized rsfMRI, longitudinal PET imaging, and longitudinal cognitive performance data to investigate the factors involved in the earliest tau accumulation in cognitively unimpaired older adults. We found that the interaction of A β pathology and/or ApoE genotype, baseline tau pathology, and functional connectivity between hippocampus and key regions of downstream tau accumulation was associated with the fastest increases in tau pathology in these regions. These pathology-connectivity interactions were further associated with domain-specific decline in cognitive function in these unimpaired individuals. Taken together, these results suggest that the strength of connectivity between hippocampus and downstream regions is modulated by the degree of baseline AD pathology to predict tau accumulation, and the interactions between these factors have the potential to explain differences in rates and distribution of tau accumulation at the earliest stages of cognitive impairment.

A particularly intriguing finding motivating the joint study of network connectivity and neurodegenerative disease is that patterns of regional brain atrophy tend to match the topography of functional and structural networks in healthy individuals¹². This insight has led to the investigation of functional connectivity in aging and Alzheimer's disease as a potential mechanism that drives the spread of pathology throughout the brain, with corresponding consequences for regional brain atrophy and domain-specific cognitive decline. From the cortical origin of tau in the transentorhinal region, tau may spread along pathways of strong functional connectivity first to hippocampus¹³⁰ and subsequently to other areas of cortex¹⁹ known to accumulate pathology and leading to neurodegeneration later in disease progression⁸³. Our results support this view, showing that the association between tau accumulation and functional connectivity between hippocampus and both precuneus and inferior temporal cortex in part depends on the degree of baseline AD pathology. We found this relationship to be somewhat more robust for the precuneus than for inferior temporal cortex, which may reflect differences in fMRI signal in these regions, as inferior temporal areas tend to have a relatively high degree of signal disruption¹⁴¹. Still, strength of hippocampal-medial parietal lobe connectivity has previously been shown to relate to tau pathology burden in the medial parietal lobe cross-sectionally^{33,130}, and disruption of hippocampal network connectivity has been proposed as the basis of cognitive deficits in AD¹⁴².

We further showed that the relationship between functional connectivity and tau accumulation was modulated by both baseline tau and global A β burden. A β has been associated with changes in network connectivity early in disease progression¹³², and modeling of tau spreading in individuals along the AD continuum has suggested that there are both local and remote tau/A β interactions that influence the propagation of tau pathology¹²⁴. Thus, greater

cortical A β pathology in individuals in our study may reflect changes in connectivity between hippocampus and downstream cortical areas that facilitate the fastest accumulation of tau. We also found that ApoE genotype modulated this relationship, as carriers of the ApoE4 gene exhibited greater rate tau accumulation in precuneus with greater HC-PrC functional connectivity and baseline tau pathology. This finding may be related to the underlying influence of ApoE4 genotype on AD pathology, as patterns of tau spread in cortex are spatially linked with ApoE messenger RNA expression¹⁴³. Further, A β burden has been proposed as a mediating factor in the relationship between ApoE4 risk and change in tau pathology over time in nondemented individuals¹⁴⁰. It may therefore be that for unimpaired individuals at the earliest stages of tau pathology spread, ApoE4 positivity modulates the relationship between connectivity and tau accumulation via its influence on cortical A β burden. Furthermore, given our finding that ApoE4 status modulated this relationship independently of A β , ApoE4 genotype may have additional influence on cellular hyperactivity^{133,134,144}, further driving downstream tau pathology spread¹⁴⁵. However, this framework is complicated by our finding that the strongest relationship between functional connectivity and tau accumulation in IT was in fact found in ApoE4 noncarriers. One possible explanation is that because IT is an area of very early neocortical tau accumulation, ApoE4 carriers already demonstrate alterations in network connectivity^{135,136} such that greater connectivity is no longer associated with the greatest degree of tau accumulation. This finding also underscores that there are likely multiple interacting factors that influence the extent and distribution of downstream pathology accumulation, and it may be that excitatory changes associated with ApoE genotype^{134,135} outweigh those associated with intrinsic connectivity strength in some pathways. This possibly should be further investigated in larger samples with more ApoE genotypic diversity.

Our finding that HC-PrC pathology-connectivity interactions was related to rate of visuospatial memory decline, more so than verbal memory decline, represents a compelling neuropsychological consequence of the modulation of functional connectivity by AD pathology. Both in individuals with lower levels of baseline A β and in ApoE4- individuals, we observed that greater functional connectivity strength was associated with slower rates of visuospatial memory decline even with greater high baseline hippocampal tau pathology. This relationship was markedly different at high levels of cortical A β and in ApoE4+ individuals, however, where greater hippocampal tau and HC-PrC was associated with the steepest rates of visuospatial memory decline (Figure 5). This finding comports with the observed relationships between HC-PrC pathology-connectivity interaction and tau accumulation, in that the 3-way interaction between functional connectivity, baseline tau, and baseline A β /ApoE4 genotype is associated not only with faster tau pathology accumulation but also faster cognitive decline. Furthermore, It is also notable that we observed this relationship to be particularly strong for visuospatial memory decline and HC-PrC connectivity given the proposed role of medial parietal structures in both episodic memory and visuospatial processing^{39,68}. Because we did not observe strong associations between HC-IT connectivity and tau accumulation in the BACS sample, future work is needed to assess if this connectivity is also related to cognitive decline in domains that rely on temporal structures such as object/face recognition^{39,146}. Taken together, the present findings suggest that greater functional connectivity between medial temporal lobe and neocortical regions in the absence of AD pathology is in fact beneficial for cognitive function, but the presence of A β and/or ApoE4 genotype may alter the excitatory/inhibitory balance of neural circuits along robust functional connections^{65,147}, leading to the spread of pathological tau protein and subsequent cognitive decline.

Conclusion

The present study provides evidence that longitudinal tau accumulation can be predicted by the interaction of baseline AD pathology and resting state functional connectivity between vulnerable regions of the brain. Within the framework of networks as both conduits and drivers of neurodegenerative pathology in the aging brain²², functional connections may be viewed as the pathways along which tau pathology spreads, and factors such as upstream tau pathology, global A β burden, and ApoE genotype represent modulating factors that influence the spatiotemporal pattern of future tau spreading. By focusing on cognitively unimpaired individuals i.e. those in the earliest stages of tau propagation, this study points to characteristics that could help identify which individuals are at greatest risk of progression to AD and could therefore benefit the most from pathology-lowering interventions. Future work should focus on the integrity of structural connections measured with diffusion MRI to provide further insight into how the structural and functional pathways in the brain provide a roadmap for neuropathologies to propagate, and what other modulating factors have the potential to exacerbate or slow the spread of pathology along these pathways.

Supplementary Materials

	BACS CU (n = 67)	ADNI CU (n = 43)	BACS vs. ADNI
	Mean (<i>SD</i>) or <i>n</i> (%)		
Age (years)	77.1 (5.8)	75.4 (7.3)	<i>p</i> = 0.22
Centiloids	23.7 (32.6)	34.6 (45.9)	<i>p</i> = 0.18
Meta-ROI tau slope (SUVR/year)	0.02 (0.01)	0.02 (0.01)	<i>p</i> = 0.20
rsfMRI-tau interval (days)	54.2 (54.3)	30.7 (45)	<i>p</i> = 0.02
Sex (female)	38 (57%)	29 (67%)	<i>p</i> = 0.36
Aβ+	33 (49%)	19 (44%)	<i>p</i> = 0.75
APOε4+	22 (34%)	13 (31%)	<i>p</i> = 0.88

Table S1. Demographics of separated BACS and ADNI cohorts of cognitively unimpaired (CU) older adults.

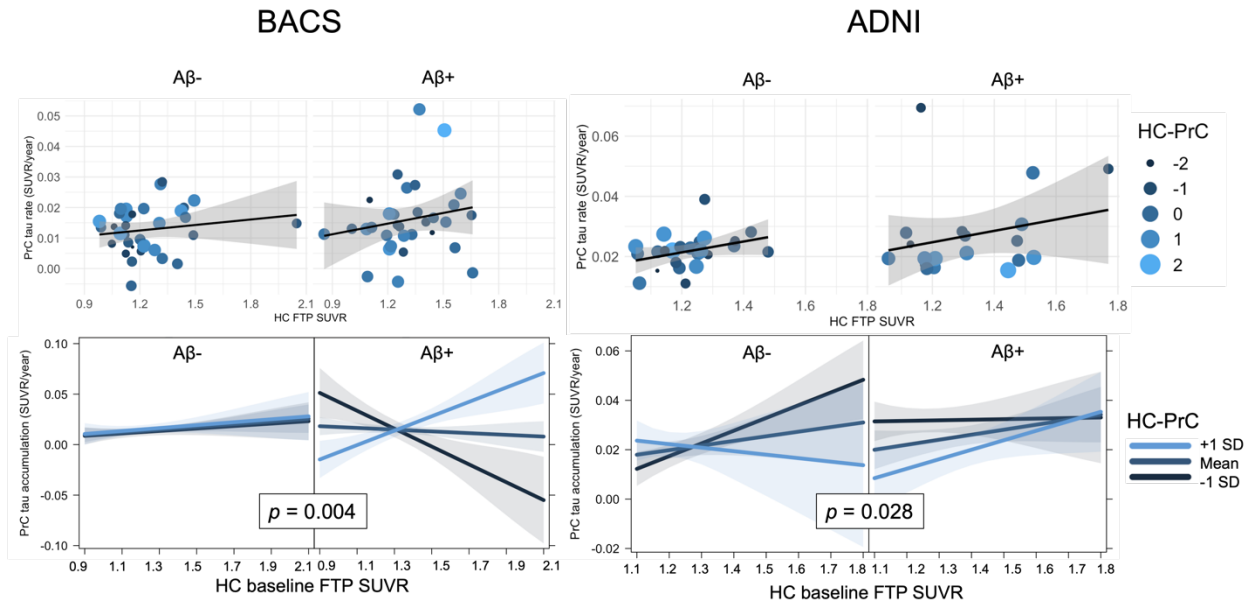


Figure S1. Pathology- connectivity interaction is associated with precuneus tau accumulation in separate cohorts. Lines represent predicted association for 3 different levels of HC-PrC connectivity. Panels visualize predicted associations at mean Centiloid value of A β - (*left*) and A β + (*right*) participants.

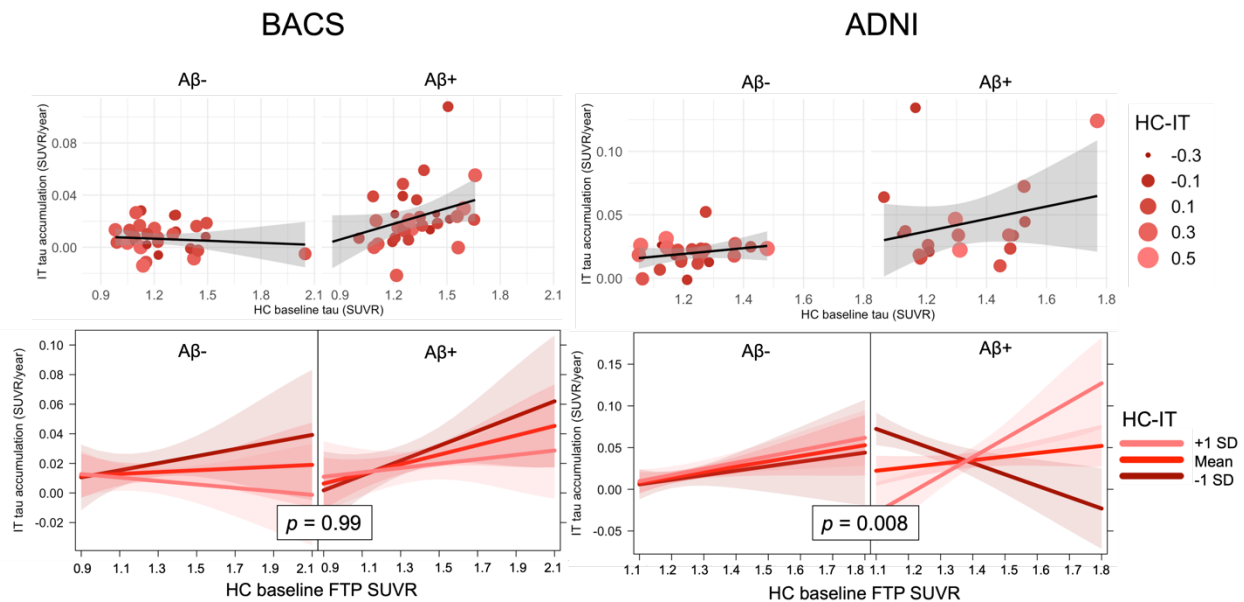


Figure S2. Pathology-connectivity interaction is associated with inferior temporal tau accumulation in separate cohorts. Lines represent predicted association for 3 different levels of HC-IT connectivity. Panels visualize predicted associations at mean Centiloid value of A β - (*left*) and A β + (*right*) participants.

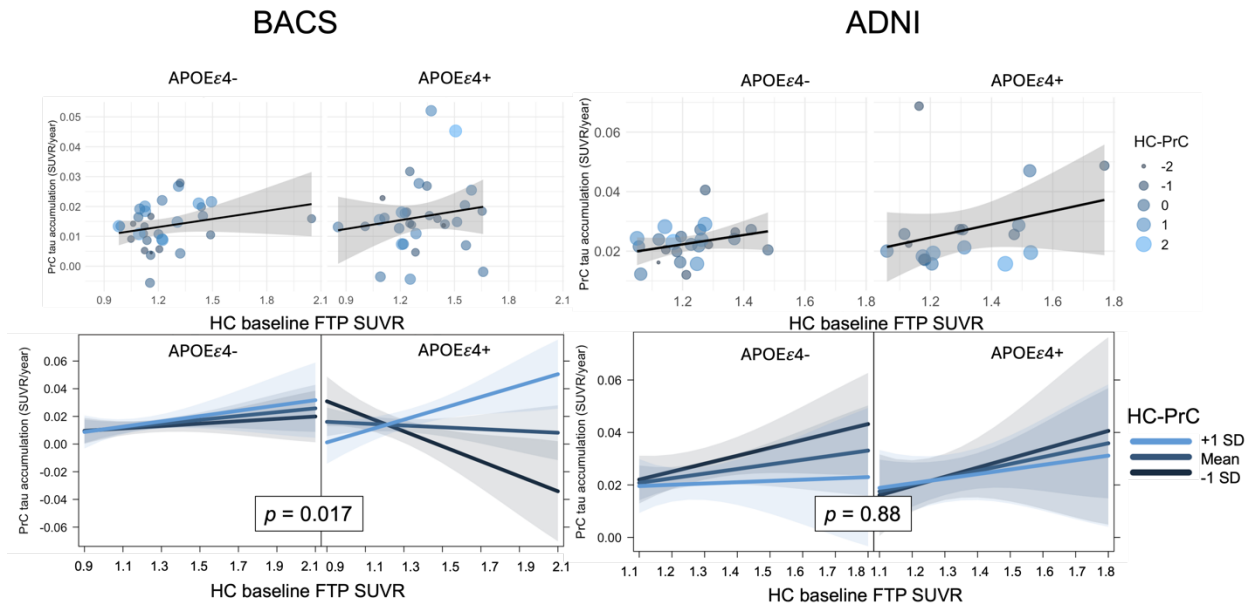


Figure S3. Connectivity modulated by ApoE4 genotype is associated with precuneus tau accumulation in separate cohorts. Lines represent predicted association for 3 different levels of functional connectivity. Panels visualize predicted associations for ApoE4- (left) and ApoE4+ (right) participants.

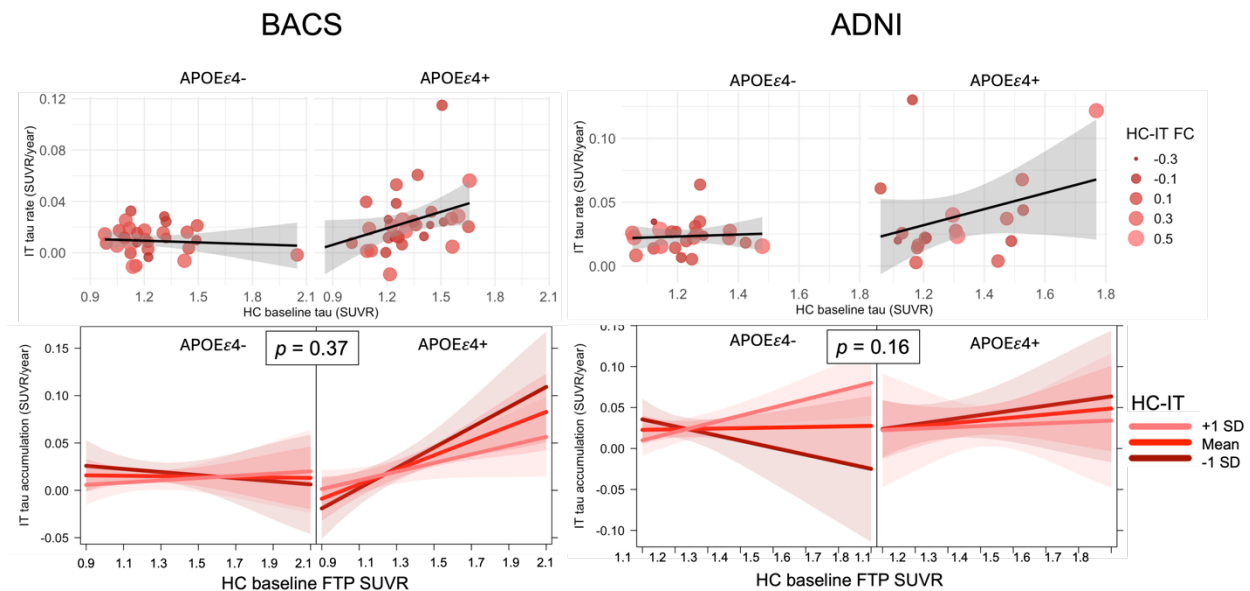


Figure S4. Connectivity modulated by ApoE4 genotype is associated with inferior temporal tau accumulation in separate cohorts. Lines represent predicted association for 3 different levels of functional connectivity. Panels visualize predicted associations for ApoE4- (left) and ApoE4+ (right) participants.

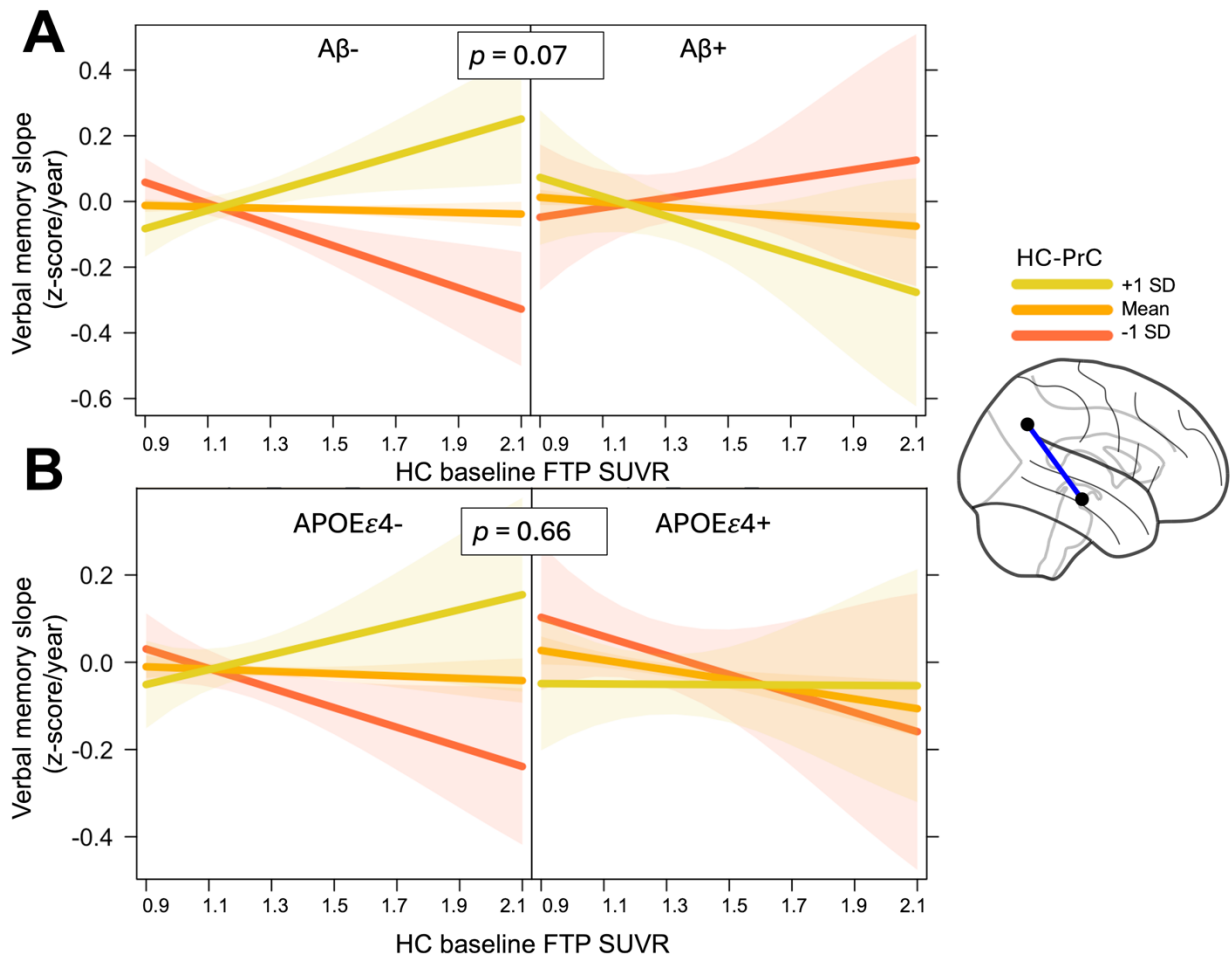


Figure S5. Association of HC-PrC pathology-connectivity interaction and verbal memory decline. (A) Visualization of 3-way interaction between hippocampus-precuneus functional connectivity (HC-PrC), baseline HC tau, and Centiloids. (B) Visualization of 3-way interaction between hippocampus-precuneus functional connectivity (HC-PrC), baseline HC tau, and *ApoE4* status. Lines represent predicted association for 3 different levels of functional connectivity. Panels visualize predicted associations for *ApoE4*- (left) and *ApoE4*+ (right) participants.

Conclusion

Here, we outline the contributions of functional networks of the aging brain in facilitating the spread and accumulation of AD-related tau pathology, as well as the corresponding consequences for cognitive function that this pathology may illicit. In Chapter 1, we show that resting state functional connectivity strength between medial temporal lobe and medial parietal cortex is associated with the degree of downstream medial parietal tau burden, and that the interaction of pathology and connectivity is associated with worse memory performance. In Chapter 2, we show that functional networks specific to performance in a given cognitive domain, in particular episodic memory, have lower overall strength in the presence of tau pathology before the onset of widespread neurodegeneration. Finally in Chapter 3, we show that the rate and distribution of tau accumulation over time is influenced by baseline functional connectivity and AD pathology, along with corresponding declines in memory performance. Taken together, this work furthers our understanding of the reciprocal relationships between pathology accumulation and function networks in the aging brain, underscoring the importance of this relationship for cognitive function and identifying neural connectivity as a potential target for interventions aimed at reducing the spread and accumulation of tau pathology in individuals at risk for disease-related cognitive decline.

From the early observation that networks of functional connectivity overlap with patterns of neurodegeneration in distinct AD subtypes¹², a robust body of literature has outlined how functional networks facilitate the stereotyped spread of tau pathology throughout the brain in aging and AD. The work described here adds to this body of research by pointing to factors that can be used to understand connectivity-mediated tau spread in cognitively unimpaired older adults who are at the earliest stages of pathology accumulation. By uncovering how functional networks contribute to neurodegenerative disease and what consequences these pathologies have for networks supporting cognitive function, this work may be used to better understand the aging human brain and the cognitive consequences of Alzheimer's disease dementia that are so devastating for so many.

Despite all this evidence, there are many unanswered questions surrounding the role of functional networks in aging and AD. Future work should seek to incorporate measures of structural connectivity between brain regions to increase the validity and reproducibility of functional neuroimaging measures in predicting pathology spread. In addition, it remains to be seen if connectivity can be used to explain why some individuals develop Alzheimer's disease and others do not, as well as why different variants and subtypes of AD present in different individuals. Ultimately, it may be that pathways of strong network connectivity that are critical for brain function throughout life are hijacked in neurodegenerative disease, initiating a syndrome of cognitive decline specific to individual profiles of brain connectivity.

References

1. Alzheimer & Association. Alzheimer's Association 2024 Alzheimer's Disease Facts and Figures. *Alzheimer's Assoc.* **20**, 1–146 (2024).
2. Jack, C. R. *et al.* Serial PIB and MRI in normal, mild cognitive impairment and Alzheimers disease: Implications for sequence of pathological events in Alzheimers disease. *Brain* **132**, 1355–1365 (2009).
3. Hansson, O., Blennow, K., Zetterberg, H. & Dage, J. Blood biomarkers for Alzheimer's disease in clinical practice and trials. *Nat. Aging* **3**, 506–519 (2023).
4. Cummings, J., Osse, A. M. L., Cammann, D., Powell, J. & Chen, J. Anti-Amyloid Monoclonal Antibodies for the Treatment of Alzheimer's Disease. *BioDrugs* **38**, 5–22 (2024).
5. Braak, H. & Braak, E. Neuropathological staging of Alzheimer-related changes. *Acta Neuropathol.* 239–259 (1991) doi:10.1007/BF00308809.
6. Crary, J. F. *et al.* Primary age-related tauopathy (PART): a common pathology associated with human aging John. *Acta Neuropathol.* **128**, 755–766 (2014).
7. Maass, A. *et al.* Entorhinal tau pathology, episodic memory decline, and neurodegeneration in aging. *J. Neurosci.* **38**, 530–543 (2018).
8. Ziontz, J. *et al.* Tau pathology in cognitively normal older adults. *Alzheimer's Dement. Diagnosis, Assess. Dis. Monit.* **11**, 637–645 (2019).
9. Aschenbrenner, A. J., Gordon, B. A., Benzinger, T. L. S., Morris, J. C. & Hassenstab, J. J. Influence of tau PET, amyloid PET, and hippocampal volume on cognition in Alzheimer disease. *Neurology* 10.1212/WNL.0000000000006075 (2018) doi:10.1212/WNL.0000000000006075.
10. Jagust, W. Imaging the evolution and pathophysiology of Alzheimer disease. *Nat. Rev. Neurosci.* **19**, 687–700 (2018).
11. Fox, M. D. *et al.* The human brain is intrinsically organized into dynamic, anticorrelated functional networks. *Proc. Natl. Acad. Sci. U. S. A.* **102**, 9673–9678 (2005).
12. Seeley, W. W., Crawford, R. K., Zhou, J., Miller, B. L. & Greicius, M. D. Neurodegenerative Diseases Target Large-Scale Human Brain Networks. *Neuron* **62**, 42–52 (2009).
13. Cope, T. E. *et al.* Tau burden and the functional connectome in Alzheimer's disease and progressive supranuclear palsy. (2018) doi:10.1093/brain/awx347.
14. Meisl, G. *et al.* In vivo rate-determining steps of tau seed accumulation in Alzheimer's disease. *Sci. Adv.* **7**, (2021).
15. Wu, J. W. *et al.* Neuronal activity enhances tau propagation and tau pathology in vivo. *Nat. Neurosci.* **19**, 1085–1092 (2016).
16. Pooler, A. M., Phillips, E. C., Lau, D. H. W., Noble, W. & Hanger, D. P. Physiological release of endogenous tau is stimulated by neuronal activity. *EMBO Rep.* **14**, 389–394 (2013).
17. Ruan, Z. *et al.* Alzheimer's disease brain-derived extracellular vesicles spread tau pathology in interneurons. *Brain* **144**, 288–309 (2021).
18. Zhou, L. *et al.* Tau association with synaptic vesicles causes presynaptic dysfunction. *Nat. Commun.* **8**, 1–13 (2017).
19. Adams, J. N., Maass, A., Harrison, T. M., Baker, S. L. & Jagust, W. J. Cortical tau deposition follows patterns of entorhinal functional connectivity in aging. *Elife* **8**, 1–22

- (2019).
20. Franzmeier, N. *et al.* Functional connectivity associated with tau levels in ageing, Alzheimer's, and small vessel disease. *Brain* 1093–1107 (2019) doi:10.1093/brain/awz026.
 21. Franzmeier, N. *et al.* Functional brain architecture is associated with the rate of tau accumulation in Alzheimer's disease Nicolai. *Nat. Commun.* **11**, 1–17 (2020).
 22. Vogel, J. W. *et al.* Connectome-based modelling of neurodegenerative diseases: towards precision medicine and mechanistic insight. *Nat. Rev. Neurosci.* **24**, 620–639 (2023).
 23. Therriault, J. *et al.* Intrinsic connectivity of the human brain provides scaffold for tau aggregation in clinical variants of Alzheimer's disease. *Sci. Transl. Med.* **14**, (2022).
 24. Hoening, M. C. *et al.* Networks of tau distribution in Alzheimer's disease. *Brain* 568–581 (2018) doi:10.1093/brain/awx353.
 25. Vogel, J. W. *et al.* Spread of pathological tau proteins through communicating neurons in human Alzheimer's disease. *Nat. Commun.* **11**, 2612 (2020).
 26. Johnson, K. A. *et al.* Tau positron emission tomographic imaging in aging and early Alzheimer disease. *Ann. Neurol.* **79**, 110–119 (2016).
 27. Schöll, M. *et al.* PET Imaging of Tau Deposition in the Aging Human Brain. *Neuron* **89**, 971–982 (2016).
 28. Braak, H. & Braak, E. On areas of transition between entorhinal allocortex and temporal isocortex in the human brain. Normal morphology and lamina-specific pathology in Alzheimer's disease. *Acta Neuropathol.* **68**, 325–332 (1985).
 29. Braak, H. & Braak, E. Staging of alzheimer's disease-related neurofibrillary changes. *Neurobiol. Aging* **16**, 271–278 (1995).
 30. He, Z. *et al.* Amyloid- β plaques enhance Alzheimer's brain tau-seeded pathologies by facilitating neuritic plaque tau aggregation. *Nat. Med.* **24**, 29–38 (2018).
 31. Ahmed, Z. *et al.* A novel in vivo model of tau propagation with rapid and progressive neurofibrillary tangle pathology: The pattern of spread is determined by connectivity, not proximity. *Acta Neuropathol.* **127**, 667–683 (2014).
 32. Cope, T. E. *et al.* Tau burden and the functional connectome in Alzheimer's disease and progressive supranuclear palsy. *Brain* **141**, 550–567 (2018).
 33. Jacobs, H. I. L. *et al.* Structural tract alterations predict downstream tau accumulation in amyloid-positive older individuals. *Nat. Neurosci.* **21**, 424–431 (2018).
 34. Franzmeier, N. *et al.* Patient-centered connectivity-based prediction of tau pathology spread in Alzheimer's disease. *Sci. Adv.* **6**, (2020).
 35. Van Hoesen, G. W., Pandya, D. N. & Butters, N. Some connections of the entorhinal (area 28) and perirhinal (area 35) cortices of the rhesus monkey. II. Frontal lobe afferents. *Brain Res.* **95**, 25–38 (1975).
 36. Witter, M. P., Groenewegen, H. J., Lopes da Silva, F. H. & Lohman, A. H. M. Functional organization of the extrinsic and intrinsic circuitry of the parahippocampal region. *Prog. Neurobiol.* **33**, 161–253 (1989).
 37. Maass, A. *et al.* Comparison of multiple tau-PET measures as biomarkers in aging and Alzheimer's disease. *Neuroimage* **157**, 448–463 (2017).
 38. Harrison, T. M. *et al.* Longitudinal tau accumulation and atrophy in aging and Alzheimer disease. *Ann. Neurol.* **85**, 229–240 (2019).
 39. Ranganath, C. & Ritchey, M. Two cortical systems for memory-guided behaviour. *Nat. Rev. Neurosci.* **13**, 713–726 (2012).

40. Ritchey, M., Libby, L. A. & Ranganath, C. *Cortico-hippocampal systems involved in memory and cognition: The PMAT framework. Progress in Brain Research* vol. 219 (Elsevier B.V., 2015).
41. Maass, A. *et al.* Alzheimer's pathology targets distinct memory networks in the ageing brain. *Brain* **142**, 2492–2509 (2019).
42. Chrastil, E. R. Heterogeneity in human retrosplenial cortex: A review of function and connectivity. *Behav. Neurosci.* **132**, 317–338 (2018).
43. Desikan, R. S. *et al.* An automated labeling system for subdividing the human cerebral cortex on MRI scans into gyral based regions of interest. *Neuroimage* **31**, 968–980 (2006).
44. Fan, L. *et al.* The Human Brainnetome Atlas: A New Brain Atlas Based on Connectional Architecture. *Cereb. Cortex* **26**, 3508–3526 (2016).
45. Maass, A., Berron, D., Libby, L. A., Ranganath, C. & Düzel, E. Functional subregions of the human entorhinal cortex. *Elife* **4**, 1–20 (2015).
46. Whitfield-Gabrieli, S. & Nieto-Castanon, A. Conn: A Functional Connectivity Toolbox for Correlated and Anticorrelated Brain Networks. *Brain Connect.* **2**, 125–141 (2012).
47. Mathis, C. A. *et al.* Synthesis and evaluation of ¹¹C-labeled 6-substituted 2-arylbenzothiazoles as amyloid imaging agents. *J. Med. Chem.* 1–15 (2009).
48. Baker, S. L., Maass, A. & Jagust, W. J. Considerations and code for partial volume correcting [¹⁸F]-AV-1451 tau PET data. *Data Br.* **15**, 648–657 (2017).
49. Rousset, O. G., Ma, Y. & Evans, A. C. Correction for partial volume effects in PET: Principle and validation. *J. Nucl. Med.* **39**, 904–911 (1998).
50. Logan, J. Graphical analysis of PET data applied to reversible and irreversible tracers. *Nucl. Med. Biol.* **27**, 661–670 (2000).
51. Price, J. C. *et al.* Kinetic modeling of amyloid binding in humans using PET imaging and Pittsburgh Compound-B. *J. Cereb. Blood Flow Metab.* **25**, 1528–1547 (2005).
52. Mormino, E. C. *et al.* Not quite PIB-positive, not quite PIB-negative: Slight PIB elevations in elderly normal control subjects are biologically relevant. *Neuroimage* **59**, 1152–1160 (2012).
53. Harrison, T. M. *et al.* Tau deposition is associated with functional isolation of the hippocampus in aging. *Nat. Commun.* **10**, (2019).
54. Vonk, J. M. J. *et al.* Semantic loss marks early Alzheimer's disease-related neurodegeneration in older adults without dementia. *Alzheimer's Dement. Diagnosis, Assess. Dis. Monit.* **12**, 1–14 (2020).
55. Schultz, A. P. *et al.* Phases of Hyperconnectivity and Hypoconnectivity in the Default Mode and Salience Networks Track with Amyloid and Tau in Clinically Normal Individuals. *J. Neurosci.* **37**, 4323–4331 (2017).
56. Huijbers, W. *et al.* Tau accumulation in clinically normal older adults is associated with hippocampal hyperactivity. *J. Neurosci.* (2018) doi:10.1523/JNEUROSCI.1397-18.2018.
57. Vogel, J. W. *et al.* Four distinct trajectories of tau deposition identified in Alzheimer's disease. *Nat. Med.* (2021) doi:10.1038/s41591-021-01309-6.
58. Schröder, T. N., Haak, K. V., Jimenez, N. I. Z., Beckmann, C. F. & Doeller, C. F. Functional topography of the human entorhinal cortex. *Elife* **4**, 1–17 (2015).
59. Kaufman, S. K., Del Tredici, K., Thomas, T. L., Braak, H. & Diamond, M. I. Tau seeding activity begins in the transentorhinal/entorhinal regions and anticipates phospho-tau pathology in Alzheimer's disease and PART. *Acta Neuropathol.* **136**, 57–67 (2018).
60. Sepulcre, J. *et al.* Tau and amyloid- β proteins distinctively associate to functional network

- changes in the aging brain. *Alzheimer's Dement.* 1–9 (2017)
doi:10.1016/j.jalz.2017.02.011.
61. Berron, D., van Westen, D., Ossenkoppele, R., Strandberg, O. & Hansson, O. Medial temporal lobe connectivity and its associations with cognition in early Alzheimer's disease. *Brain* (2020) doi:10.1093/brain/awaa068.
 62. Wang, L. *et al.* Intrinsic connectivity between the hippocampus and posteromedial cortex predicts memory performance in cognitively intact older individuals. *Neuroimage* **51**, 910–917 (2010).
 63. Kaboodvand, N., Bäckman, L., Nyberg, L. & Salami, A. The retrosplenial cortex: A memory gateway between the cortical default mode network and the medial temporal lobe. *Hum. Brain Mapp.* **39**, 2020–2034 (2018).
 64. Warren, J. D. *et al.* Molecular nexopathies: A new paradigm of neurodegenerative disease. *Trends Neurosci.* **36**, 561–569 (2013).
 65. Harris, S. S., Wolf, F., De Strooper, B. & Busche, M. A. Tipping the Scales: Peptide-Dependent Dysregulation of Neural Circuit Dynamics in Alzheimer's Disease. *Neuron* 1–19 (2020) doi:10.1016/j.neuron.2020.06.005.
 66. Jones, D. T. *et al.* Tau, amyloid, and cascading network failure across the Alzheimer's disease spectrum. *Cortex* **97**, 143–159 (2017).
 67. Flicker, C., Bartus, R. T., Crook, T. H. & Ferris, S. H. Effects of aging and dementia upon recent visuospatial memory. *Neurobiol. Aging* **5**, 275–283 (1984).
 68. Bushara, K. O. *et al.* Modality-specific frontal and parietal areas for auditory and visual spatial localization in humans. *Nat. Neurosci.* **2**, 759–766 (1999).
 69. Iachini, T., Iavarone, A., Senese, V., Ruotolo, F. & Ruggiero, G. Visuospatial Memory in Healthy Elderly, AD and MCI: A Review. *Curr. Aging Sci.* **2**, 43–59 (2012).
 70. Lithfous, S., Dufour, A. & Després, O. Spatial navigation in normal aging and the prodromal stage of Alzheimer's disease: Insights from imaging and behavioral studies. *Ageing Res. Rev.* **12**, 201–213 (2013).
 71. Dehmelt, L. & Halpain, S. The MAP2/Tau family of microtubule-associated proteins Gene organization and evolutionary history. *Genome Biol.* **6**, 1–10 (2004).
 72. Hanger, D. P. *et al.* Intracellular and extracellular roles for tau in neurodegenerative disease. *J. Alzheimer's Dis.* **40**, (2014).
 73. Sperling, R. A. *et al.* The impact of amyloid-beta and tau on prospective cognitive decline in older individuals. *Ann. Neurol.* **85**, 181–193 (2019).
 74. Schöll, M. *et al.* PET Imaging of Tau Deposition in the Aging Human Brain. *Neuron* **89**, 971–982 (2016).
 75. Buckner, R. L. Memory and executive function in aging and ad: Multiple factors that cause decline and reserve factors that compensate. *Neuron* vol. 44 195–208 (2004).
 76. Bejanin, A. *et al.* Tau pathology and neurodegeneration contribute to cognitive impairment in Alzheimer's disease. *Brain* **140**, 3286–3300 (2017).
 77. Hanseeuw, B. J. *et al.* Association of Amyloid and Tau with Cognition in Preclinical Alzheimer Disease: A Longitudinal Study. *JAMA Neurol.* **76**, 915–924 (2019).
 78. Tideman, P. *et al.* Association of β -Amyloid Accumulation with Executive Function in Adults with Unimpaired Cognition. *Neurology* **98**, E1525–E1533 (2022).
 79. Ossenkoppele, R. *et al.* Amyloid and tau PET-positive cognitively unimpaired individuals are at high risk for future cognitive decline. *Nat. Med.* **28**, 2381–2387 (2022).
 80. Mak, E. *et al.* In vivo coupling of tau pathology and cortical thinning in Alzheimer's

- disease. *Alzheimer's Dement. Diagnosis, Assess. Dis. Monit.* **10**, 678–687 (2018).
81. Harrison, T. M., Du, R., Klencklen, G., Baker, S. L. & Jagust, W. J. Distinct effects of beta-amyloid and tau on cortical thickness in cognitively healthy older adults. *Alzheimer's Dement.* **17**, 1085–1096 (2021).
 82. Berron, D. *et al.* Early stages of tau pathology and its associations with functional connectivity, atrophy and memory. *Brain* **144**, 2771–2783 (2021).
 83. La Joie, R. *et al.* Prospective longitudinal atrophy in Alzheimer's disease correlates with the intensity and topography of baseline tau-PET. *Sci. Transl. Med.* **12**, 1–13 (2020).
 84. Spillantini, M. G. & Goedert, M. Tau pathology and neurodegeneration. *Lancet Neurol.* **12**, 609–622 (2013).
 85. Ossenkoppele, R. *et al.* Accuracy of Tau Positron Emission Tomography as a Prognostic Marker in Preclinical and Prodromal Alzheimer Disease: A Head-to-Head Comparison against Amyloid Positron Emission Tomography and Magnetic Resonance Imaging. *JAMA Neurol.* **78**, 961–971 (2021).
 86. Fox, M. D. & Raichle, M. E. Spontaneous fluctuations in brain activity observed with functional magnetic resonance imaging. *Nat. Rev. Neurosci.* **8**, 700–711 (2007).
 87. Cole, M. W., Bassett, D. S., Power, J. D., Braver, T. S. & Petersen, S. E. Intrinsic and task-evoked network architectures of the human brain. *Neuron* **83**, 238–251 (2014).
 88. Cole, M. W., Ito, T., Bassett, D. S. & Schultz, D. H. Activity flow over resting-state networks shapes cognitive task activations. *Nat. Neurosci.* **19**, 1718–1726 (2016).
 89. Ossenkoppele, R. *et al.* Tau PET patterns mirror clinical and neuroanatomical variability in Alzheimer's disease. *Brain* **139**, 1551–1567 (2016).
 90. Schultz, A. P. *et al.* Phases of Hyperconnectivity and Hypoconnectivity in the Default Mode and Salience Networks Track with Amyloid and Tau in Clinically Normal Individuals. *J. Neurosci.* **37**, 4323–4331 (2017).
 91. Buckley, R. F. *et al.* Functional network integrity presages cognitive decline in preclinical Alzheimer disease. *Neurology* **89**, 29–37 (2017).
 92. Yeo, B. T. *et al.* The organization of the human cerebral cortex estimated by intrinsic functional connectivity. *J. Neurophysiol.* **106**, 1125–1165 (2011).
 93. Rosenberg, M. D. *et al.* A neuromarker of sustained attention from whole-brain functional connectivity. *Nat. Neurosci.* **19**, 165–171 (2015).
 94. Lee, J. J. *et al.* A neuroimaging biomarker for sustained experimental and clinical pain. *Nat. Med.* **27**, 174–182 (2021).
 95. Beaty, R. E. *et al.* Robust prediction of individual creative ability from brain functional connectivity. *Proc. Natl. Acad. Sci. U. S. A.* **115**, 1087–1092 (2018).
 96. Henneghan, A. M. *et al.* Predicting Patient Reported Outcomes of Cognitive Function Using Connectome-Based Predictive Modeling in Breast Cancer. *Brain Topogr.* **33**, 135–142 (2020).
 97. Ju, S. *et al.* Connectome-based predictive modeling shows sex differences in brain-based predictors of memory performance. *Front. Dement.* **2**, (2023).
 98. Gao, S., Greene, A. S., Constable, R. T. & Scheinost, D. Combining multiple connectomes improves predictive modeling of phenotypic measures. *Neuroimage* **201**, 116038 (2019).
 99. Greene, A. S., Gao, S., Scheinost, D. & Constable, R. T. Task-induced brain state manipulation improves prediction of individual traits. *Nat. Commun.* **9**, (2018).
 100. Fountain-Zaragoza, S., Samimy, S., Rosenberg, M. D. & Prakash, R. S. Connectome-

- based models predict attentional control in aging adults. *Neuroimage* **186**, 1–13 (2019).
101. Gao, M. *et al.* Connectome-based models can predict processing speed in older adults. *Neuroimage* **223**, 117290 (2020).
 102. Boyle, R. *et al.* Connectome-based predictive modelling of cognitive reserve using task-based functional connectivity. *Eur. J. Neurosci.* **57**, 490–510 (2023).
 103. Shen, X. *et al.* Using connectome-based predictive modeling to predict individual behavior from brain connectivity. *Nat. Protoc.* **12**, 506–518 (2017).
 104. Tibshirani, R. Regression Shrinkage and Selection Via the Lasso. *J. R. Stat. Soc. Ser. B* **58**, 267–288 (1996).
 105. Schwarz, G. Estimating the Dimension of a Model. *Ann. Stat.* **6**, 461–464 (1978).
 106. Jack, C. R. *et al.* Defining imaging biomarker cut points for brain aging and Alzheimer’s disease. *Alzheimer’s Dement.* **13**, 205–216 (2017).
 107. Leuzy, A. *et al.* A multicenter comparison of [18F]flortaucipir, [18F]RO948, and [18F]MK6240 tau PET tracers to detect a common target ROI for differential diagnosis. *Eur. J. Nucl. Med. Mol. Imaging* **48**, 2295–2305 (2021).
 108. Gibbons, L. E. *et al.* A composite score for executive functioning, validated in Alzheimer’s Disease Neuroimaging Initiative (ADNI) participants with baseline mild cognitive impairment. *Brain Imaging Behav.* **6**, 517–527 (2012).
 109. Gilbert, S. J. & Burgess, P. W. Executive function. *Curr. Biol.* **18**, 110–114 (2008).
 110. Voets, N. L. *et al.* Aberrant functional connectivity in dissociable hippocampal networks is associated with deficits in memory. *J. Neurosci.* **34**, 4920–4928 (2014).
 111. Gonneaud, J. *et al.* Accelerated functional brain aging in pre-clinical familial Alzheimer’s disease. *Nat. Commun.* **12**, 5346 (2021).
 112. Liem, F., Geerligs, L., Damoiseaux, J. & Margulies, D. Functional Connectivity in Aging. 1–36 (2019) doi:10.31234/osf.io/whsud.
 113. Shen, X. *et al.* Using connectome-based predictive modeling to predict individual behavior from brain connectivity. *Nat. Protoc.* **12**, 506–518 (2017).
 114. Ossenkoppele, R. *et al.* Associations between tau, A β , and cortical thickness with cognition in Alzheimer disease. *Neurology* **92**, e601–e612 (2019).
 115. Jones, D. T. *et al.* Cascading network failure across the Alzheimer’s disease spectrum. *Brain* **139**, 547–562 (2016).
 116. Finn, E. S. Is it time to put rest to rest? *Trends Cogn. Sci.* **25**, 1021–1032 (2021).
 117. Jack, C. R. *et al.* NIA-AA Research Framework: Toward a biological definition of Alzheimer’s disease. *Alzheimer’s Dement.* **14**, 535–562 (2018).
 118. Crary, J. F. *et al.* Primary age-related tauopathy (PART): a common pathology associated with human aging. *Acta Neuropathol.* **128**, 755–766 (2014).
 119. Iaccarino, L. *et al.* Local and distant relationships between amyloid, tau and neurodegeneration in Alzheimer’s Disease. *NeuroImage Clin.* **17**, 452–464 (2018).
 120. Bennett, R. E. *et al.* Enhanced Tau Aggregation in the Presence of Amyloid β . *Am. J. Pathol.* **187**, 1601–1612 (2017).
 121. He, Z. *et al.* Amyloid- β plaques enhance Alzheimer’s brain tau-seeded pathologies by facilitating neuritic plaque tau aggregation. *Nat. Med.* **24**, 29–38 (2018).
 122. Schöll, M. *et al.* PET Imaging of Tau Deposition in the Aging Human Brain. *Neuron* **89**, 971–982 (2016).
 123. Sanchez, J. S. *et al.* The cortical origin and initial spread of medial temporal tauopathy in Alzheimer’s disease assessed with positron emission tomography. *Sci. Transl. Med.* **13**,

- (2021).
124. Lee, W. J. *et al.* Regional A β -tau interactions promote onset and acceleration of Alzheimer's disease tau spreading. *Neuron* 1–12 (2022)
doi:10.1016/j.neuron.2022.03.034.
 125. Scott, M. R. *et al.* Inferior temporal tau is associated with accelerated prospective cortical thinning in clinically normal older adults. *Neuroimage* **220**, 116991 (2020).
 126. Halawa, O. A. *et al.* Inferior and medial temporal tau and cortical amyloid are associated with daily functional impairment in Alzheimer's disease. *Alzheimer's Res. Ther.* **11**, 1–10 (2019).
 127. Jack, C. R. *et al.* Longitudinal tau PET in ageing and Alzheimer's disease. *Brain* **141**, 1517–1528 (2018).
 128. Sperling, R. A. *et al.* Amyloid Deposition Is Associated with Impaired Default Network Function in Older Persons without Dementia. *Neuron* **63**, 178–188 (2009).
 129. Epstein, R. A., Patai, E. Z., Julian, J. B. & Spiers, H. J. The cognitive map in humans: Spatial navigation and beyond. *Nat. Neurosci.* **20**, 1504–1513 (2017).
 130. Ziontz, J., Adams, J. N., Harrison, T. M., Baker, S. L. & Jagust, W. J. Hippocampal Connectivity with Retrosplenial Cortex is Linked to Neocortical Tau Accumulation and Memory Function. *J. Neurosci.* **41**, 8839–8847 (2021).
 131. Targa Dias Anastacio, H., Matosin, N. & Ooi, L. Neuronal hyperexcitability in Alzheimer's disease: what are the drivers behind this aberrant phenotype? *Transl. Psychiatry* **12**, (2022).
 132. Giorgio, J., Adams, J. N., Maass, A., Jagust, W. J. & Breakspear, M. Amyloid induced hyperexcitability in default mode network drives medial temporal hyperactivity and early tau accumulation. *Neuron* **112**, 676-686.e4 (2024).
 133. Koutsodendris, N. *et al.* Neuronal APOE4 removal protects against tau-mediated gliosis, neurodegeneration and myelin deficits. *Nat. Aging* **3**, 275–296 (2023).
 134. Nuriel, T. *et al.* Neuronal hyperactivity due to loss of inhibitory tone in APOE4 mice lacking Alzheimer's disease-like pathology. *Nat. Commun.* **8**, (2017).
 135. Filippini, N. *et al.* Distinct patterns of brain activity in young carriers of the APOE- ϵ 4 allele. *Proc. Natl. Acad. Sci. U. S. A.* **106**, 7209–7214 (2009).
 136. Cacciaglia, R. *et al.* Genotypic effects of APOE- ϵ 4 on resting-state connectivity in cognitively intact individuals support functional brain compensation. *Cereb. Cortex* **33**, 2748–2760 (2023).
 137. Baek, M. S. *et al.* Effect of APOE ϵ 4 genotype on amyloid- β and tau accumulation in Alzheimer's disease. *Alzheimer's Res. Ther.* **12**, 1–12 (2020).
 138. Buckley, R. F. *et al.* Associations between baseline amyloid, sex, and APOE on subsequent tau accumulation in cerebrospinal fluid. *Neurobiol. Aging* **78**, 178–185 (2019).
 139. Young, C. B. *et al.* APOE effects on regional tau in preclinical Alzheimer's disease. *Mol. Neurodegener.* **18**, 1–14 (2023).
 140. Steward, A. *et al.* ApoE4 and Connectivity-Mediated Spreading of Tau Pathology at Lower Amyloid Levels. *JAMA Neurol.* **80**, 1295–1306 (2023).
 141. Deichmann, R., Josephs, O., Hutton, C., Corfield, D. R. & Turner, R. Compensation of susceptibility-induced bold sensitivity losses in echo-planar fMRI imaging. *Neuroimage* **15**, 120–135 (2002).
 142. LaJoie, R. *et al.* Intrinsic connectivity identifies the hippocampus as a main crossroad between alzheimer's and semantic dementia-targeted networks. *Neuron* **81**, 1417–1428

- (2014).
143. Montal, V. *et al.* Network Tau spreading is vulnerable to the expression gradients of APOE and glutamatergic-related genes. *Sci. Transl. Med.* **14**, 1–11 (2022).
 144. Ferrari-Souza, J. P. *et al.* APOE ϵ 4 associates with microglial activation independently of A β plaques and tau tangles. *Sci. Adv.* **9**, 1–10 (2023).
 145. Therriault, J. *et al.* Association of Apolipoprotein e ϵ 4 with Medial Temporal Tau Independent of Amyloid- β . *JAMA Neurol.* **77**, 470–479 (2020).
 146. Peelen, M. V & Caramazza, A. Conceptual Object Representations in Human Anterior Temporal Cortex. **32**, 15728–15736 (2012).
 147. Ranasinghe, K. G. *et al.* Altered excitatory and inhibitory neuronal subpopulation parameters are distinctly associated with tau and amyloid in Alzheimer’s disease. *Elife* **11**, 1–26 (2022).
 148. Baker, S. L., Harrison, T. M., Maass, A., Joie, R. La & Jagust, W. J. Effect of off-target binding on 18F-flortaucipir variability in healthy controls across the life span. *J. Nucl. Med.* **60**, 1444–1451 (2019).
 149. Giorgio, J. *et al.* A robust and interpretable machine learning approach using multimodal biological data to predict future pathological tau accumulation. *Nat. Commun.* **13**, 1–14 (2022).